Risk and Performance Based Fire Safety Design of Steel and Composite Structures

David James Lange

Doctor of Philosophy
The University of Edinburgh
2009

Declaration

The research which is detailed in this thesis has been completed solely by myself at the University of Edinburgh under the supervision of Professor Asif Usmani and Professor Jose Torero. Where other sources are used, appropriate references are made.

David Lange

The University of Edinburgh 2009

Abstract

For the development of performance based design on a proper scientific basis the use of the concept of risk is inevitable. However, the application of this concept to actual structural design is not simple because of the large ranges of probability and consequences of events which exist. This is compounded by a plethora of different actions that can be taken to reduce the probabilities of the events and also the magnitude of the consequences. It is the reduction in the magnitude of these consequences which is essentially the goal of design.

This work aims to address the challenges posed by the application of the concepts of performance based design for structures in fire. Simple methodologies have been developed for the assessment of the consequences of an extreme event. These methodologies are based upon fundamental behaviour of structures in fire.

A methodology has been developed which can be used to assess the capacity/deflection behaviour through the complete thermal deflection of floor slabs. This takes into account positive effects on the capacity of floor slabs of the membrane stress at the slabs boundaries at low deflections as well as the final capacity provided by the tensile membrane action of the reinforcement mesh at high deflections.

For vertical stability of structures in fire, analytical equations to describe the behaviour of floor systems at the perimeter of a building are developed. From these equations, the resulting pull-in forces on external columns can be calculated as well as the resulting horizontal load applied to the column. From this, a simple stability assessment is proposed which can be used to

assess the consequences of multiple floor fires on tall buildings.

These analytical methodologies are brought together in a risk based framework for structural design which can be used to identify areas in a building or structural components which pose a high residual risk. These elements can be qualitatively 'ranked' according to their relative risk and appropriate measures taken to reduce the risk to an acceptable level. The framework is illustrated via 2 case studies. The first is of a typical small office building, and the second is of a prestige office development.

Acknowledgements

This work has been supported by Corus Group plc. and the EPSRC through an industrial CASE award.

I would like to acknowledge the support and help of my friends and colleagues at the University of Edinburgh; in particular my academic supervisors Professors Asif Usmani and Jose Torero.

Publications

Journal Papers

Charlotte Roben, A. Usmani, G. Flint, A. Jowsey, and **D. Lange**; Tall building collapse mechanisms initiated by fire; Part 1, Mechanisms Explained; submitted to the Structural Engineer, July 2007; under revision

David Lange, C Roben, A. Usmani; Tall building collapse mechanisms initiated by fire; Part 2, Design Method; submitted to the Structural Engineer, July 2007; under revision

Conference Papers

David Lange, Asif Usmani, Neil Cameron, Wolfgang Winkler and Jose Torero; A performance based design methodology for composite floor slabs in fire; Proceedings of the 4th International Workshop Structures in Fire (SiF '06) 10-12 May 2006

David Lange, Asif Usmani and Jose Torero; A Risk Based Framework for Performance Based Fire Safety Design of Steel and Composite Structures; Fifth International Conference on Advances in Steel Structures (ICASS 2007) 5-7 December 2007

David Lange, Asif Usmani and Jose Torero; The Reliability of Structures in Fire, Proceedings of the 5th International Workshop Structures in Fire (SiF '08) 28-30 May 2008

David Lange, Asif Usmani; Collapse of tall buildings in multi-storey fires; 9th International Symposium on Fire Safety Science; 21-26 September 2008

Other Presentations

David Lange, C. Roben, A. Usmani; Tall building collapse mechanisms initiated by fire: Design Method; presentation at Steel in Fire Forum, April 2007

David Lange, Asif Usmani and Jose Torero; Development of a risk based framework for performance based fire safety design of steel and composite structures; presentation at Corus Academia symposium, March 2008

Contents

List of Figures

List of Tables

1

Introduction

1.1 Background to the Project

For the Development of performance based design on a proper scientific basis the use of the concepts of risk and reliability is inevitable. The application of the concepts of performance based methodology to actual design is not simple because of the large ranges of probability and consequences of events which exist. This is compounded by a plethora of different actions that can be taken to reduce the probabilities of the events and also the magnitude of the consequences, which is essentially the goal of design.

Clearly while the use of this concept poses major challenges, it also offers enormous opportunities because of the element of choice inherent in the concept. The designer using these concepts has numerous choices to address his design problem to enable him to arrive at a solution for which the 'risk is acceptable'.

Risk is defined as a function of probability and consequence. For our purposes, the probability refers to some undesirable event over a period of time (which in fire terms could be described as a fire event over a certain critical magnitude of severity during the design life of the building). Consequence refers to the effects of the occurrence of the event (in fire terms it would mean a loss of life, damage to property, damage to business and longer term damage to society for major events).

Reliability is defined as the probability of 'success', or the complement of the probability of failure. A risk-based approach will also allow the calculation of quantitative estimates of reliability for particular design solutions, and hence provide stakeholders with a numerical measure for guiding their choice between various solutions.

1.2 Research aims

Although design codes allow for the implementation of performance based design techniques, the analysis required to understand and quantify complete structural response is typically computationally intensive. Where numerical techniques have been validated by classical theories and their validity demonstrated in well understood ambient conditions, counterpart 'classical' theories for elevated temperature response have not until relatively recently existed. Numerical analysis of the Cardington tests as well as other deliberate or accidental fires in large buildings has helped to develop and improve an understanding of structural behaviour at elevated temperatures. Where numerous 'simple' analytical techniques have been developed to determine response of buildings subject to fire attack, there has been no known attempt made to develop and combine these techniques in a comprehensive risk or reliability based design methodology. The primary aim of this project is, therefore:

- To develop a performance based design methodology for structures in fire, addressing the concepts of risk and reliability;

To accomplish this, the following has to be addressed as part of the design framework:

- the probability of a fire event and the consequences of said fire have to be defined; and,
- a method for the determination of the reliability of a structure given a fire has to be employed in the framework.

As inherently modular, performance based design methodologies require additional components which satisfy the performance criteria upon which they are based. Therefore an additional research goal occurs as a result of the nature of the primary research goal:

- To draw on previous research which has been carried out in the determination of structural response and capacity in fire and develop this research where necessary into a useable tool which can be incorporated into the design framework.

1.3 Thesis Overview

The following is a summary of the chapters in this thesis:

Chapter 2. Basic Fire Modelling for Structures

In this chapter, various fire models available for structural fire engineering are introduced. An overview of their level of complexity is given as well as the level of complexity involved in their use. Basics of heat trasnfer to structural elements are also described.

Chapter 3. Overview of the Behaviour of Structures in Fire

In this chapter, an overview and a brief review of the behaviour of structures in fire is given. A brief history of researcgh in the field is given, followed by a description of some of the fundamental principles which govern the behaviour of structures in fire, along with their analytical description.

Behaviour of materials under elevated tempertures is briefly described.

Chapter 4. Performance Based Design

The basic principles of performance based design are laid out, describing the basic elements of a performance based design framework. An overviw of some of the curreent methodologies is given and their application to fire is discussed.

Chapter 5. Risk and Reliability

In this chaper the meanings of risk and reliability are described as well as their difference and the different applications of the concepts. Following this, a simple risk informed framework for the design of structures in fire is described. The framework incorporates a risk assessment to identify areas of relatively high risk wihtin a building. This is then followed by an assesment of the reliability of the structure based on real possible fires to evaluate the current design evolution,

Chapter 6. Floor slab design

This chapter describes the behaviour and capacity of floor slabs over a complete deflection history. An analytical methodology for the determination of tensile membrane capacity of floor slabs in fire is described. The forces on the floor slab at low displacements are used to derive a methodology for the calculation of the capacity of a thermally 'pre-stressed' floor slab at low deflections.

Chapter 7. Performance based design framework

This chapter describes two possible collapse mechanisms for tall structures in fire. These mechanisms have been identified previously using numerical modelling. Following the description of these collapse mechanisms a simple method for calculating the forces which govern the potential for collapse is described and a methodology for the assessment of tall building stability in fire is described.

Chapter 8. Case Study: the SCI buildings

Using the buildings which were designed by the Steel Construction Institute (the SCI) for their comparative study of building costs, the response of two buildings using different structural configurations is determined analytically and changes are suggested using the design framework proposed which allow the structure to achieve target reliability.

Chapter 9. Discussion and conclusions

A general discussion is given here, summarising the results, conclusions and any issues which have been brought up in previous chapters.
Possible further work is suggested.

2

Basic Fire Modelling for Structural Design

2.1 Introduction

Before beginning any structural design process, the loads which have to be resisted need to be determined. For structural design for fire resistance, regardless of whether or not the solution is one of protection or another solution, as will be disucessed in detail later in this thesis, the fire which the structure is required to resist must be defined.

Various fire models exist, with varying degrees of control over their complexity, and some are more suited to use in determining structural loads than others. With an increase in complexity of the fire model generally comes an associated increase in the level of input required by the user. The models can broadly be divided into five categories, which are listed in ascending order of complexity [12]:

- Nominal fire curves;
- Parametric fire curves;
- One zone fire models;
- Multi-zone fire models, and;
- Field models

These models are described briefly below, however for more information as to the uses and limitations of these models, additional references should be consulted.

2.2 Nominal fire curves

Standard temeprature time curves represent an average compartment gas temperature which varies over the duration of the fire. They are specified in codes for single structureal element testing methods and being empirical they do not incorporate any aditional variables, apart from fire duration, to describe the compartment temperature, fire duration, or the fires growth rate. Their use is limited, especially for rational structural design for fire, except as a basis for comparison with other more appropriate test methods [13]. The standard British fire curve is the same as the ISO 834 fire curve, and is given by the equation:

$$\Theta_g = \Theta_a + 345log_{10}(8t + 1) \tag{2.1}$$

The British standard fire is intended to be used where the fuel load is mainly composed of cellulosic material, i.e. wood. Where the fuel source is hydrocarbon based a more severe fire can occur with an increased heating rate. In these instances, an alternative design fire is given in the Eurocodes as:

$$\Theta_g = 1080(1 - 0.325e^{-.167t} - 0.675e^{-2.5t}) + \Theta_a \tag{2.2}$$

The american ASTM E119 fire curve is not described as an equation, but rather by a series of data points, Table 2.1, which give temperature values at different times [14].

A comparison of the three nominal fire curves is shown in figure 2.1. It is apparent that there is little difference between the British or ISO curves and the ASTM fire curve. The maximum temperature achieved in the hydrocarbon fire curve is lower than that achieved over a long duration standard fire, although the increase in temperature is faster and the fire could be considered to be more severe for a shorter duration (measures of severity are largely subjective and a severe fire could be considered such based on any of the following: a more aggressive heating rate; a longer duration; or a higher achieved temperature).

Time (Minutes)	ASTM E119 Temperature (^{O}C)
0	20
5	538
10	704
30	843
60	927
120	1010
240	1093
480	1260

Table 2.1: ASTM E119 fire curve

2.3 Parametric fire curves

Parametric fire curves are described in Eurocode 1 part 1-2 [15]. They provide a more rational indication of compartment temperatures than those prescribed by nominal fire curves. They are based on full-scale compartment fire tests and take into account both the physical characteristics of the compartment: the geometry and the effect of the bounding surfaces; and fuel load in the occupancy.

During the heating phase of the fire, the temperature is described via the following relationship wiht time:

$$\Theta_g = \Theta_a + 1325(1 - 0.324e^{-0.2t^*} - 0.204e^{-1.7t^*} - 0.472e^{-19t^*}) \tag{2.3}$$

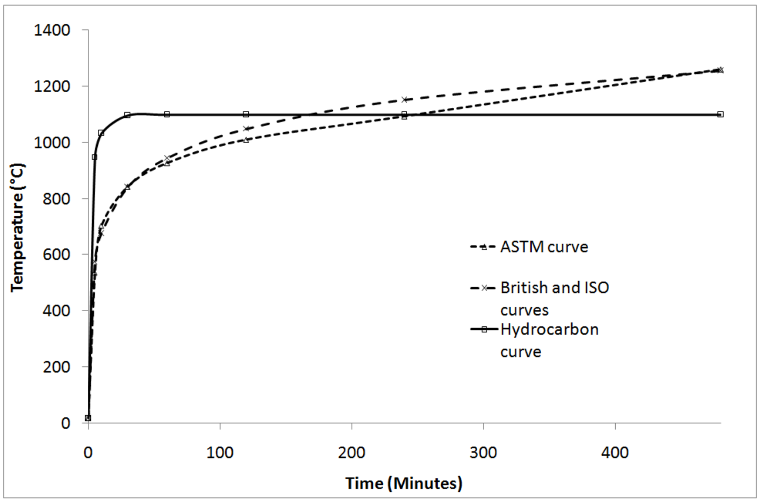

Figure 2.1: Nominal fire curve comparison

Where t^* is the notional time given by the current time multiplied by a factor Γ representing the opening factor and the compartment boundarys thermal inertia and their ratios to some reference values:

$$\Gamma = \frac{(F_v/b)^2}{(0.04/1160)^2} \tag{2.4}$$

Where F_v is the ventilation factor (or opening factor) of the compartment and b is the square root of the thermal inertia of the wall linings. The ventilation factor is given by the expression:

$$F_v = \frac{A_v}{A_t}\sqrt{H_v} \tag{2.5}$$

Where A_v is the sum of the areas of the openings, A_t is the total area of the compartment boundaries and H_v is the weighted avergae height of all of the window and door openings [14].

The Eurocode parametric fire curve is very similar to the so-called "'Swedish"' curves of Magnusson and Thelanderson.

Both nominal and parametric fire models describe the fire as an average compartment tempertaure time curve.

Alternative parametric fire curves have been developed as alternative to the Eurocode parametric fire, with specific attention paid to their relevance for structural fire engineering [16]. A number of analyses are run using the zone model CFAST to study the effects on the fire of fire load, ventilation conditions, geometry and thermal properties of the enclosure. The model relies on the rate of heat release as input, and accounts for traveling fires by allowing breakthrough between cells of a compartment and an adjustment of the heat release rate. However this approach is ultimately conservative since there is no indication of near and far exposure to the fire and the inherent assumption appears to be that once ignited, all material contribution to the fire load is cumulative with no expiry time.

2.4 One Zone Fire Models

One zone fire models have uniform temperature distribution throughout the compartment, and the gas temperature is calculated by solving the heat and mass balance equations for the system [14]. A one zone model takes account of the transfer of mass between the inside of the compartment and its surroundings and between the fire and the gas in the compartment. As with the Eurocode paramteric fire, one zone models take account of energy transfe between the gas, the compartment surroundings, the compartment boundaries and the fire, figure2.2. The physical variables used to describe the model are [17]:

- Θ_g, the gas temperature
- m, the mass of the gas inside the compartment
- V, the volume of the compartment
- E, the internal energy of the compartment
- ρ, the density of the gas inside of the compartment
- p, the compartment pressure

The major assumption of the one-zone model is that the physical properties of the gas are uniformly distributed throughout the compartment.

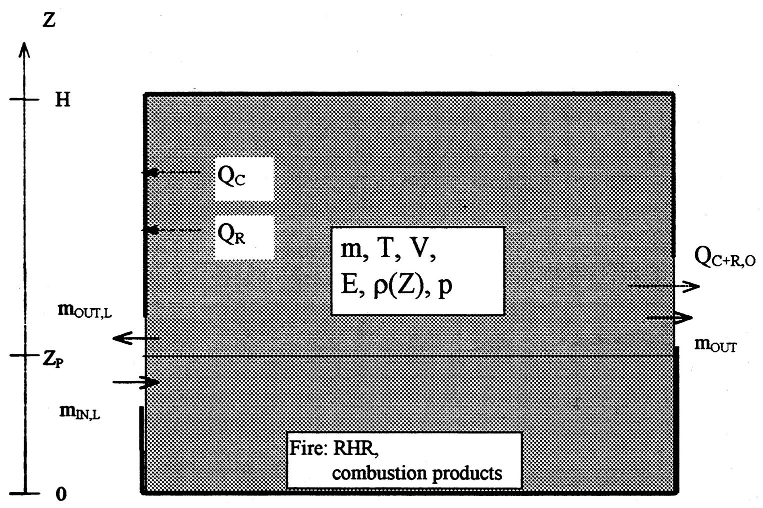

Figure 2.2: One Zone fire model

The rate of heat release into the compartment from the fire controls the amount of energy allowed into the system; this is balanced with the energy in the compartment and the energy lost via openings and through the compartment boundaries.

2.5 Multi Zone Fire Models

A multi-zone fire models is similar in concept to a one zone fire model, with the important assumption that the compartment can be divided into two separate regions, figure ??: a hot gas, or smoke, layer abover a cooler gas layer. Two zone models require the mass and energency balance to be resolved between the two layers iun the compartment as well as the exterior of the compartment. They are therefore more onerous than one-zone models. However, they are particularly suited to situations where the fire is localised [12].

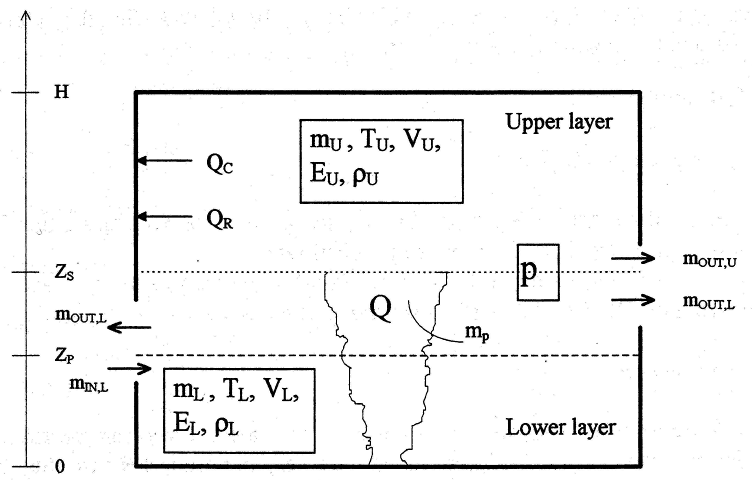

Figure 2.3: Two zone fire model

There are eleven variables which describe two zone models, constrained by the following equations [17]:

$$\rho_i = m_i/V_i$$
$$E_i = c_v m_i T_i$$
$$p = R\rho_i T_i$$
$$V = V_u + V_L$$

Where in the above set of equations, the upper and lower layers are denoted by i=U,L. Differential relationships between these variables can be derived from the mass and energy balance equations.

2.6 Field Models

Although similar to multi-zone models, field models solve the equations for mass and energy at discrete points in space rather than in two separate layers. Complex compartment geometries can be considered using field models, and non-linear temperature dependant material properties can be more easily incorporated into the models. Some examples of field models which are frequently used for fire modeling are NISTS Fire Dynamics Simulator (FDS) [18], Ansys CFX [19] and the BRE's JASMINE model [20].

Field models are computationally intensive and any results obtained from field models are extremely sensitive to the input chosen by the user [21, 22].

2.7 Temperature of Structures Exposed to Fire

There are three mechanisms which control the through depth of a structural element exposed to fire: conduction, convection and radiation. Conductive heat transfer describes the balance of energy through a solid or via a solid interface; convective heat transfer describes the transfer of energy through a gas-solid interface; and radiative heat transfer describes the transfer of energy to a solid via the electromagnetic spectrum from a radiative heat source.

Using the nominal temperature time curves described above provides a mean compartment temperature. For simplicity this is often taken to be the temperature of the exposed surface of all structural components within the compartment. This results in the through depth temperature distribution of most structural elements being controlled by conduction rather than convection or radiation. For thermally thin materials such as steel and other metals, the temperature of the element is often assumed to follow the mean compartment temperature.

Where a steel beam is protected by some material in contact with the section, BS 7974 [2] provides a simple equation for calculating the mean temperature of the section given a gas temperature time curve:

$$\Delta T_m = \frac{1}{\rho_m C_m}(\frac{H_p}{A})\frac{k_i}{d_i}(T_g - T_m)\Delta t \tag{2.6}$$

Additionally, Eurocode 2 Annex A provides calculated temperature profiles for slabs and beams [15]. Annex B of the same document provides a simplified calculation method.

Through the modelling of the Cardington tests, some simplifications were made regarding the through depth temperature distribution of floor slabs and other thermally thick structural elements. The non-linear temperature distribution was idealised as an equivalent average temperature increase, ΔT, and through depth thermal gradient, T, z, Figure 2.4 [23, 24]. All that is required in this method is that the elongation and curvature strains imposed by the idealised temperature increase and gradient are equivalent to those imposed upon the section by the original through depth temperature distribution.

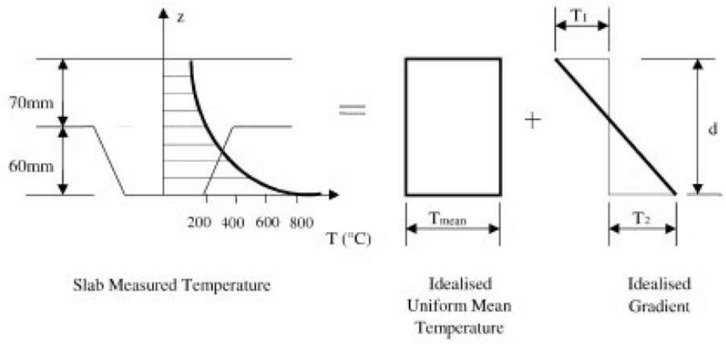

Figure 2.4: idealised temperature distribution through a concrete slab

2.8 Summary

In this chapter an overview was given of the various fire models which can be used for structural applications. Although the nominal fire curve, including the parametric fire curves are code based and used in design codes to specify temperatures of fire compartments the more complicated models are permitted as required to rationalise design solutions which are not code based, as will be discussed in later chapters. The application of these fire models to structures and various methods of calculating the temperature distribuion ina heated structural element was also described as well as the mechanisms which permit heat trasnfer.

3

Overview of the Basics of Structures in Fire

3.1 Introduction

Traditional structural design for fire centres on a furnace test of an unrestrained structural component. The component is subjected to a 'standard fire' of some prescribed duration following which the capacity of the component is checked to ensure that it meets any loading requirements which it is required to. Testing focuses on the loss of stiffness and strength of the material, and where the component fails, passive fire protection is applied to ensure that it could not reach the 'critical' temperature for the duration of the furnace test.

On the 23rd of June 1990, a fire broke out in the partially completed structure of Broadgate phase 8 - a 14 storey composite office building which was largely completed but which had no passive fire protection installed. The building did not collapse, although it did suffer very large deflections as a result of the elevated temperatures.

Although it was widely known at the time that current fire testing techniques were scientifically unsound - failure of elements in a real fire inside of a highly redundant structure bears little resemblance to failure of elements in a furnace test - the Broadgate fire led to a more focussed and concerted effort to understand real frame behaviour in real fires. This was made manifest in the Cardington tests - a set of full scale tests which were carried out on a composite steel structure inside of the airship hangars at Cardington, in Bedfordshire.

This work, undertaken jointly by Corus (then British Steel) and the Building research Establishment (BRE) consisted of 6 full scale fire tests designed and carried out in order to facilitate a better understanding of the behaviour of frames subject to fire. The tests were carried out between January 1995 and July 1996. The UK governments department for the environment transport and regions funded the partners in technology (DETR PiT) project in 1996 - a consortium of establishments undertook to analyse the results and develop numerical models to aid in the understanding and analysis of the underlying mechanics which govern structural response to fire.

The understanding of the principles which govern the behaviour of structures subject to fire has led to the development of analytical techniques to describe their behaviour.

This chapter presents a broad overview of the research carried out in the late 1990's and the early 2000's. For more detailed information a number of sources can be looked at, some of which are referenced here, however for a good introduction to the behaviour of structures in fire, the original PiT project report [25] as well as a number of PhD theses from the University of Edinburgh [1, 26, 27] give a comprehensive overview of the background to the Cardington tests, their results, and the outcome of the modelling which followed.

3.2 The Cardington Tests

The Cardington building was an 8 story composite steel frame, designed and constructed to represent a typical office building in the UK [28]. It was a braced frame comprised of a composite floor system constructed from an A142 anti-cracking mesh embedded in a concrete slab with a minimum depth of 130mm. In plan, the building measured 21 x 45 metres, and it was 33m in height. Of the six tests which were carried out on the structure 4 were planned by British Steel plc, and the remaining two were planned by the BRE.

The aims of the tests were threefold:

1. To provide data for numerical analysis of the behaviour of composite steel frames in fire;
2. To demonstrate the behaviour of multi-storey frames in fire; and,
3. To provide a platform from which to build an understanding of the behaviour of multi-storey frames in fire upon which design recommendations and, ultimately, practical methodologies can be based.

The layout of the British Steel tests is shown in figure 3.1. These consisted of, in order, test 1: a restrained beam test, test 2: a plane frame test, test 3: a corner test and test 4: a demonstration test. The BRE tests were of a corner compartment, and a large compartment; their layout is shown in figure 3.2.

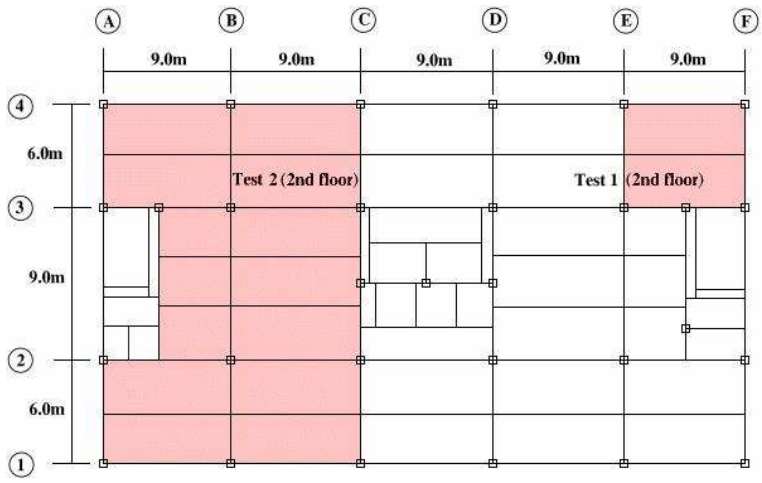

Figure 3.1: British Steel fire tests layout [1]

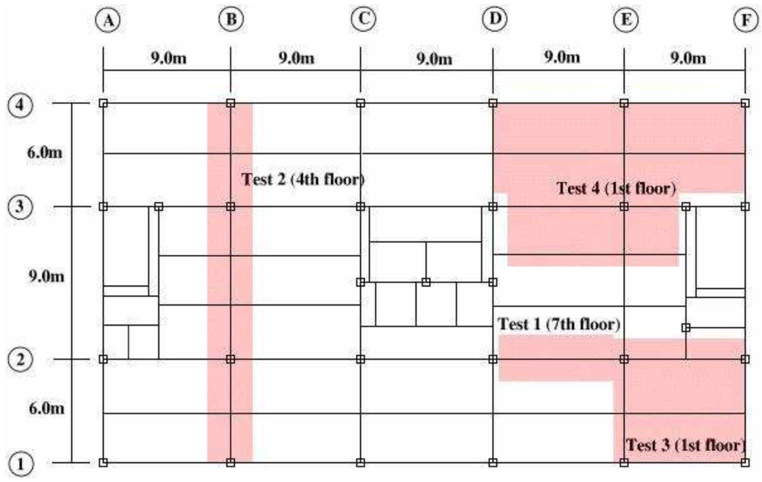

Figure 3.2: BRE fire tests layout [1]

3.2.1 British Steel Test 1

The first British Steel test was the restrained beam test. It was carried out on the 7th floor and was designed to demonstrate the real behaviour of a single structural element which is restrained by the surrounding structure. The beam was connected to columns at either end via partial depth end-plates. It was subject to a furnace fire over most of its length - 0.5m was left outside of the furnace at either end.

2 things of note were observed in this test. Aside from the expected large vertical mid-span displacements in the beam, the lower flanges of the beam and lower depths of the web yielded plastically at either end as a result of large compressive forces restraining the beams thermal expansion. The large displacements during heating were not fully recovered upon cooling.

3.2.2 British Steel Test 2

The second British Steel test was conducted over the entire length of a series of 3 beams spanning across the buildings shorter span. It also encompassed the 4 exposed columns which the beam was connected to, which were left unprotected for the purposes of this test. The objective of the test was to observe the behaviour of connections in fire as well as to observe the behaviour of the frame in the vicinity of the connections. This was the only test where the columns were exposed to heat directly without passive protection being applied up to the level of the floor.

The assembly was heated by a furnace, as in the previous test. Similar behaviour was observed as to the first test: plastic yield and buckling distortions were observed in the lower flanges of the beams at either end, and squashing of the column heads occurred directly beneath the floor system. Large displacements occurred upon heating which were not fully recovered upon cooling.

3.2.3 British Steel Test 3

The British Steel corner test was designed to study the entire compartment, and in particular the large deflection 'membrane' behaviour of the heated floor. Similar behaviour was observed to the previous tests, large displacements and buckling of the lower flanges as a result of the restraint provided by the adjacent unheated structure.

3.2.4 British Steel Test 4

The 4th British Steel test was designed to demonstrate that the behaviour observed in the previous tests would occur in a large compartment subject to a 'real' fire. The test compartment was the largest of all of the tests carried out by British Steel, and it covered fully two bays of the structure and a large portion of the neighbouring bays.

Again, large displacements were observed upon heating that remained partially after cooling. Buckling of the flanges of the beams occurred adjacent to the connections to the column. Cracking of the concrete floor slab was observed around the columns, but there was no indication that the structure was near to failure.

3.2.5 BRE Test 1

The first BRE fire test was conducted on a single corner compartment on the 2nd floor. Although there was a deflection of the structure remaining after the fire, there was no local buckling observed.

3.2.6 BRE Test 2

The second BRE test was carried out over two full bays of the structure on the 2nd floor. Like most of the British Steel tests, the columns were protected to the level of the floor. Similar behaviour was observed to the British Steel tests - large displacements in the floor system and beams, accompanied by local buckling of the lower flanges of the beams about the column connections.

3.2.7 Summary

In all of the tests which were carried out, large deflections were seen to occur in the horizontal components - the floor slabs and the primary and secondary beams. However, there was no indication that the structure was ever anywhere near failure during any of the tests. In all but the 1st BRE test which was carried out, local buckling was observed at either end of the steel beams as a result of large compressive forces developing in the steel upon heating.

Contrary to the philosophy behind the standard furnace test, the behaviour of a composite steel frame in fire is not controlled by the behaviour of the components subject to heating in a determinate mechanical test. The behaviour is determined by the ability of a heated component to expand due to temperature increases; and by the ability of the surrounding structure to resist this expansion.

3.3 Numerical Studies

A number of numerical studies to understand the behaviour of structures under thermal actions had been undertaken prior to the Cardington tests. Some examples of these modelled the behaviour of steel frames subject to fire using sub frames taking account of the restraint provided by the adjacent structure [29]. However, there were no available experimental results with which to compare the data and the only validation that was made was using existing, codified, limiting temperatures.

The PiT project was a joint collaboration between teams at the University of Edinburgh, the BRE, Imperial College London, British Steel and the SCI. Its goal was [28]:

> To understand and exploit the results of the large scale fire tests at Cardington so that rational design guidance can be developed for composite steel frameworks at the fire limit state

This was achieved through the development of numerical models of the existing test data to verify the ability of numerical techniques to model the phenomena observed [30,31]. These models were then simplified to accurately predict the behaviour of steel framed structures under thermal effects [32]. Similar models were then developed separately to test the assumptions which had been made in the original and simplified models [33].

Following the understanding which had been gained from these models and the results of the Cardington tests, analytical techniques were developed to accurately predict and explain the response of multi-storey frames to fire.

3.4 Analytical Techniques for Describing the Behaviour of Structures in Fire

3.4.1 Thermal Displacements

The overriding factor which controls the behaviour of steel structures in fire is the thermal strain and the combination of expansion and restraint which describes the response of the structure. As will be discussed, this combination may allow for alternative thermally enhanced mechanisms to mobilise which allow the structure to sustain the mechanical load to which it is subjected. The thermal strain is the product of the coefficient of thermal expansion and of the temperature increase of the material.

$$\epsilon_T = \alpha \Delta T \tag{3.1}$$

It is mechanically separate and distinct from the mechanical strain, although it does contribute to the overall total strain [34, 35]:

$$\epsilon_{tot} = \epsilon_{mech} + \epsilon_T \tag{3.2}$$

Considering a determinate beam in fire - one end is supported on a roller support, and the other is simply supported, i.e. it is free to rotate about the support but restrained against axial translation. The thermal displacements consist of two components, one dependant upon the expansion strain caused by the equivalent uniform temperature increase (ΔT) and the other on curvature strain imposed by the equivalent uniform temperature gradient ($T_{,z}$) through the depth of the composite section. The first component, the additional length generated by the outward translation of the support at the perimeter of the structure caused by the thermal expansion of the floor system, is as shown in figure 3.3.

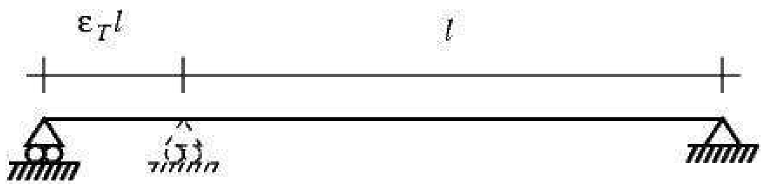

Figure 3.3: Thermal deflection due to expansion

$$L_T = L(1 + \epsilon_T) \tag{3.3}$$

The second component is the inward translation of the support at the perimeter of the structure caused by the bowing of the floor system after the application of the thermal gradient as shown in figure 3.4. The bowing strains cause a vertical deflection of the floor system. In combination with the expansion strains, the thermal curvature strains lead to some horizontal, u_T, and some vertical, w_T, displacement in the floor system, dependant upon the thermal curvature $\phi = \alpha T_{,z}$.

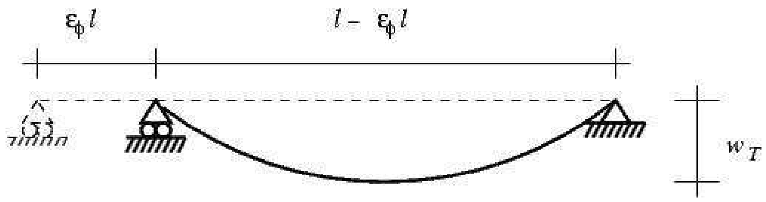

Figure 3.4: Thermal deflection due to curvature

$$\epsilon_\phi = 1 - \frac{sin\frac{L\phi}{2}}{\frac{L\phi}{2}} \tag{3.4}$$

$$w_T = \frac{2L}{\pi}\sqrt{\epsilon_\phi + \frac{{\epsilon_\phi}^2}{2}} \tag{3.5}$$

3.4.2 Thermal Force

Where the thermal strains are accommodated in the structure by deformations there is no resulting stress in the material. Where the strains are not accommodated by some displacement of the structure they induce some thermal stress:

$$\sigma_T = E\epsilon_T \tag{3.6}$$

Where no lateral translation is allowed in the floor system, the distance between the supports is fixed. Therefore thermal expansion and thermal bowing induce lateral forces, N_T, and N_ϕ, at the support, dependant upon the thermal deflection, w_T [35], figure 3.5. The thermal force at the restrained

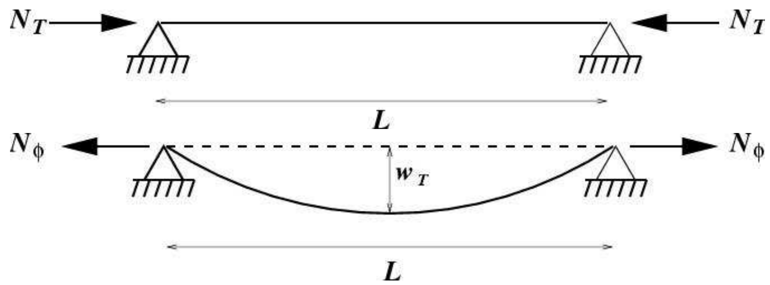

Figure 3.5: thermal forces in the floor system

ends of the beam is equivalent to the thermal force in the section:

$$N_T = E_s(T)A_s\epsilon_T \tag{3.7}$$

$$N_\phi = \left(\sqrt{\frac{1}{2}\left(\frac{\pi w_T}{L}\right)^2 + 1} - 1\right) E_s(T)A_s \tag{3.8}$$

The total horizontal force at the supports from the thermal loading is the combined load from the thermal forces:

$$N_{tot} = N_T + N_\phi \tag{3.9}$$

Thermal loading on the section is presented in two components, both related to the temperature distribution: a thermal force, N_T, caused by the restraint against expansion of the slab heated by the mean temperature; and as a thermal moment, M_T, caused by the expansion due to the temperature gradient present in the section [36].

$$N_T = Eb\alpha \int_{-h/2}^{h/2} T(z)\ dz = EA\alpha\Delta T \tag{3.10}$$

$$M_T = Eb\alpha \int_{-h/2}^{h/2} T(z)z\ dz = E\alpha T_{,z}I \tag{3.11}$$

3.5 Alternative Load Carrying Mechanisms

Although it was widely recognised as a potential action in both ambient and elevated temperature design for floor systems at large displacements, the results of the 3rd and 4th British Steel Cardington tests demonstrated the potential for structures to adopt a catenary or a membrane mechanism in fire.

These mechanisms are greatly enhanced by the presence of non-mechanical thermal strains in the structure which allow the load to effectively 'hang' without the build up of large mechanical strains in the material which lead to rupture.

They are discussed further in later chapters.

3.6 Material Properties

Despite the potentially positive effect that thermal expansion may have on a structure by mobilising alternative mechanisms, thermal action on material tends to have some negative effect on its stiffness and its strength. BS 7974 and Eurocodes 2 and 4 provide descriptions of the behaviour of materials at elevated temperatures [2, 37, 38]. This behaviour is relatively intuitive - an increase in temperature is accompanied by a decrease in both stiffness and strength - and is only summarised here.

3.6.1 Steel at Elevated Temperatures

The factors which describe stress-strain behaviour of structural steel is shown in figure 3.6. The yield plateau, not including strain hardening (represented by the dashed line), is relatively constant between 0 and 400C, although the modulus of elasticity, or Young's modulus, reduces with relatively low temperature increases. These factors are an approximation and assume a constant strain hardening.

For hot rolled reinforcing steels, the stress-strain behaviour at elevated temperature can be described using the same tables and figures as for structural steel. Poisson's ratio of steel is relatively constant at all temperatures, and

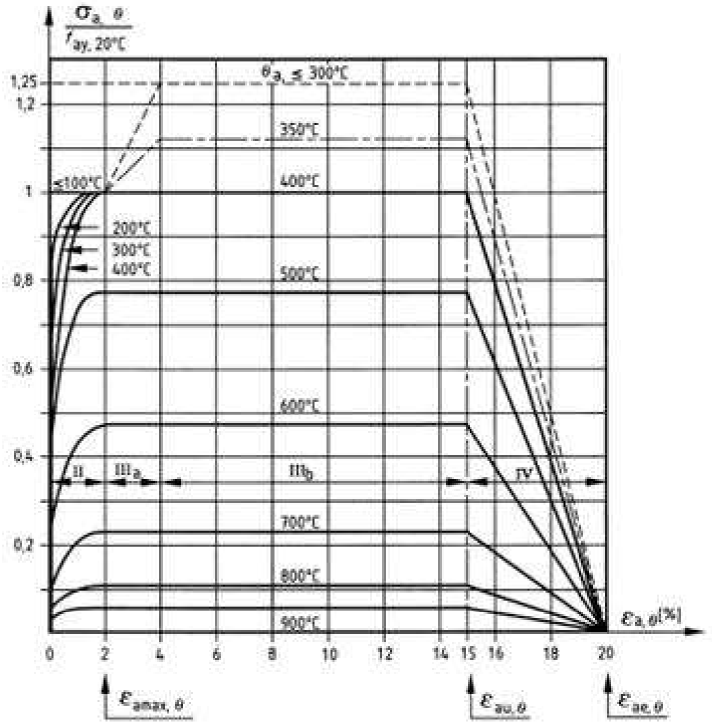

Figure 3.6: stress-strain behaviour of structural steel at ambient and elevated temperatures [2]

is normally taken to be 0.3.

Although the coefficient of thermal expansion varies with temperature [37], figure 3.7, it is commonly assumed to have a nominal value of $\alpha = 1.2x10-5$.

3.6.2 Concrete at Elevated Temperatures

The reduction in the compressive strength of concrete at elevated temperatures is shown in figure 3.8. Peak compressive strain increases with increasing

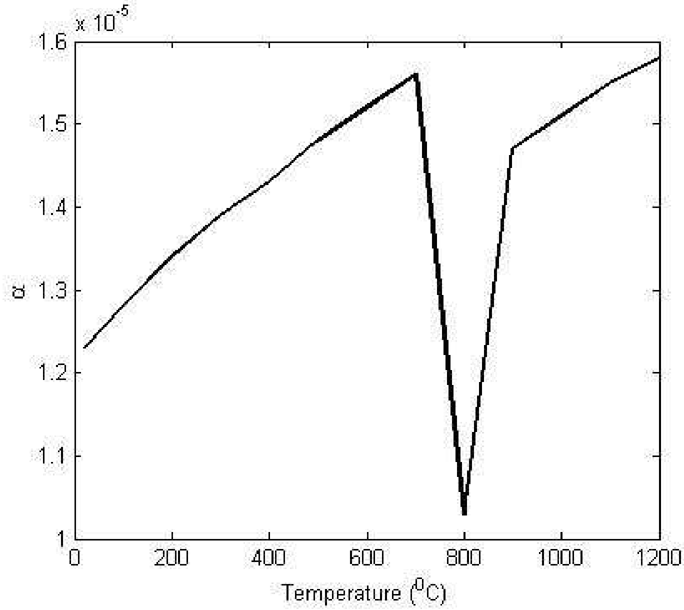

Figure 3.7: coefficient of thermal expansion variation with temperature

temperature, although peak compressive stress decreases. Figure 3.9 shows the reduction factors for peak tensile strength of concrete at elevated temperatures. Compressive strength of concrete is normally assumed to be negligible in design, and where it is considered it is usually taken as around 10% of the peak compressive strength.

3.7 Summary

Structural fire engineering has benefited in recent years from a growing understanding of the fundamental mechanics which control the behaviour of structures in fire. While the design and analysis of structures at ambient temperatures has had the benefit of many years of research and a fundamental analytical understanding of the behaviour of structures, an appreciation

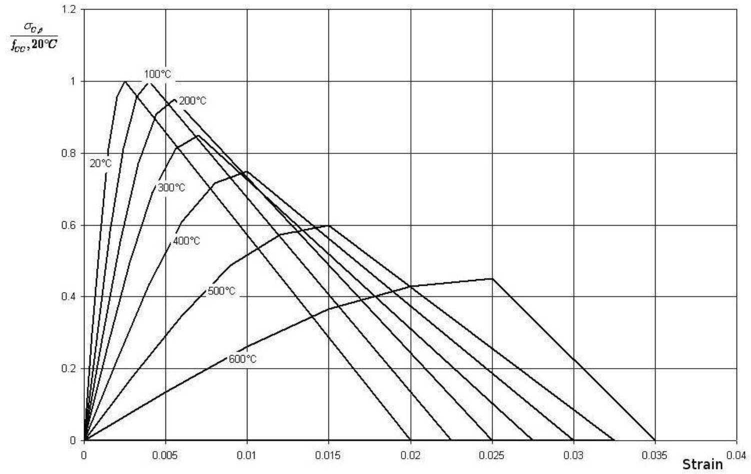

Figure 3.8: reduction factors of compressive strength of concrete at elevated temperatures

of the principles of structures in fire has only relatively recently been available for structures in fire.

Theories and mechanisms identified and developed through the numerical analysis of the response of real structures to deliberate or accidental fires has allowed for the validation of simple analytical theories which accurately describe and predict the behaviour of structural systems to elevated temperatures.

Although temperature dependant material properties are of importance when analysing the response of real frames in fire, these methods have departed from the traditional emphasis on the effect of temperature on structural stiffness and strength. They therefore allow for a more rational and proportionate response to the problem of structural design for fire attack.

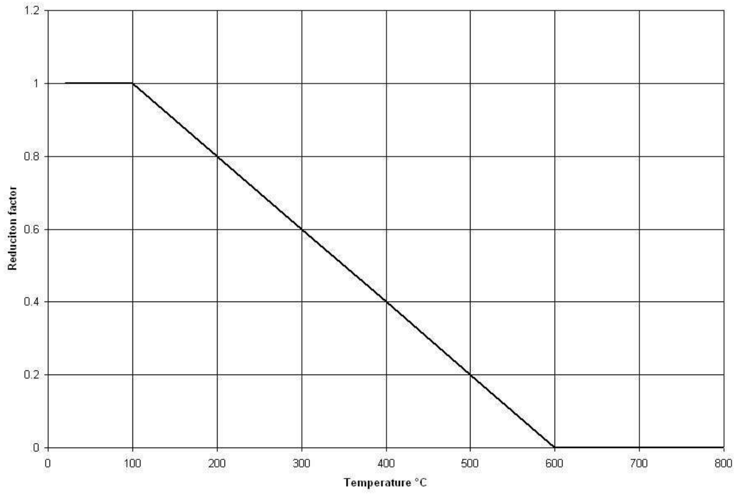

Figure 3.9: reduction factors of tensile strength of concrete at elevated temperatures

4

Performance Based Design

4.1 Introduction

Performance based design is an alternative to prescriptive code based design which has developed over the last few years in a number of engineering disciplines. It changes the goal of design from that of attaining a 'deemed to satisfy' solution to a solution which can be shown to meet performance goals as set out at the beginning of a project. The performance goals are the statement of intent of the design. They can meet any number of criteria: financial; life safety; environmental; structural stability or integrity; cost to repair or recover or any combination of these goals. They are specified in standard cases by authorities having jurisdiction and are normally disposed to the assurance of life safety and reducing environmental contamination as opposed to other goals. However, for low probability/extreme consequence events such as earthquakes or fires, there is a great deal of scope for both improvement of safety and cost saving. This can be achieved by adopting an approach to the design of the building which not only considers the life safety and environmental consequences of the event but also other factors which may be of interest to the project owners such as the cost to repair or replace in the event of a fire.

While prescriptive codes describe how a structure should be designed to meet performance goals which are hidden in the design codes, performance based codes should allow for a specification of the performance goal and should allow for any solution to be composed which can be demonstrated to meet these goals. The performance goals specified depend upon the type of design being carried out: severe weather; earthquake; fire. In fire safety engineering, prescriptive codes specify how to achieve minimum levels of fire resistance times for structures, performance based codes should detail how levels of performance should be calculated and allow sufficient scope for the Engineer to design a solution which achieves the desired performance.

Prescriptive codes rely upon a similar philosophy to traditional fire testing techniques: elements are protected from thermal effects to prevent a loss of strength and stiffness by ensuring an appropriate level of insulation from temperature increases. A fully performance based code would allow the user to define the required performance goal for a structural element in situ in the structure, with the appropriate static, dynamic and fire loading. For a complete building system, however, it may also look at methods of fire suppression, containment, and methods of reducing the impact of a fire attack.

4.2 History of Performance Based Design

Performance based codes for building design first began appearing in the USA in the 1970's [39], and their proliferation across most of the building regulations in place worldwide has been steady. Notably in Europe, where the Conseil International de Batiment (CIB) issuing a report in 1982 in which prescriptive codes were found to be restrictive and inefficient. The report detailed performance requirements and how they can be gleaned from prescriptive codes and also gave some sample solutions of how these performance goals could be applied . The current Eurocodes, developed by the CIB, all accept a performance based solution as opposed to the 'deemed to satisfy' prescriptive solution.

4.3 Fundamentals of Performance Based Design

Performance based design is based upon three main criteria [40]:

- Definition of the objectives of the design process

- Investigation of the alternative designs available to meet the objectives
- Reliability and risk assessment of alternatives to select the most efficient solution

The basic elements of a performance based design framework are defined in such a way as to allow the user freedom to compose any solution to the problem, allowing also the freedom to employ new techniques and technology as they become available. The objectives must be clearly stated at the outset of the project, and any design solution which fulfils these objectives whilst still adhering to the performance targets of the design framework should be permitted. It should be noted that although the targets in terms of life, property and business protection may remain similar to those prescribed in prescriptive design codes, these targets should remain independent of the prescriptive building code performance goals.

There are many justifications for the use of performance based design codes as opposed to prescriptive design codes. Although prescriptive codes are still in use in many countries it is generally accepted that these are flawed in many ways [39].

Prescriptive codes are based upon previous experience: safety and design criteria were prescribed individually and independently of each other. However, this is rarely the most cost effective and resource efficient method of design, since the inefficiency of prescriptive techniques tends to lead to an overlapping of fire safety measures. The use of performance based codes allows for the use of advances in both fire science and engineering to facilitate an optimum design, one which meets not only the code safety objectives but also the needs of the designer and of the user.

While the prescriptive codes are simple and easy to work with, Performance based design allows the engineer a degree of flexibility in selecting a method for design so that a structure resists both a fire load as well as a static design load. It is possible for the engineer to innovate, and use the behaviour of materials and structural arrangements to their advantage, possibly reducing cost, and with the ultimate goal of optimising the final design. Ultimately, a performance based approach increases the range of solutions which are open to the design engineer over a prescriptive approach, figure 4.1 [3].

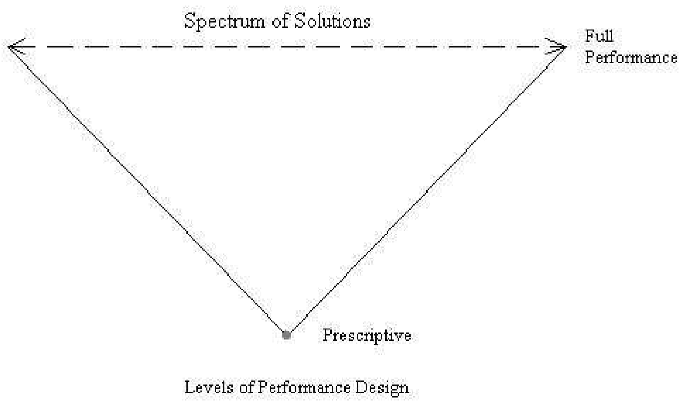

Figure 4.1: Expanding spectrum of solutions [3]

4.4 Performance Based Design Frameworks

Traditional design techniques approach the design of structures for accidental and severe loading in a very linear manner, approaching the problem by defining the loading and then applying this loading to the structure. This is particularly well illustrated for earthquake engineering in many instances , for example Irfanoglu [41] presents a comprehensive framework for performance based earthquake design which uses utility functions to assess performance under multiple objectives.

The application of the concepts of performance based design to fire engineering has also been attempted, in particular by Hamilton et al. [4], where the authors propose a Performance Based Fire Engineering Methodology which follows the linear process of Fire Hazard Analysis, Structural Analysis, Damage Assessment and finally loss and risk assessment. This methodology is an exact mapping of a performance based structural engineering methodology for earthquake design developed at the John A. Blume Pacific Earthquake Engineering Research (PEER) Centre, figure 4.2, with Seismic Hazard Analysis replaced by Fire Hazard Analysis. This same linear methodology can

PROCESS	VARIABLE	DISCIPLINE	PARAMETERS	EXAMPLES
Seismic Hazard Analysis	IM	seismology & geotechnical engineering	fault location type and length of rupture (magnitude of event) site/soil conditions	• $S_a(T_1)$ • PGA, PGV • Aires intensity • …
Structural Analysis	IM→EDP	structural & geotechnical engineering	foundation and structural system dynamic mass & damping …	• story drift • floor accelerations • component forces & deformations • …
Damage Assessment	EDP→DM	structural, mech. & elec. engrg.; construction; architecture; loss modeling	deformation sensitive component fragilities (walls, beams, columns) acceleration sensitive component fragilities (equipment, contents)	• component strength/deformation limits • damage (repair) states • hazards (falling, blocked egress, chemical release, etc.) • collapse
Loss & Risk Analysis	DM→DV	construction & cost estimating; loss modeling	occupancy time of earthquake post-eq recovery resources	• fatalities • direct $ losses • repair time/downtime

Figure 4.2: PEER earthquake engineering performance based design methodology [4]

be utilised for the performance based design of almost any system under any form of extreme extrinsic loading. However while the acceleration and location of earthquakes is independent of the structure which is being designed; fire loading is inherently intrinsic and varies with the structure in question and with the features of the building. The 'worst case' fire varies from component to component and from performance goal to performance goal.

Barry [5] describes a complete performance based design framework which flows the steps of Appraisal, Analysis, Performance and Assessment, figure 4.3. A complete set of design fires and fire scenarios is developed and the performance of a system is assessed. Although this methodology focuses on industrial risk assessment rather than structural design, a number of the concepts in the work are relevant and can be applied to structures in fire. Of

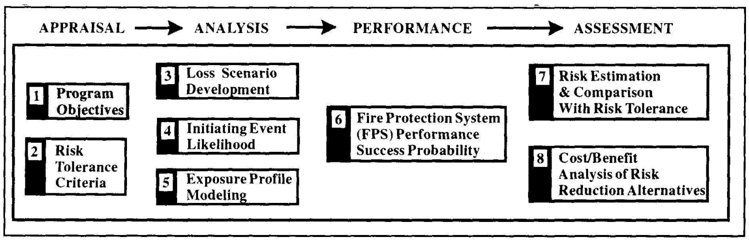

Figure 4.3: Performance system model [5]

particular relevance is the development of a number of possible fire scenarios for a component or system and the assessment of building performance as a result of these events and based upon the likelihood of the initiating event. Although this is onerous in terms of the amount of calculation required for design and assessment, this is one of the only solutions which allows for anything other than an ad-hoc design methodology which is based upon a single design fire.

In Barry's book, the actual event probability for risk assessment is estimated using an event tree. This process is used to achieve a ranking of high risk components of the system for mitigation in the framework.

4.5 Performance Goals

Moving from performance based codes to prescriptive codes has led to a requirement for the explicit statement of performance goals and requirements of the system. While the methodologies employed to both quantify and assess system performance are left open where performance based design is allowed, the acceptable levels of performance for buildings has to be classified and prescribed externally. A common approach to the allowance of performance based design in building codes is the use of a hierarchical system for the overall design of buildings which allows for both a performance based and a prescriptive based approach [6, 42], figure 4.4. In this approach, the functional requirements are consistent for both prescriptive and performance based codes, and whether a 'deemed to satisfy' solution is implemented or a fully performance based solution is engineered depends upon the decisions made earlier in the project, while the performance requirements and the acceptable methods are being determined or stated. This approach in turn has led to a necessity for the classification of buildings for extreme events where the performance requirements are stated based on the type of building and its utilisation.

Mowrer [6] proposes a fire performance matrix, table 4.1, which is based upon the performance groups defined in the ASCE 7 standard:

- Group 1 - this group includes buildings which are normally unoccupied, such as agricultural buildings and sheds. Significant loss of life is

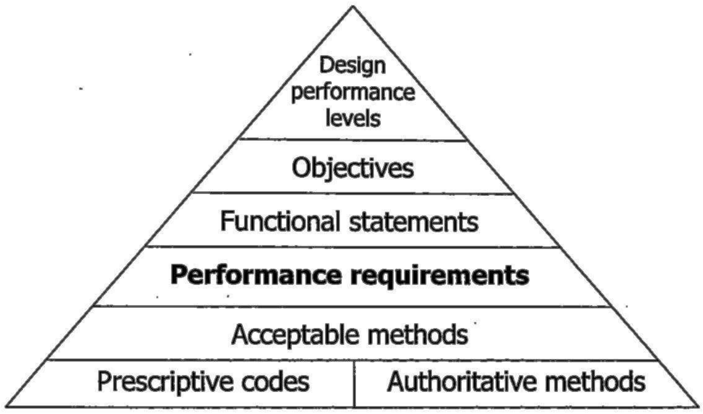

Figure 4.4: Hierarchical approach to performance-based design [6]

unlikely given occurrence of a fire in these buildings.

- Group 2 - this group includes most other buildings, such as residential, retail and commercial structures. Occupants are not restricted in their mobility.
- Group 3 - this group includes buildings which are occupied by large groups of people, services or by people with reduced mobility. Loss of life is likely given an extreme event.
- Group 4 - these buildings are deemed high consequence buildings. They are essential for public welfare and include hospitals, police stations and fire stations.

In the performance matrix, performance levels are defined for structural applications as:

- Mild - No damage
- Moderate - Moderate, repairable

	Performance Groups			
Performance Level	I	II	III	IV
Severe	Infrequent	Rare	Very Rare	Extremely Rare
High	Frequent	Infrequent	Rare	Very Rare
Moderate	Very Frequent	Frequent	Infrequent	Rare
Mild	Very Frequent	Very Frequent	Frequent	Infrequent

Table 4.1: fire performance matrix [6]

- High - Significant, repairable
- Severe - Substantial, irreparable

These performance goals are, fundamentally, qualitative and their specific application to design is only valid in a general sense.

Beller [42] addresses the suitability of qualitative and quantitative statements of goals in performance based design codes. Since performance based codes are meant to provide a link or a dialogue of the process which society expects a building to perform to and the design which is meant to meet these objectives. Therefore both qualitative and quantitative statement of goals is necessary, although at different stages in the process of design. Qualitative statements reflect the expectations which society and the profession places upon a structure, whereas quantitative goals reflect the suitability of the final design to meet these goals.

A method for determining reliability acceptance criteria for exceptional structures is detailed in [43]. Although this details consequences of extreme events in terms of life, economy, cultural assets and the environment as opposed to structural consequences.

Figure 4.5 [7] illustrates schematically building performance goals in fire in terms of evacuation and structural integrity. Performance goals over the course of fire growth are prescribed for the room of origin; the floor of origin; and the entire building in terms of tenability limits of the compartments and the integrity of the structure in fire. Design codes allow for the reduction in design loading given extreme events [44]. During a fire attack on a building the design loading may vary with the time of exposure. Early on in a fire, the design static loading will be very similar to ambient static loading, with this value reducing as fire progresses until the structure is required to sustain only its own self weight. The characteristic design load is therefore a function of time. This method of determining performance goal takes account of a number of different performance criteria of importance to fire safety engineering, and the specification of tenability limits as a function of evacuation times is of use to fire safety engineers. The specification of the goal of structural integrity seems to be a reasonable goal since no fire will burn indefinitely. The loss of structural integrity shown in figure 4.5 should therefore not be allowed to occur.

4.6 Summary

Performance based design is a concept which offers designers the ability to specify their own criteria for acceptance of a solution. They are effectively

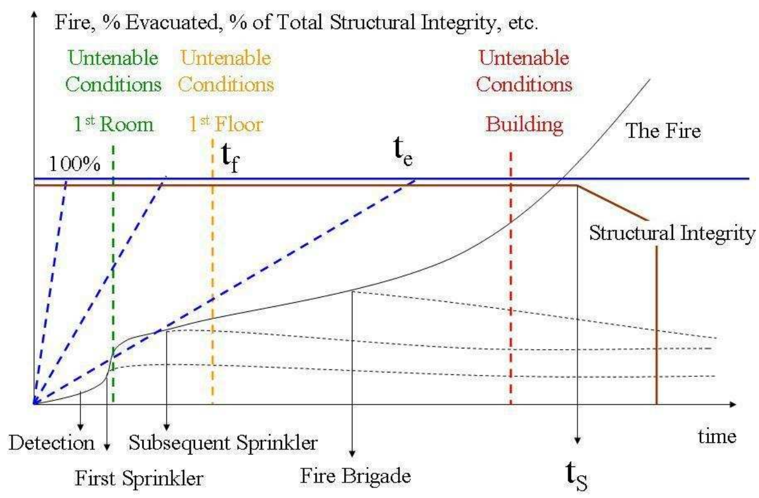

Figure 4.5: performance timeline of building response [7]

open design codes and allow any method of specifying a solution to the problem so long as it meets the expectations which are placed upon it.

Since performance goals are descriptive rather then qualitative they reflect a commissioning bodies willingness to accept a certain amount of risk in commissioning a solution. Because of this they are particularly suited to low probability high consequence events such as earthquake, extreme weather or fire.

5

Risk and Reliability

5.1 Risk Assessment

The concept of risk is a very subjective one. What constitutes a high risk to one person may be deemed to be a low risk to another, depending upon their perspective. While risk is determined by the product of the probability and the consequence of an event, equation(1.1), as a meaningful measure for design unless it is based upon reliable statistical data it is limited by the fact that any risk acceptance decision is a value judgement dependant upon the risk analysis done in the first place and upon the experience and opinion of the engineer doing the analysis.

$$Risk = Probability \ \times \ Consequence \tag{5.1}$$

As discussed in the previous chapter, as a value judgement, risk represents the goals which society expects a structure or building to achieve. A comprehensive risk assessment will enable the identification and ranking of high risk areas for more detailed design.

5.2 Risk Based Design Goal

The consideration of fire as a load in every part of a building is an onerous task and in many cases it is not practical due to time or financial constraints. especially for such a low probability event.

The potential for a serious fire event occurring in different areas of a building is largely dependant upon the use and occupancy of those areas. Similarly, the potential consequences in terms of structural stability or integrity are largely dependant upon the design. However, by assessing both the likelihood and the consequences of a fire event in an area regions of higher risk can be identified for more detailed design.

The purpose of this identification as part of a design framework will be to rank compartments in terms of overall risk and to demonstrate by other means that components conform to any predetermined design goals. These high risk regions should be individually checked for acceptance until a suitably low risk is found for the entire building. A suitable risk based framework for structural design should describe methodologies to identify these higher risk areas and their systematic targeting according to some risk or hazard ranking in order to reduce the overall risk to the structure.

5.3 Acceptable Risk

The lower level of acceptable risk will depend upon a number of factors, including but not limited to: the building owners, the authority having jurisdiction, the insurers, and the building occupants. It will also depend upon the proposed use of the building: some occupancies have naturally higher risk associated with them either as a result of processes being carried out within the building, for manufacturing or other facilities, or as a result of arson or terrorist attacks on, for example, schools or on high profile public buildings.

This concept of acceptable risk is recognised, although not explicitly, in a number of current design codes where life safety objectives are altered depending upon the occupancy.

5.4 Fire Probability

Much of the previous work on risk based fire safety design has tended to employ annual return periods of fires of given severities, similar to the way in which earthquake probability is defined. Lin [45] uses a Poisson process to model the probability of fires based upon numbers of annual fire occurrences and floor area. This is similar in approach to work by Ramachandran [46], where the risk from a fire is defined as the product of the probability of fire occurrence and the floor area damaged. While potentially viable as statistical measures of fire loss, these methods are generally unsuitable for structural design since fire is often man made, not a natural phenomenon, and probabilities derived from fire statistics do not reflect the poor informativeness of the relatively small sample group of fire ignition.

Some local bodies or groups maintain their own records and statistics of fire occurences and these are subject to analysis and interpretation, however these analyses range from the very informative [47] and useful for developing a range of scenarios, including estimates of fire growth rate and fuel load by occupancy type, to the descriptive [48]. Any rational attempt to design based on these analyses will be only applicable for the region or country from which the statistics are collected and will not be a general application of the concepts. Of use, however, may be some sort of a map which collects fire statistics and from which social factors can also be incorporated into the design information.

The following corollaries are therefore proposed for the design of buildings for fire:

1. For Structural design, a building has to be designed under the assumption that a meaningful fire will occur, i.e. P(fire occurring)=1.

2. The quantification of the probability of a particular fire event occurring

in a building cannot be simply described as a probability over a return period. This is at odds with existing frameworks for exceptional and accidental loading and suggests that other design frameworks cannot simply have their wording changed to address fire loading.

3. It is unscientific to use historical data to derive statistics for use within a design process and draw probability distributions of fire duration or temperatures for use in a risk assessment.

4. The perceived risk should be associated with real and possible fires in the building being designed and the subjective consequence of these fires on the structure. This data should be based upon information about the individual construction project and its proposed usage.

The second, third and fourth points above are addressed in work by Hostikka and Keski-Rahkonnen [49], where the probability of the fire and the associated consequences are directly related to assumed probability distributions of the variables associated with the fire model and system being designed. Although this work was not focussed on the risk as a result of fire, it did model the probabilities of a number of fire events occurring as a product of a number of assumed distributions of input variables for the model which was considered the most likely outcome of an event.

5.5 Risk Matrix

A risk matrix is a simple graphical tool for assessing risk. It correlates the likelihood of an event with its severity to provide a simple visual assessment of the risk associated with the occurrence of the event. NFPA 551 [8] provides a simple example of this concept, figure 5.1. In the example, the

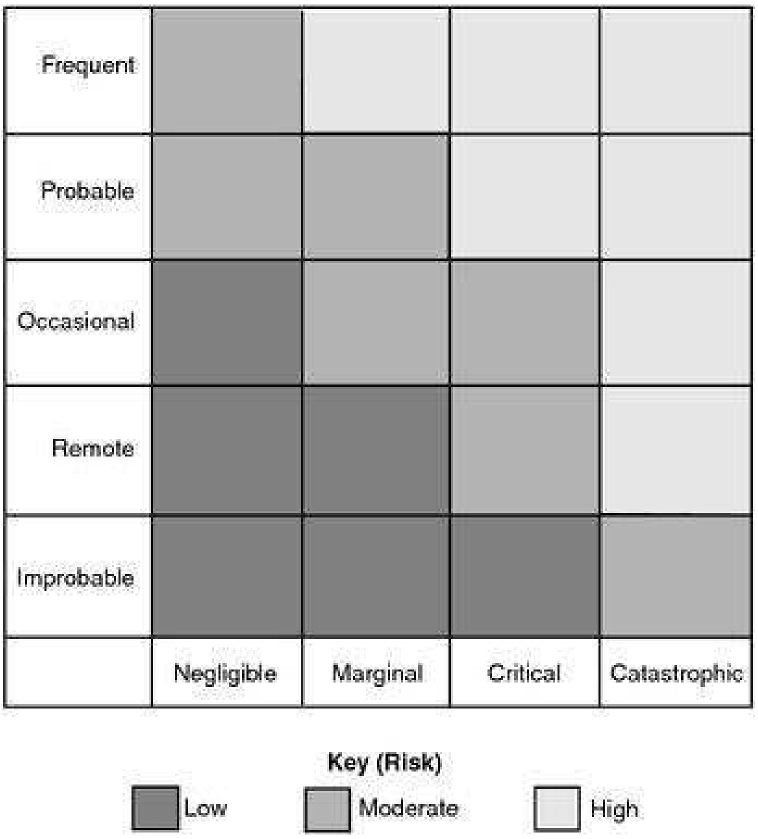

Figure 5.1: NFPA risk matrix [8]

consequences are listed along the horizontal axis and the probabilities are listed along the vertical axis. High consequence - high probability events have higher risk than low probability - low consequence events. All combinations of the intermediate categories have some intermediate level of risk associated with them. In this example there are three risk classifications which are distributed between the different combinations.

This is a common management tool for assessing risks and is used widely in one form or another throughout the construction industry.

5.6 Reliability

The current Eurocodes present a design framework which is based upon the First Order Reliability Method, or FORM. The targets of the Eurocodes are based upon indices of Safety or Reliability. The reliability of a system (or component) is a measure of the probability that the load on the system will be less than the systems resistance. This concept is the basis for the partial safety factors which are prevalent throughout design codes worldwide, and it therefore seems only natural to apply it to structural fire safety design.

5.6.1 Reliability Theory

The standard stress-strength model is shown in figure 5.2. The load on the system is represented by normally distributed random variable Q, and the resistance of the system is represented by normally distributed random variable R. The probability of failure of the system is the probability that the resistance will be less than the load, equation 5.2.

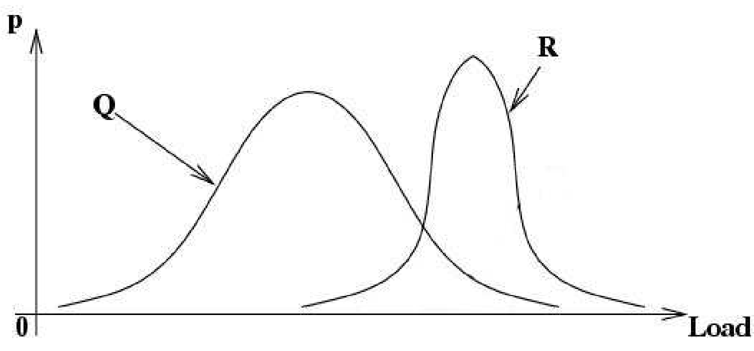

Figure 5.2: The standard stress-strength model

$$P_f = P(R < Q) \tag{5.2}$$

For some characteristic value, $Q*$, of Q, this is:

$$P_f = P(R < Q^*) = \int_{Q^*}^{\infty} R \; dLoad \tag{5.3}$$

In cases where Q is also unknown:

$$P_f = P(R < Q) = \int_{-\infty}^{\infty} \int_{Q}^{\infty} RQ \; d^2Load \tag{5.4}$$

The reliability of a system, S_R, is the probability that the strength is greater than the stress on the system, i.e. $S_R = P(Q < R)$ [50].

$$S_R = P(Q < R^*) = \int_{-\infty}^{R^*} Q \; dLoad \tag{5.5}$$

$$S_R = P(Q < R) = \int_{-\infty}^{\infty} \int_{-\infty}^{R} QR \; d^2Load \tag{5.6}$$

The conventional factor of safety of a system is the ratio of the resistance to the load applied [51].

$$FS = \frac{R^*}{Q^*} \tag{5.7}$$

Factors of safety are prescribed such that probabilistically the resistance of a system will be such that the system will be able to withstand a design load. For serviceability limit states these factors are applied to the loads, whereas for ultimate states the factors are applied to the system.

The margin of safety is the margin between the load and the resistance of the system. For characteristic values of these, figure 5.3, this is given be equation 5.8.

$$M = R^* - Q^* \tag{5.8}$$

For normally distributed values of Q and R, the margin of safety is also

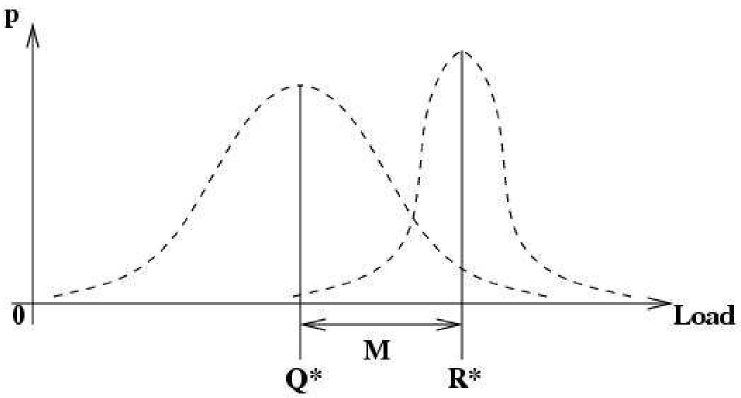

Figure 5.3: the margin of safety

normally distributed [40], and has mean and variance dependant upon the mean and variance of Q and R.

$$\mu_M = \mu_R \ - \ \mu_Q \tag{5.9}$$

$$var(M) = \sigma_M^2 = \sigma_R^2 \ + \ \sigma_Q^2 \tag{5.10}$$

The reliability factor, β, is the number of standard deviations of the margin of safety between its mean and 0, figure 5.4.

$$\beta = \frac{\mu_M}{\sigma_M} \tag{5.11}$$

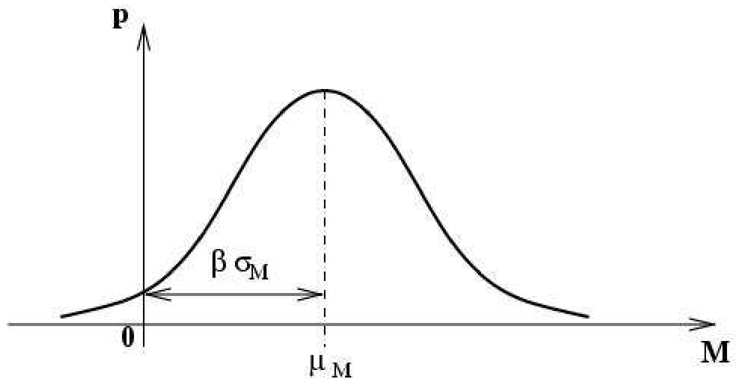

Figure 5.4: the reliability factor

5.7 Reliability of Structures in Fire

A number of sources suggest that the concept of reliability should be applied to structures in fire. The SFPE handbook describes the concept of reliability as a tool for measuring the failure rate of a system [52], and also for estimating physical responses of material and components in fire [53]. Alternative sources describe the concepts of reliability within the derivation of a performance based framework for structural design [40, 50], although there is little or no illustration or discussion of the proposed application.

The relationship between the reliability of a component or a series of components and the features of the building in which it is contained is not one that is normally addressed as part of a reliability calculation. However, it is known that the details of a compartment control the potential thermal load within and on a building and this interaction is of primary importance in the determination of structural reliability in fire. It must therefore be included as a factor in the acceptance or otherwise of a design.

Given a protected component, such as an encased column; or a component which is not exposed to any increase in temperature; the 'thermal loading' of surrounding components will manifest itself through additional thermo-mechanical loads which need to be considered in addition to the dead and live loading of the structure. For unprotected components or components which adopt an alternative, thermally enhanced or controlled, mechanism for carrying the static load 'thermal loading' in terms of the temperature increase of the component needs to be considered when selecting the active mechanism, this is in addition to the thermo-mechanical loading which needs to be considered and the 'standard' dead and live 'static' loading.

While the current design codes do allow for a reduction in static loading when a fire occurs, the load which a structure must be designed to resist does not vary with the magnitude of the fire, and it is still generally a prescribed one. Additional loads will, nevertheless, manifest themselves as a result of the structures adoption of alternative mechanisms. Without restating the static load imposed upon a structure, a framework for structural fire safety design which includes an assessment of reliability can be developed and which is in line with existing design methodologies for static and dynamic loading.

5.7.1 Thermal Load Variation

As discussed in previous chapters, the list of variables which affect the development and spread of a fire in a compartment is potentially endless, and the more complicated the model used, the more variables which need to be defined. From the robust nominal standard fire curve; where the duration of the fire has to be declared, to the finest celled field model; where the equations for mass, energy and momentum have to be solved in every field, add to that energy loss through the boundaries and radiative heat transfer and the number of variables can become unmanageable. A balance has to be struck between reasonable certainty in the model, appropriateness of the model for the purpose it is required, and complexity of the model.

The variables which affect the temperature in a compartment fire can broadly be separated into two groups: constant and non-constant variables. The constant variables are those which are not changing on a day to day basis; e.g. variables such as construction material properties, compartment geometry, compartment boundary construction, and occupancy. Although these variables have some random distribution, they are generally specified in the design process at ambient temperatures by nominal values. It should be noted that suitable research into the variation of material properties at elevated temperatures has not been carried out, and the only values which can be relied upon are the variation of the materials at ambient temperatures. Those variables which are non-constant are those which can change throughout not just the life of the building but from day to day use of the building; e.g. fuel load, fuel distribution (compartment configuration), and ventilation conditions. These indeterminate variables are those which cannot be foreseen during the design process and only a range of values with indefinable probabilities can be determined.

According to Knight [54], there are three types of probability relevant to decision making:

1. "'a priori probability"', which applies where there is "'absolute homogeneous classification of instances, completely identical except for really indeterminate factors"';

2. "'statistical probability"', namely, "'empirical evaluation of the frequency of association between predicates"'; and

3. "'estimates"', which "'must be radically distinguished from probability or chance of either type"'

Evidently, "a priori" probability and "statistical" probability are ill suited to the study of fire since there is neither homogeneity between events nor a large enough number of samples for there to be a reasonable informativeness in the frequencies obtained. From the points listed, it is clear that the probability of a fire falls into the third classification of probability as defined by Knight: estimates. It is proposed to use estimates of the variables which affect compartment temperature in determining reliability in fire. In designing a sample set of fires using assumed probabilities of the input variables for the fire model, no dependency upon the probability of a fire occurring is required, this is accounted for in the risk assessment stage of the design process by assessing the relative likelihood of occurrence of a fire in each location. This proposed estimation of a sample set of fires satisfies the 2nd 3rd and 4th corollaries listed above, and allows the design to be based upon a range of possible real fires in a building.

5.7.2 Reliability Calculation

The loading and the resistance of any component in fire is a complex product of a number of variables, and the determination of the actual reliability can only be achieved by integrating the load and resistance function where necessary of the mechanism being designed for over the entire sample space of variables.

5.7.2.1 Performance Function

Describing the complex system, Z, of load and resistance using the performance function of the variables which describe the system, X [55]:

$$Z = Z(X_1, X_2, ..., X_n) = Resistance \ - \ Load \tag{5.12}$$

Each of these variables has some distribution either random or deterministic, and the reliability of the system is given by:

$$S_R = 1 - P_f = 1 - \int ... \int f_{x_1,x_2,...,x_n}(x_1, x_2, ..., x_n) dx_1 dx_2, ..., dx_n \tag{5.13}$$

The use of the performance function must consider the effects of fire at each stage of the design process. At the initial statement of the problem the active mechanism should be considered, whether it is a thermally enhanced one, or changing with the exposure. The actual analysis of the structure should consider all loads; dead loads, live loads and any additional thermo-mechanical loads:

$$Q = f\left(\begin{array}{c} Dead\ Loads \\ \\ Live\ Loads \\ \\ Thermo - mechanical\ Loads \end{array}\right)$$

The actual integration of the performance function and the determination of the reliability of a structure, system or component is an onerous one which becomes more and more complicated with increasing complexity of both the structural model and the model which is used to describe the fire. Since the number of variables becomes increasingly difficult to manage, alternative methods for the integration of the performance function are required. There are two common methods for doing this [55]: Taylor series expansion and Monte Carlo analysis.

5.7.2.2 Monte Carlo Analysis

Monte Carlo analysis is a random sampling technique which draws on a library of variables and their distributions to generate N random events. As with statistical probability, the informativeness of the resulting distribution increases with the number of events, N.

$$S_R = 1 - \frac{N_f}{N} \tag{5.14}$$

5.8 Reliability Goals

For any given system, of resistance R, subjected to a load, Q, the reliability of the system will vary with the degree of exposure, figure 5.5. The goal of design must be to improve the resistance of the system so that the performance goal in terms of reliability of the project is met for all reasonable exposure values, as set out at the beginning of the project. The reliability goal of the system can be reduced in accordance with the increased 'tolerable' risk to the structure with increased exposure. Figure 5.6 shows the expected

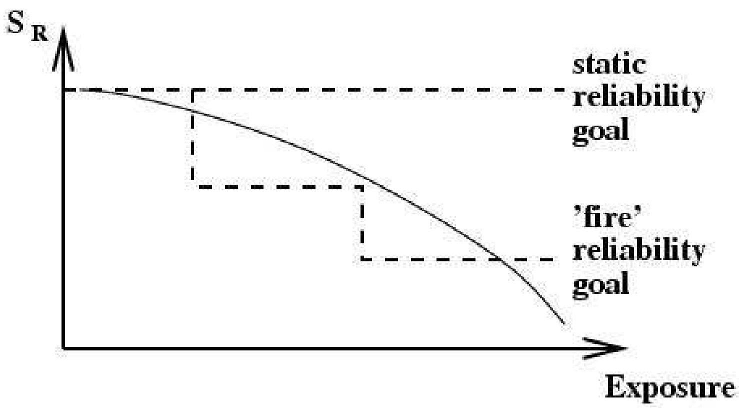

Figure 5.5: variation with exposure of the reliability and reliability goal

evolution of the stress-strength model over the duration of exposure to a fire, including a stepped reduction in the load on the structure as well as a gradual change in the resistance of the system. At ambient, the stress-strength model is as described above, with Q_a and R_a the static design values for strength and resistance. Allowing for the reduction in design loading, the required load resistance (strength) of the structure, $R(T, t)$ is reduced over the time to evacuation while the actual structural resistance (stress), changes with increased duration of exposure to fire. Since the fire will never be known at the outset of the project, the performance goals of the building have to be set irrespective of the fire itself, hence the stress, $Q(t)$ does not vary with the actual fire but rather the duration of exposure. Following some exceptional and prolonged level of exposure it should be expected that the system will no longer be able to sustain its own self weight and collapse of the structure will ensue. Diamantidis [56] lists the Eurocode [11] classification system based

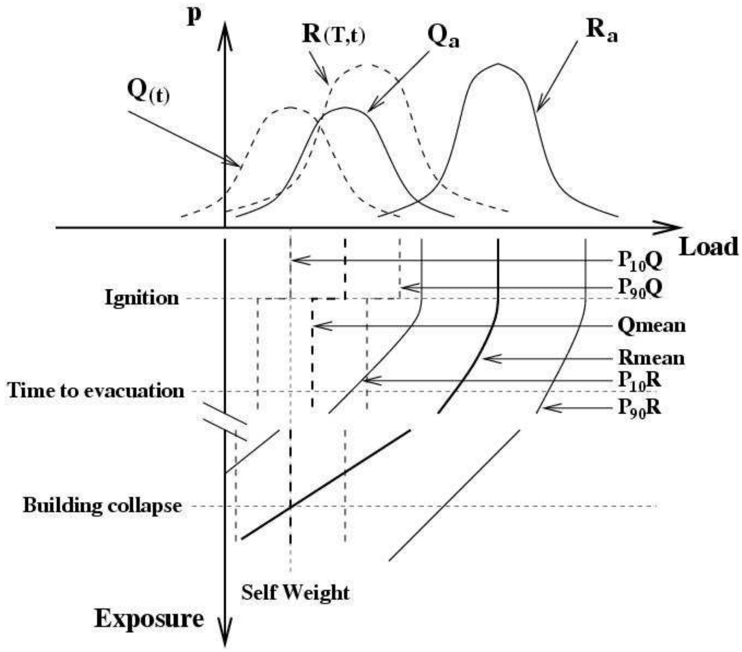

Figure 5.6: reliability variation with exposure

upon consequences of failure, although he defines the ratio of expected loss, ρ, between total costs including; initial construction costs and losses due to failure; and construction costs. Target reliability indices and probabilities of failure for these classes are then defined, table 5.1.

Class 1 - Minor consequences: Risk to life, given a failure, is small to negligible and economic consequences are small or negligible - ρ is less than 2

1	2	3	4
Relative cost of safety measure	Minor consequences of failure	Moderate consequences of failure	Large consequences of failure
Large	$\beta = 3.1$ ($P_f \approx 10^{-3}$)	$\beta = 3.3$ ($P_f \approx 5 \times 10^{-4}$)	$\beta = 3.7$ ($P_f \approx 10^{-4}$)
Normal	$\beta = 3.7$ ($P_f \approx 10^{-4}$)	$\beta = 4.2$ ($P_f \approx 10^{-5}$)	$\beta = 4.4$ ($P_f \approx 5 \times 10^{-6}$)
Small	$\beta = 4.2$ ($P_f \approx 10^{-5}$)	$\beta = 4.4$ ($P_f \approx 5 \times 10^{-5}$)	$\beta = 4.7$ ($P_f \approx 10^{-6}$)

Table 5.1: reliability index targets [11]

Class 2 - Moderate consequences: Risk to life, given a failure, is medium or economic consequences are considerable - ρ is between 2 and 5

Class 3 - Major consequences: Risk to life, given a failure, is high or economic consequences are significant - ρ is between 5 and 10

Using an order of magnitude approach, the probability of failure of the performance goals is related to the allowable frequency of occurrence of the event. The probability of failure can be mapped to the reliability index [51], and reliability targets set for structures exposed to fire based upon the performance group classification described in the previous chapter and the performance level required, table 5.2.

Relative frequency	Conditional $P(R > Q)$	β
Very frequent	$> 10^{-1}$	
Frequent	10^{-1}	1.29
Infrequent	10^{-2}	2.33
Rare	10^{-3}	3.1
Very Rare	10^{-4}	3.72
Extremely Rare	10^{-5}	4.25

Table 5.2: reliability index according to frequency

5.9 Risk Informed Framework for Structural Fire Design

As previously described, the goals of a risk assessment is to satisfy the qualitative expectations which are placed upon a structure whereas the goal in carrying out a reliability assessment of a structure is to demonstrate suitability of the solution for the purpose for which it is intended. However, because of the extremely low probability of fire and the indeterminacy of the fire loading, the calculation of the reliability of every component of a structure is uneconomical, especially where other circumstances may exist such as low fuel loads as a result of the proposed occupancy.

It is therefore proposed to employ a 2 stage design process for structures in fire. The first stage of the design process is a risk assessment of all of the components, based upon the relative probability of a fire occurring in each area of a building. The second stage is to rank each component according to this risk and to systematically determine the reliability of the components starting with the high risk components and descending through the ranked components until the reliability is suitably high or until the risk is deemed to be suitably low.

5.9.1 Risk Assessment

For the first stage of the design framework, the fire risk assessment, it is proposed to use a very simple system of risk indexing to determine high areas of risk. The benefits which arise from using this approach as opposed to more detailed risk analyses in terms of the resources required are illustrated in figure 5.7. Having discussed the poor informativeness of fire statistics and the lack of a necessity for absolute determination of risk for structural fire safety design when relative risk suffices to target areas for more detailed design risk indexing can be used to provide an informative estimate of the risk in a compartment. Since the risk assessment is used to determine areas of a structure for more detailed design consideration, the risk assessment should describe the risk which will result in a meaningful fire for structural design. Assuming that suitable air is available for materials to burn, the risk of a meaningful fire can be defined to be a product to the likelihood of there being an ignition source, the probability, and the amount of combustible materials, the consequences; or magnitude of the event.

The compartments within the structure should be grouped into a number of categories based upon these two factors and the risk should be determined using a risk matrix similar to the NFPA risk matrix shown in figure 5.1.

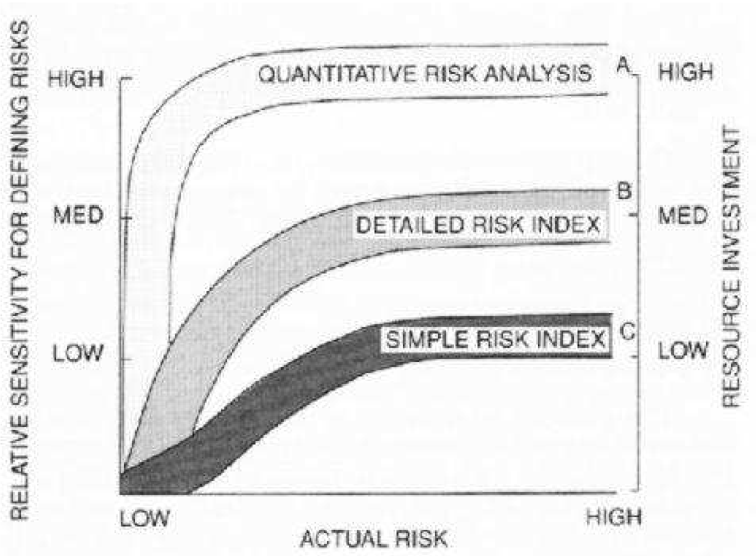

Figure 5.7: resource investment for increasing level of risk analysis [9]

For example, if compartments are divided into four groups of relative potential combustible loading (High, Medium, Low and Very Low) and the same compartments are divided into 4 groups of relative potential ignition (Very Likely, Likely, Unlikely and Very unlikely) one possible risk matrix is shown in figure 8.8. There are 4 levels of risk in the proposed matrix. The general form of the risk matrix is the same as the NFPA matrix, although the risks have been changed to reflect the fact that a very likely ignition source may include some forms of ignition where combustible materials are introduced to a fire compartment for example in the case of likely arson targets. Similarly occupancies where there is little or no risk of ignition represent generally a low risk.

The proposed risk assessment methodology can be broken down into the following stages:

		Relative potential ignition likelihood			
		Very Likely	Likely	Unlikely	Very Unlikely
Relative potential fuel load	Very High	IV	III	III	I
	High	IV	III	II	I
	Low	IV	II	I	I
	Very Low	IV	I	I	I

Figure 5.8: proposed risk matrix

1. Identification of the compartments
2. Relative potential fuel load ranking and grouping into the 4 indices proposed
3. Relative potential ignition ranking and grouping into the 4 indices proposed
4. Ranking of the components according to their relative risk

5.9.2 Reliability Assessment

The risk assessment and subsequent ranking of the components according to their relative risk reflects the qualitative aspects of the way that a building should perform in fire. Following the statement of the qualitative requirements of the building in fire, the buildings performance in scenarios which have a high expectation placed upon them should be demonstrated. Using the reliability methodologies as described earlier, this should be achieved by estimating the range of possible fires which can occur in a building and applying these fires to the structure. The reliability assessment methodology is as follows:

1. Declaration of reliability goals
2. Definition of fire scenarios
3. Assignment of components to compartments
4. Targeted reliability assessment

5.9.3 Complete Risk Based Framework

As part of a design framework for structures in fire, the two assessment methodologies should be applied successively to a proposed design and the design should be iterated until it meets some requirements. Using the performance criteria described in tables 5.1 and 5.2 the reliability of high risk components should be assessed against those of the Eurocode.

As an alternative to proposing some risk based acceptance criteria, the reliability assessment should be carried out systematically on the components, beginning with those which represent a high risk and should end when the reliability goal is met without any subsequent alteration.

The complete proposed design framework is shown in figure 5.9. The work-flow, however, for the framework should follow the steps listed above, in the order of risk assessment and then reliability assessment.

5.10 Summary

In this chapter, the fundamentals of risk and reliability were discussed as well as their application in fire safety design.

Reliability theory was summarised as well as the effect fire has on reliability and current Eurocode based reliability goals were given for structural design.

A risk informed framework for structural fire safety design of steel and composite structures was also proposed which draws on the concepts which are introduced in this chapter.

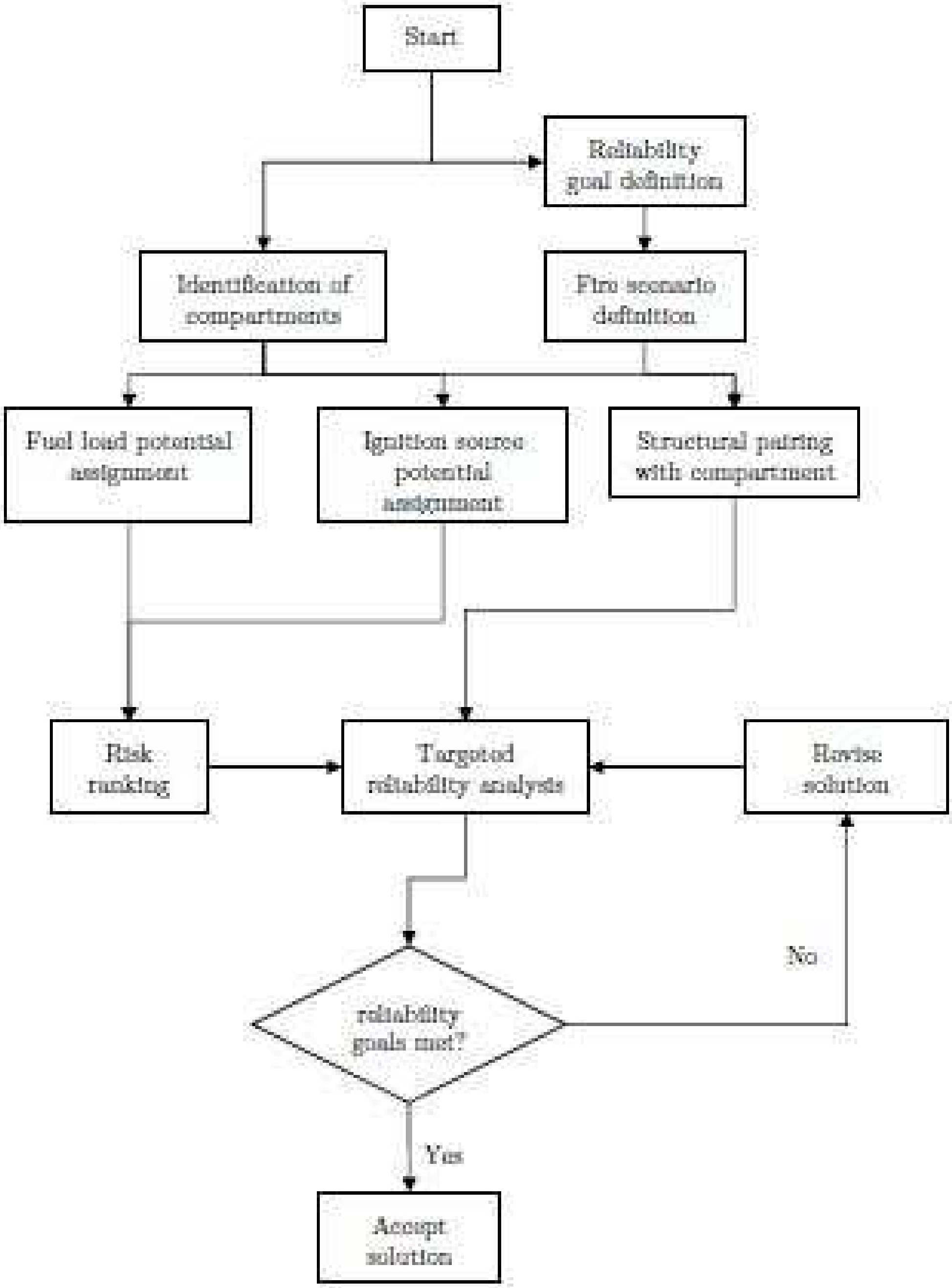

Figure 5.9: complete proposed framework

6

Floor Slab Behaviour and Design

6.1 Introduction

There have been a number of methods proposed for the determination of ultimate capacities of floor slabs in fire. For example, a compressive membrane action enhanced yield line analysis, as proposed by Bailey [57, 58], for composite floor slabs in fire; or an energy method proposed by Cameron and

Usmani [36, 59, 60], for assessing tensile membrane capacity in fire. Both of these methods deal with composite concrete floor systems subjected to large deflections in fire, although they are fundamentally different in their approaches.

Regardless of their differences, both methods provide a means of assessing the membrane capacity of composite floor slabs in fire. Both agree that the assumption that membrane capacity is the final load carrying capacity in fire depends upon the presence of large displacements. However, neither of the methods provide information for the lower limit of deflection at which it becomes of use to the designer. For example, slabs with low span/depth ratios are far less likely to experience large enough displacements to allow significant membrane action to develop than slabs with high span/depth ratios.

This chapter aims to explore the transition between the two mechanisms further.

6.2 Floor Slabs at Large Deflections

Flexural capacity in floor slabs either disappears entirely or is massively reduced at large displacements. These large displacements allow for the mobilisation of membrane action in floor slabs. Initial deflection and rotation of the slab about the supports induces an 'arching' effect or compressive membrane action - the slab pushes against the boundaries, and large compressive forces develop through the slab. Increasing deflection allows for the reduction of these compressive forces starting from the middle of the slab, and leading to areas of tension and cracking in the centre of the slab. As the deflection increases these cracks develop further outward, and the slab develops tensile membrane action anchored at or supported by the boundary. Most of this tensile membrane mechanism is likely to be provided by the reinforcing mesh. In most ambient tests, the tensile membrane capacity is similar to, or lower than, the compressive membrane capacity, and the transition from compressive membrane action to tensile membrane action is likely to be accompanied by a rapid increase in the central deflection of the floor system. The ambient load deflection behaviour of reinforced concrete slabs is summarised schematically in figure 6.1 [61, 62].

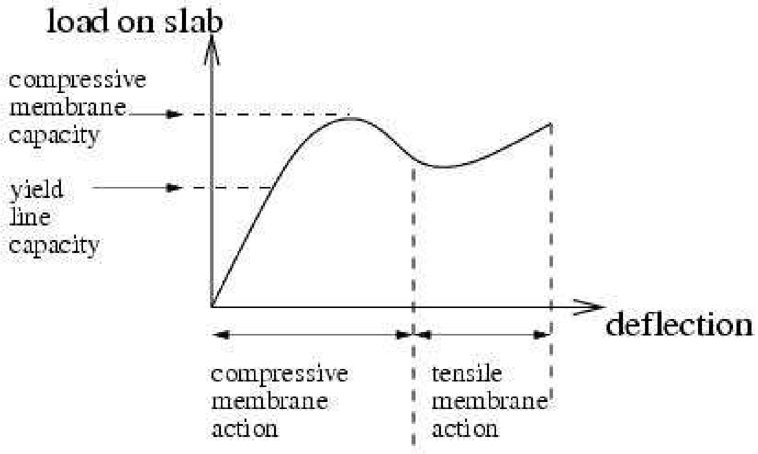

Figure 6.1: ambient load deflection behaviour of a concrete slab

Where a slab is exposed to large temperature increases as a result of fire in a structure, the increased temperature and thermal gradient induced in the slab allows large deflections to develop often simply due to thermal strains and without the extensive cracking at ambient temperature. These large thermal strains are unaccompanied by corresponding mechanical strains and therefore resulting in an increased tensile membrane capacity, figure 6.2.

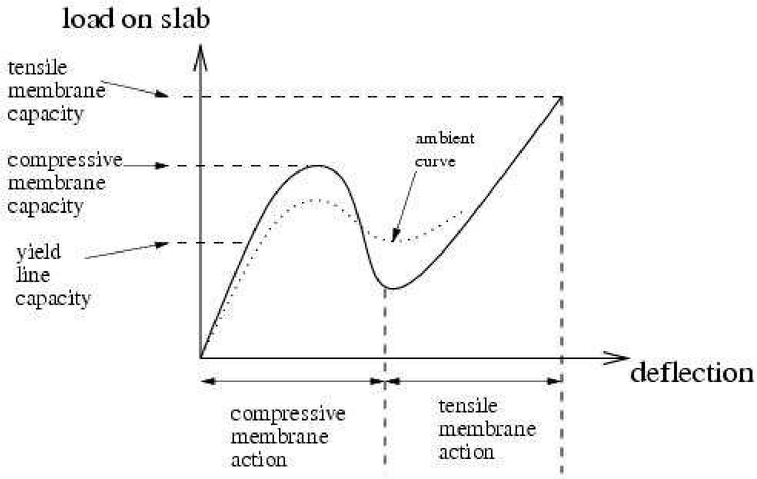

Figure 6.2: load deflection behaviour of a concrete slab at elevated temperatures

6.3 3-Dimensional Slab Modelling

The response of a slab modelled as a membrane or shell is well documented [63], and the presence of a compressive ring around the perimeter is a well acknowledged phenomenon in a deflected floor slab. However, previous research has not considered the distribution of stresses through the depth of a floor slab under heating. Compatible tensile stresses and strains will develop in the slab away from the heated surface as the heated region of concrete expands and forces the slab to adopt some deflected shape. These tensile strains will increase the available mechanical compressive strain before failure of the concrete in the section thus increasing the ultimate bending moment of a concrete section, thus increasing the flexural capacity of a floor slab. At low deflections, where the tensile membrane capacity has not been able to develop enough to sustain the static load imposed upon a floor system this additional flexural capacity may be relied upon to provide additional resistance where ambient flexural capacity can no longer be relied upon.

To explore the phenomena which lead to the replacement of a bending, or flexural, action with an overriding tensile mechanism a simple quarter model of a floor slab is analysed under a variety of conditions using the finite element method in ABAQUS. The results of this analysis illustrate the effects that thermal and static loading have on the distribution of stresses and strains through the depth of a floor slab.

The following assumptions are made regarding the slab at low deflections:

- The slab is restrained at the perimeter at mid depth against translation but free to rotate - this restraint allows for the development and utilisation of thermal pre-stressing forces which occur in the slab as a result of thermal strains
- The temperature increase through the slabs depth is idealised by an average temperature increase, ΔT; and a through depth thermal gradient, $T_{,z}$, as discussed previously

The model is exposed to two loading conditions, designed to increase the deflection of the slab via initial thermal effects and then by an increasing static loading. The model analysed is a quarter model of a 6 m x 6 m slab. A concrete deck of 100mm depth is assumed. Continuum elements with incompatible modes to avoid an over stiff response were used to model the concrete and membrane elements were embedded at mid-depth to model an

A142 mesh reinforcement. The concrete was assumed to be perfectly elastic, accounting for a reduction of stiffness with increasing temperature, according to EC2. Load history is as follows:

- thermal loading was applied in the form of a ΔT=200^{O}C and $T_{,z}$=-5^{O}C/mm
- a static loading was applied in two steps, leading to a combined deflection of ≈160mm and then ≈190mm.

The first combination of loading leads to a combined thermal and mechanical deflection of around 160mm. The resulting compressive and tensile stress vectors and their magnitudes are shown for the bottom surface of the floor slab in figures 6.3 and 6.4.

At 3/4 depth in the floor slab, figures 6.5 and 6.6, the tensile stresses are more developed than at the bottom surface of the floor slab. Figures 6.7 and 6.8 show the in plane compressive and tensile stress vectors at the slabs mid depth. There is a clear area in the centre of the slab where compressive stresses are not present. Tensile stresses are developed across the mid-spans of the slab.

Figures 6.9 and 6.10 show the compressive and tensile stresses at 1/4 depth of the concrete slab and figures 6.11 and 6.11 show the stress vectors and magnitudes at the upper surface. Both the expected compressive ring around the slabs perimeter and the tensile region in the centre of the slab are visible in these figures - the compressive ring at low level and the tensile region in midspan areas.

Following the increase of the static loading on the slab, so that the deflection is now 190mm, there is a clear 'relief' of the compressive stresses at the bottom of the floor slab caused by the increased mechanical loading. This is evident in figures 6.13 and6.14 which shows that at the lower surface of the slab compressive stresses are relieved in the middle of the slab and a compressive ring is visible around the perimeter.

The same can be seen at 3/4 of the slabs depth, figures 6.15 and 6.16, and at 1/2 of the slabs depth, figures 6.17 and 6.18. Compressive stresses are localised around the restrained corner of the slab where they are much larger than at lower deflections as a result of bending stresses restraining the uplift of the corner. Tensile stresses act perpendicular to the slabs boundary across the span.

Figures 6.19, 6.20,6.21 and 6.22 show the stress vectors and magnitudes at 1/4 depth and at the upper surface of the floor slab. Tensile stresses are dominant, and compressive stresses are present at the perimeter of the slab and in the restrained corner only. The relief of the compressive forces at the slabs lower surface is accompanied by an increase in the tensile forces at the upper surface.

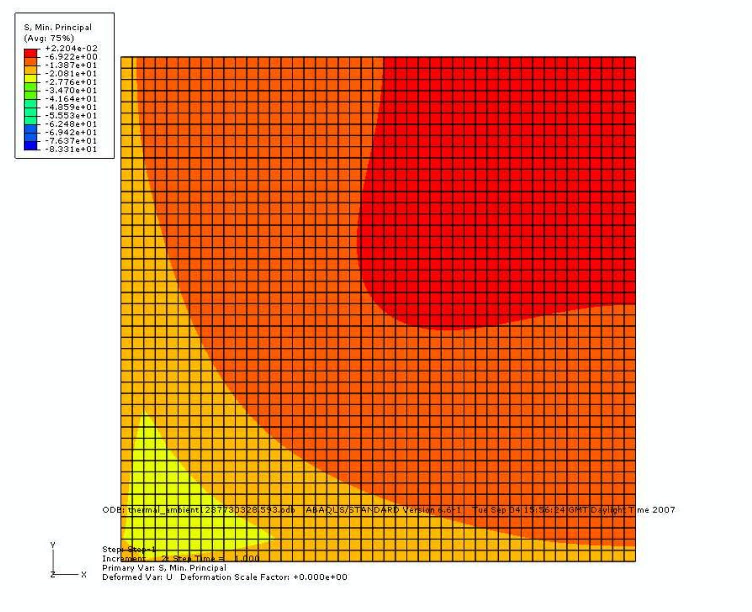

Figure 6.3: minimum stress values at the bottom slice of the floor slab for the first load case

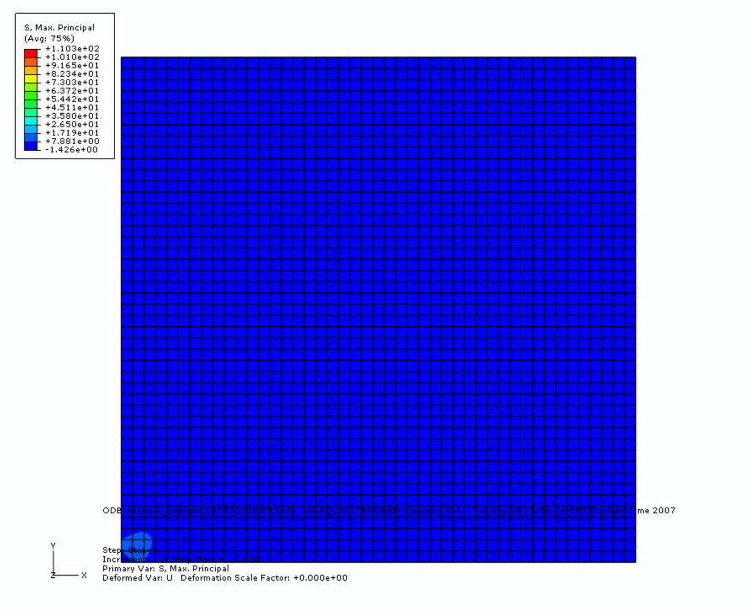

Figure 6.4: maximum stress values at the bottom slice of the floor slab for the first load case

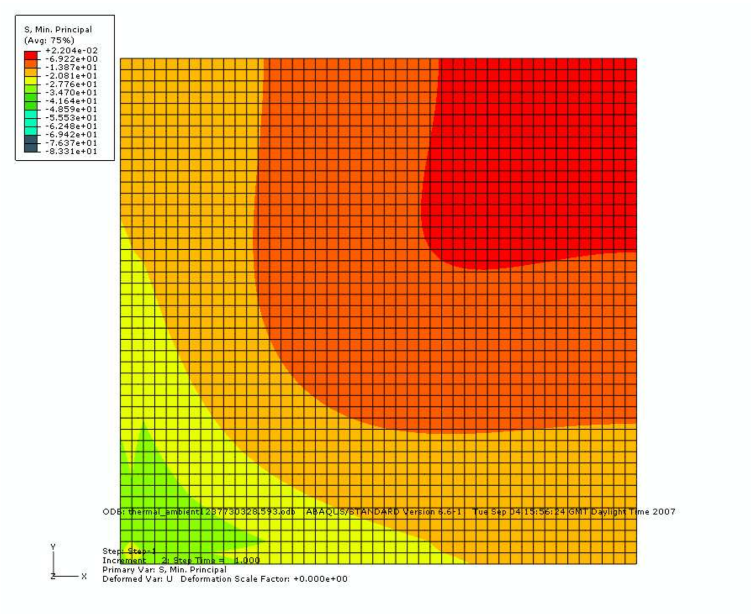

Figure 6.5: minimum stress values at 3/4 depth of the floor slab for the first load case

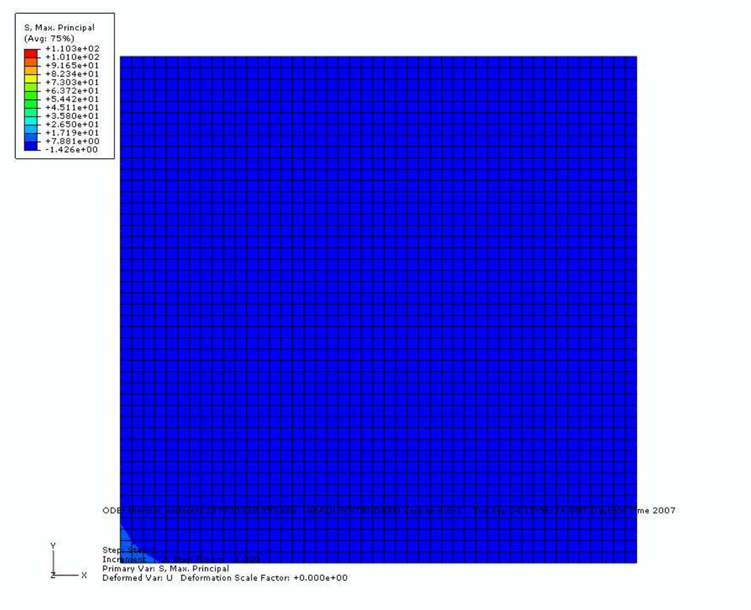

Figure 6.6: maximum stress values at 3/4 depth of the floor slab for the first load case

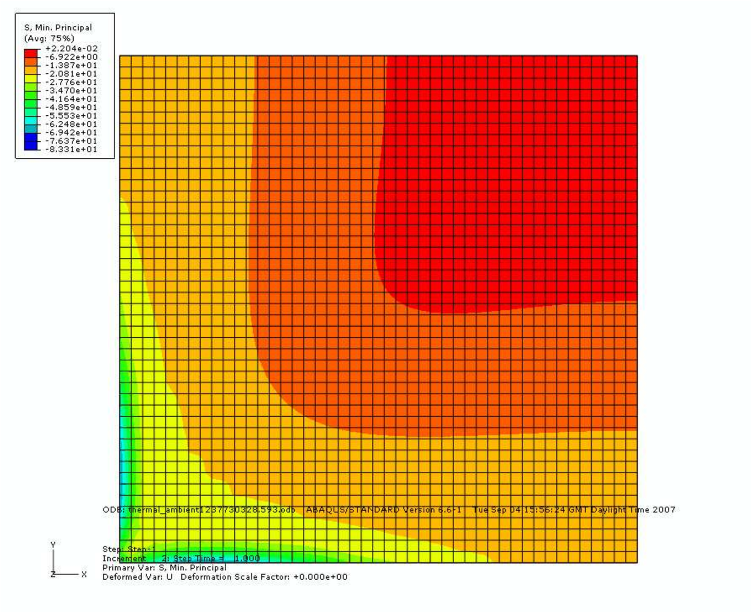

Figure 6.7: minimum stress values at mid of the floor slab for the first load case

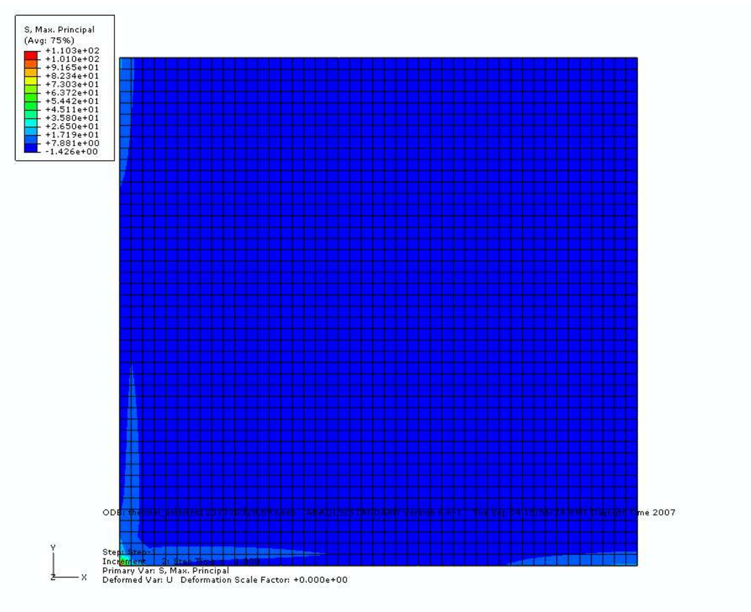

Figure 6.8: maximum stress values at mid depth of the floor slab for the first load case

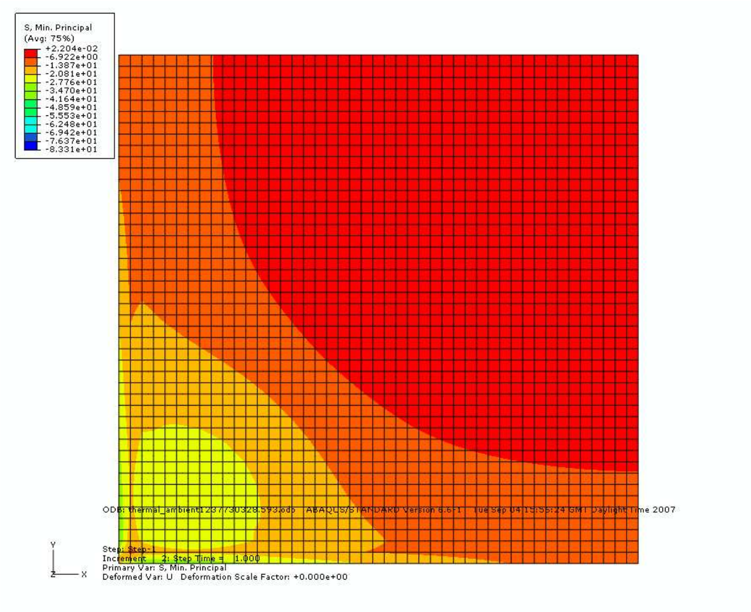

Figure 6.9: minimum stress values at quarter of the floor slab for the first load case

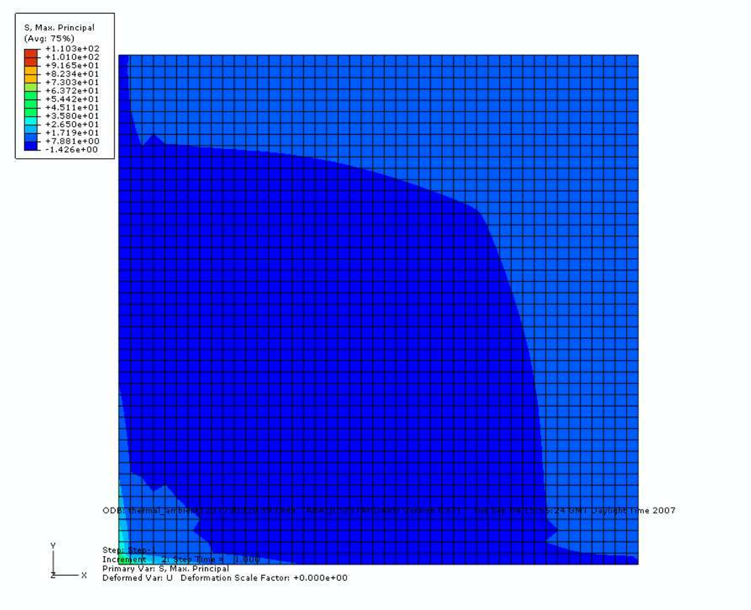

Figure 6.10: maximum stress values at quarter depth of the floor slab for the first load case

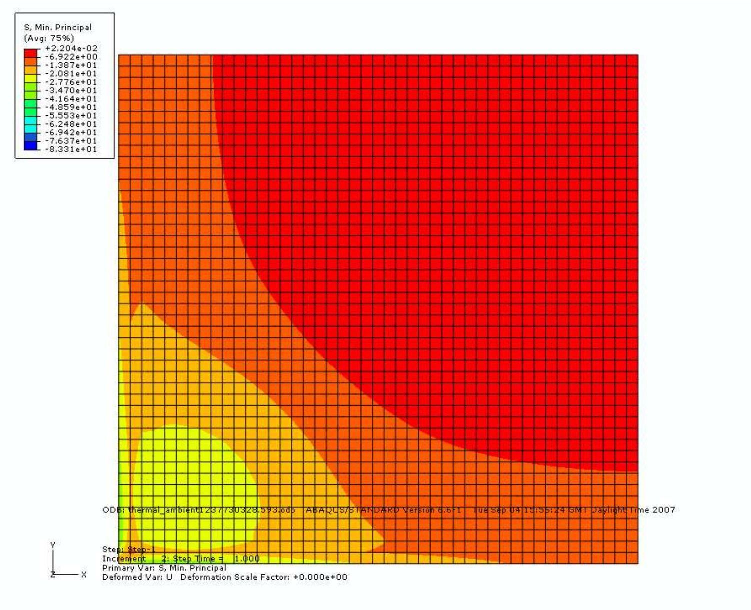

Figure 6.11: minimum stress values at the upper surface of the floor slab for the first load case

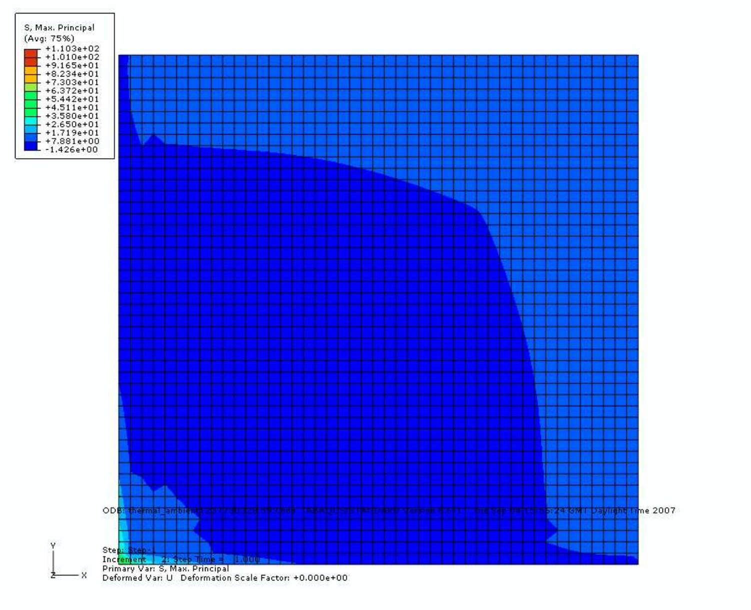

Figure 6.12: maximum stress values at the upper surface of the floor slab for the first load case

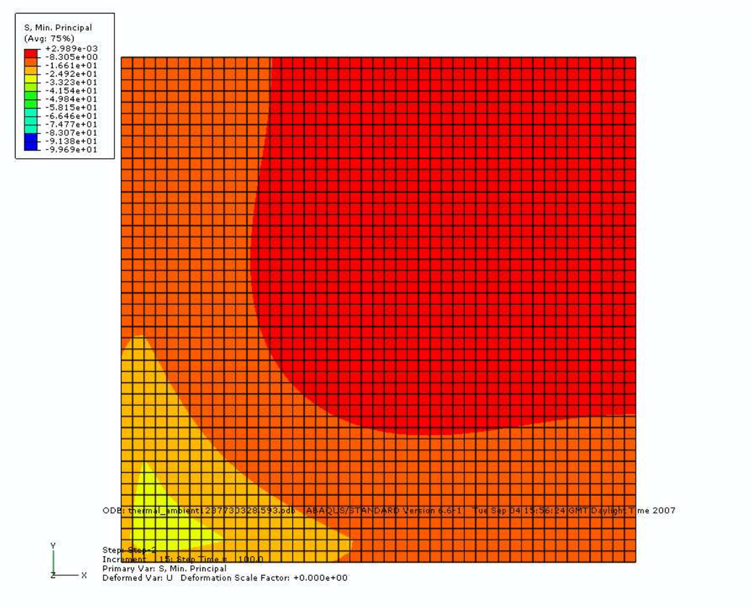

Figure 6.13: minimum stress values at the bottom slice of the floor slab for the second load case

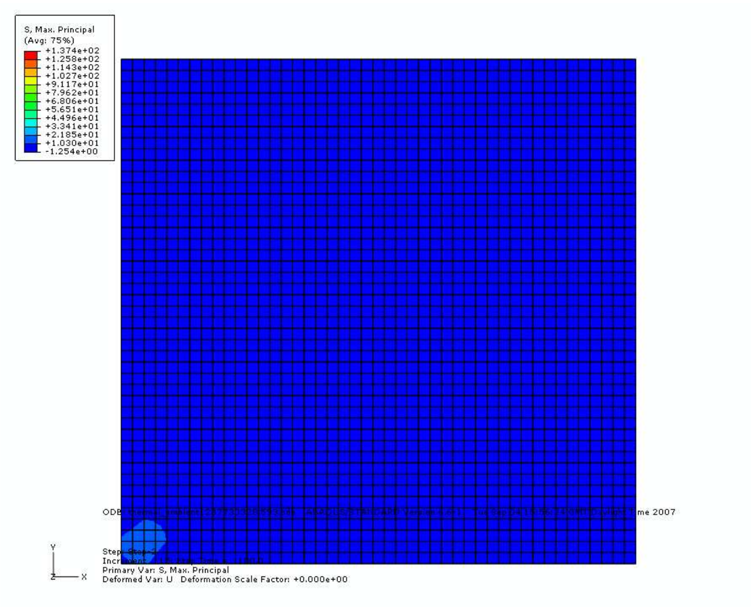

Figure 6.14: maximum stress values at the bottom slice of the floor slab for the second load case

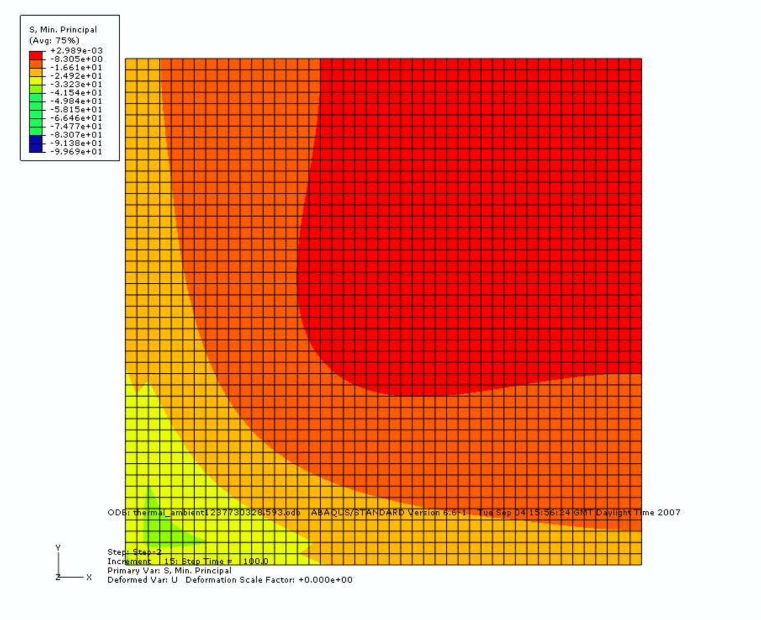

Figure 6.15: minimum stress values at 3/4 depth of the floor slab for the second load case

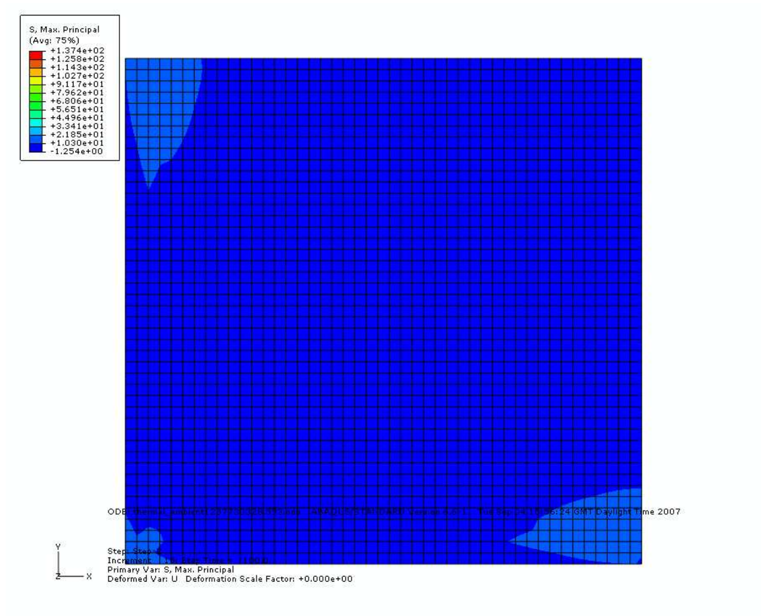

Figure 6.16: maximum stress values at 3/4 depth of the floor slab for the second load case

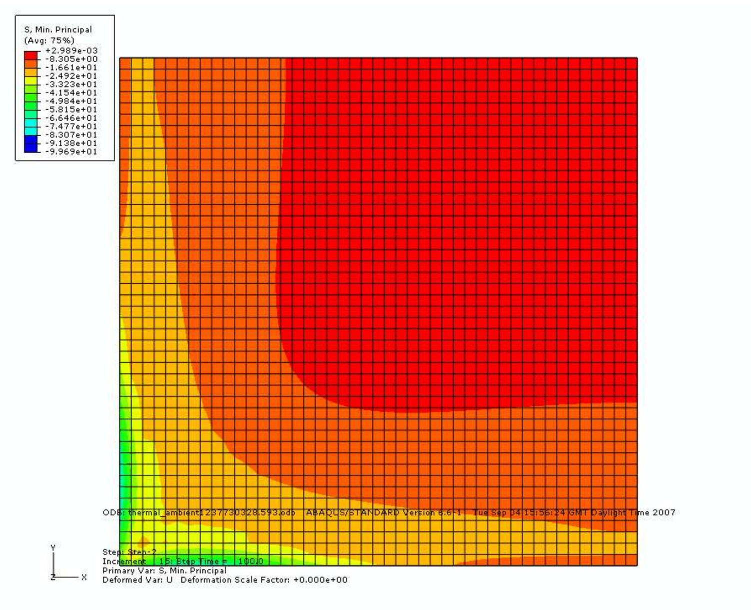

Figure 6.17: minimum stress values at mid depth of the floor slab for the second load case

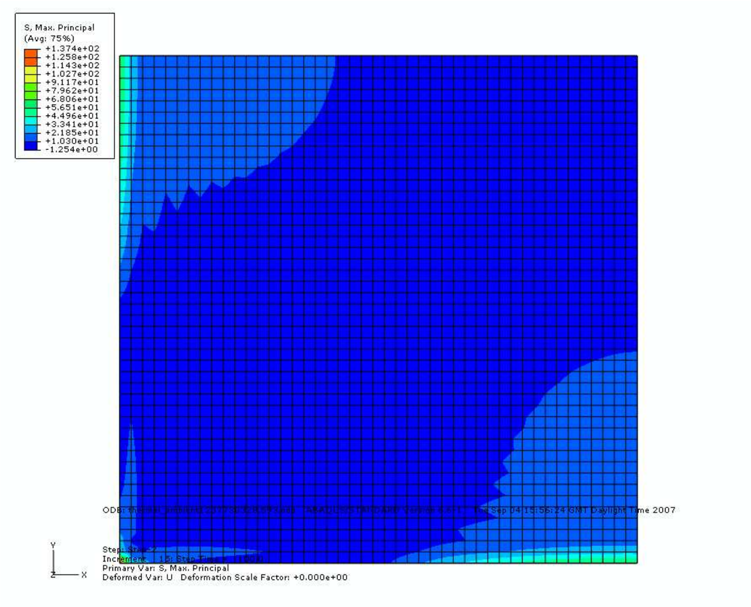

Figure 6.18: maximum stress values at mid depth of the floor slab for the second load case

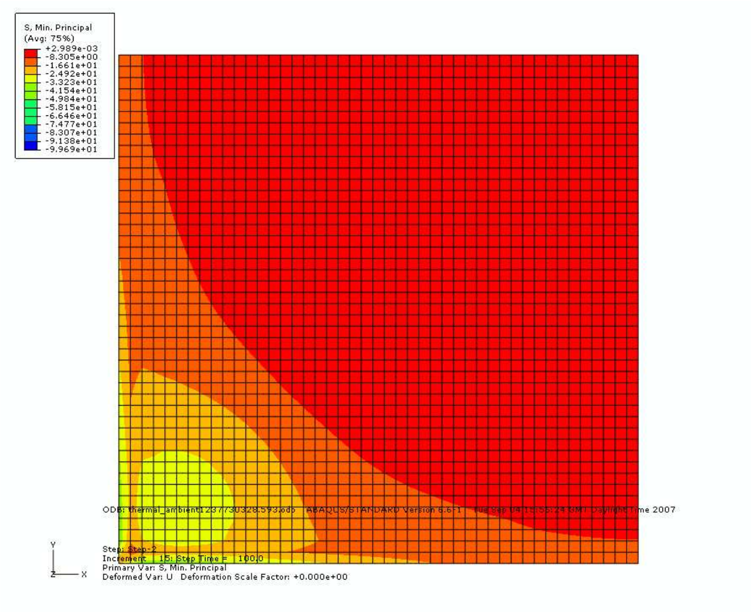

Figure 6.19: minimum stress values at quarter of the floor slab for the second load case

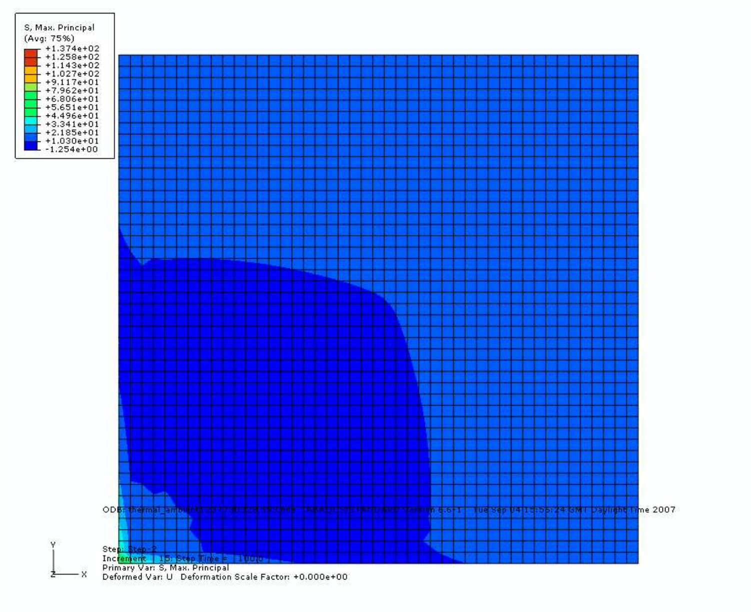

Figure 6.20: maximum stress values at quarter depth of the floor slab for the second load case

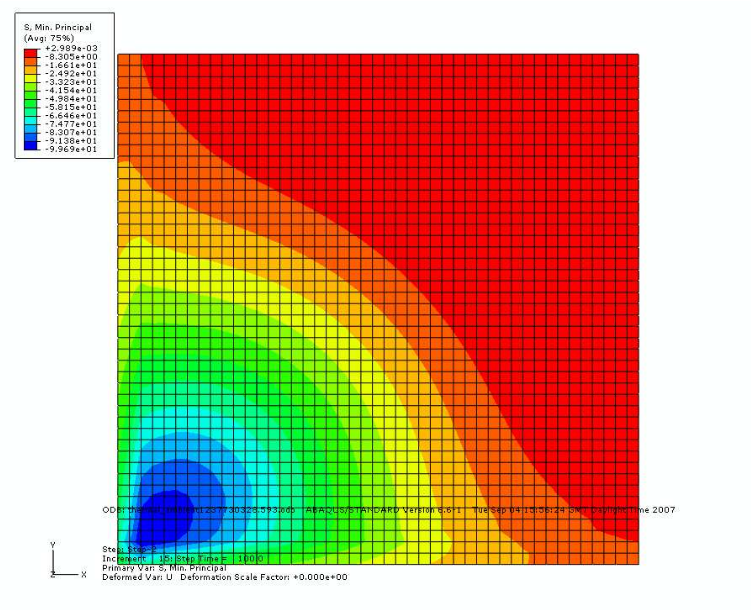

Figure 6.21: minimum stress values at the upper surface of the floor slab for the second load case

6.3.1 Summary

In summary, there are 3 aspects in the development of a slabs load bearing mechanism with increasing thermo-mechanical deflections which can be identified from the FE model:

1. A 'pre-stressing' of the concrete around the slabs perimeter due to thermal expansion inducing in-plane compressive stresses. This can lead to an increase of the moment capacity of the concrete section around the slabs perimeter, increasing the ultimate capacity of the floor slab at low deflections.

2. Displacement of the slab below available in-plane resistance to compression. This is the point at which the central region of the slab begins

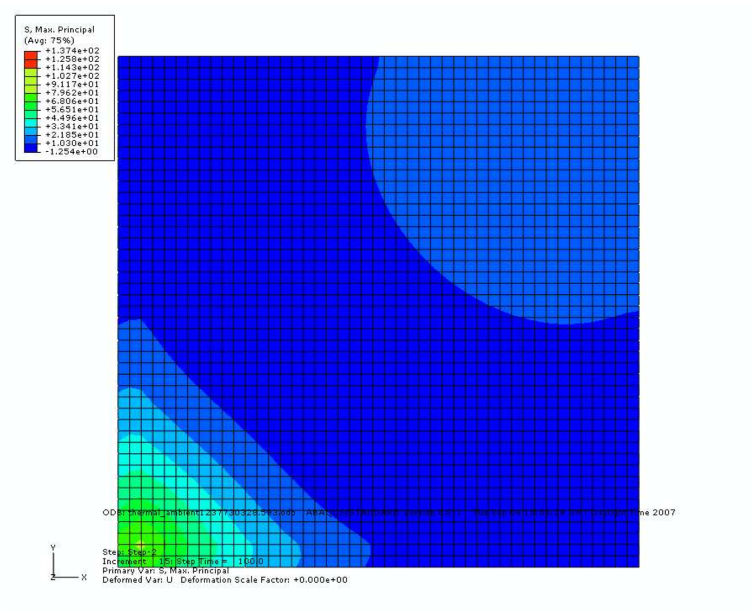

Figure 6.22: maximum stress values at the upper surface of the floor slab for the second load case

to adopt a tensile membrane mechanism, effectively hanging from the remaining compressive region which is now braced against the lateral restraint.

3. Following the adoption of a tensile membrane mechanism at the slabs central region, the perimeter of the slab continues to develop increased compressive forces due to the in plane restraint provided by the surrounding structure. These forces increase the capacity of the remaining relatively un-deformed concrete by increasing the thermally induced pre-stress which is present. Continued growth of the region adopting a tensile membrane mechanism reduces the width of the supporting compressive region.

6.4 The Bailey BRE Method

Bailey's method assumes the slab to be simply supported, arguing that the reinforcement over the supports may rupture given the localisation of strains due to the cracking of the concrete over the supports. Although this phenomenon was observed around the columns in the Cardington tests, it was not present around the entire perimeter of the heated regions, in fact evidence at the time pointed to the cracks occurring as a result of tensile strains during cooling in the supporting structure [64]. In addition to this, further work in the form of a seventh Cardington test has suggested that the reinforcement within the composite slab was not properly overlapped above the primary beams, leading to the possibility that the floor slab was effectively simply supported due to a lack of continuity of the reinforcement at the perimeter [65]. This suggestion is further backed up by experimental research carried out in New Zealand, where cracking of the concrete was seen to propagate across a slab away from initial cracking as a result of tension stiffening of the reinforcement as cracks form.

Bailey also assumes that secondary beams yield plastically at their mid point and that this plastic deformation moves outward towards the primary beams, allowing the slab to develop a standard shaped yield envelope. Whilst this location of yield is consistent with a simply supported beam in fire, secondary beams are restrained against axial movement by connection to the primary beams and are therefore not simply supported. In most cases, large compressive forces in the region of the beam-column connection lead to plastic yielding of the bottom flange of the section resulting in a change in the boundary condition of the composite beam from fixed, or moment resisting, to pinned. In lightly restrained slabs there is some evidence of concrete cracks as well which could lead to rupture of the reinforcement in this region leading to unrestrained boundary conditions. An unprotected beam at high temperature will generally not provide much bending support and will follow the deflected shape of the floor slab. Unrestrained boundary conditions mean that no mechanical stress or strain will occur as a result of thermal expansion.

Failure in this method of assessment is by rupture of reinforcement in the long span, leading to a full-width crack along the short span of the floor slab.

6.5 The Cameron Usmani Method

Cameron and Usmani observe that in the Cardington tests continuity in the reinforcement was maintained at the supports away from the columns and so in their method the slab is assumed restrained against lateral movement, but free to rotate. The method takes account of the actual observed deflected shape of the slab, and large mechanical stresses and strains occur in the slab as a result of the restraint to thermal expansion at the boundary. The concrete in the floor system is ignored in calculating tensile membrane capacity since large displacements at ultimate load will cause widespread cracking of the concrete throughout the slab leaving only continuity in the reinforcing mesh to support any load.

Failure in this calculation method is by rupture of the reinforcement in the middle of the short span, since compatibility means that tensile strains in the short span must be larger than tensile strains in the long span for a given deflection. This method also assumes that the strain in a reinforcing bar does not vary along its length and ignores the possibility of strain localisation at the supports. It is argued that given that the reinforcement in Cardington consisted of smooth bars while most current practice favours deformed bars, this may be an unsafe assumption. However, the use of a low failure strain and only in the first most highly strained single bar to define the point of failure and the maximum membrane capacity reduces this risk.

Following the Cameron/Usmani methodology, the analytical method employed for determining the tensile membrane capacity of a slab subjected to heating has three steps:

1. Calculation of the temperature distribution through the depth of the member
2. Calculation of: the deflected shape of the member, based upon the gross cross-sectional area; and the stresses and strains in the reinforcing bars associated with this deflected shape and steel temperature
3. Calculation of the limiting deflection and the internal and external work done to move from the thermal deflection to the limiting deflection, the internal work done is based on the reinforcement only and ignores any contribution from the concrete.

The methodology is summarised in this section, however for a more detailed explanation further references [27, 36, 59, 60] should be consulted.

The following assumptions are made in the derivation of the tensile membrane capacity:

- The slab is simply supported around all four sides, i.e. it is restrained against horizontal movement but free to rotate.
- The deflected shape under thermal loading is represented as a double sine function
- Where tensile membrane action develops the concrete makes no contribution to the resistance of the slab

The methodology is described here for a compartment temperature time history during the heating phase of the fire with analysis carried out at a number of discrete time steps.

The first step, the calculation of the temperature distribution through the depth of the member can be carried out in a number of ways as previously discussed. For the subsequent steps, all that is required is the equivalent temperature increase and the uniform through depth thermal gradient. Because the slab is restrained at the boundaries, the temperature distribution results in a thermal force in the section due to the average temperature increase and a thermal moment in the section due to the through depth thermal gradient.

The calculation of the deflected shape of the member takes account only of the concrete section. Applying the thermal loading to the section results in a thermal deflection, w_T. For a 1-way spanning slab of length L, and of concrete with stiffness E_C, this deflection can be calculated by solving the following cubic equation for w_T:

$$w_T^3 + \left(\frac{4I}{A} - \frac{4N_T L^2}{\pi^2 E_c A}\right) w_T + \frac{16 M_T L^2}{\pi^3 E_c A} = 0 \qquad (6.1)$$

Where I is the second moment of area of the section, A is the area, N_T is the thermal force and M_T is the thermal moment - all calculated per unit width of the section. Where a 2-way spanning slab is considered, equation 6.1 becomes:

$$\begin{aligned}&\tfrac{3}{4}\left\{(3-\nu^2)\left(1+\tfrac{L^4}{B^4}\right)+4\nu\tfrac{L^2}{B^2}\right\}\left(\tfrac{w_T}{h}\right)^3\\&+\left\{\left(1+\tfrac{L^2}{B^2}\right)^2-12\tfrac{L^2(1+\nu)N_T}{\pi^2}\left(1+\tfrac{L^2}{B^2}\right)\right\}\left(\tfrac{w_T}{h}\right)\\&-192\tfrac{L^2(1+\nu)M_T}{\pi^4E_ch^4}\left(1+\tfrac{L^2}{B^2}\right)=0\end{aligned} \tag{6.2}$$

Where h is the depth and B the breadth of the slab; and ν is the poissons ratio of the concrete. These equations both need to be solved iteratively for each time step. In the calculation of the thermally deflected shape, the creep and transient strains in the concrete are effectively ignored. Although this is not considered in the derivation of the original methodology it may lead to an underestimation of the maximum thermal deflection, however it is expected that the end result of this omission will be minimal since the concrete plays no furhter rols in this methodology after the deflected shape has been calculated.

The thermal deflection of the slab at any point, x, along the length can be calculated for a 1-way spanning slab by assuming that the deflected shape is that of a sine curve, with central deflection w_T:

$$w_T(x) = w_T sin\frac{\pi x}{L} \tag{6.3}$$

For a 2-way spanning slab the deflected shape is assumed to be that of a double sine curve, thus equation 6.3 becomes:

$$w_T(x,y) = w_T sin\frac{\pi x}{L} sin\frac{\pi y}{B} \tag{6.4}$$

The strains in the bars at the thermal deflection consist of two components, the thermal strain as a result of the increase in temperature of the steel and the strain induced in the steel as a result of the deflected shape of the concrete in which it is embedded. As discussed in earlier chapters, the total strain is the sum of the thermal strain and the mechanical strain, i.e.:

$$\epsilon_{tot} = \epsilon_{mech} + \epsilon_T \tag{6.5}$$

For a two way spanning slab, the total strains in the rebars spanning in the x and y directions are given by the following equations:

$$\epsilon_{xx,tot}(y) = \frac{w_T^2\pi^2}{8L^2}\left(1 - cos\frac{2\pi y}{B}\right) + \nu\frac{w_T^2\pi^2}{8B^2} \tag{6.6}$$

$$\epsilon_{yy,tot}(x) = \frac{w_T^2\pi^2}{8B^2}\left(1 - cos\frac{2\pi x}{L}\right) + \nu\frac{w_T^2\pi^2}{8L^2} \tag{6.7}$$

The mechanical strains are obtained by subtracting the thermal strains from equations 6.8 and 6.9:

$$\epsilon_{xx,mech}(y) = \frac{w_T^2\pi^2}{8L^2}\left(1 - cos\frac{2\pi y}{B}\right) + \nu\frac{w_T^2\pi^2}{8B^2} - \alpha T_s \tag{6.8}$$

$$\epsilon_{yy,mech}(x) = \frac{w_T^2\pi^2}{8B^2}\left(1 - cos\frac{2\pi x}{L}\right) + \nu\frac{w_T^2\pi^2}{8L^2} - \alpha T_s \tag{6.9}$$

The stress in the reinforcing bars is based upon the mechanical strains, and is therefore given by:

$$\sigma_{xx}(y) = \frac{w_T^2\pi^2 E_s}{8(1-\nu^2)}\left(\frac{1}{L^2}+\frac{\nu}{B^2}\right) - \frac{w_T^2\pi^2 E_s}{8L^2} cos\frac{2\pi y}{B} - \frac{E_s\alpha T_s}{1-\nu} \quad (6.10)$$

$$\sigma_{yy}(x) = \frac{w_T^2\pi^2 E_s}{8(1-\nu^2)}\left(\frac{1}{B^2}+\frac{\nu}{L^2}\right) - \frac{w_T^2\pi^2 E_s}{8B^2} cos\frac{2\pi x}{B} - \frac{E_s\alpha T_s}{1-\nu} \quad (6.11)$$

Where E_s is the modulus of elasticity and T_s the temperature of the steel and ν is the poisons ratio of the concrete.

If the slab is two way spanning, then the stresses and strains need only be calculated for the reinforcement running along the axis of the slab and the equations above should be modified accordingly to reflect the fact that curvature is in one direction only.

Following the application of thermal loading, the slabs response to static loading has to be determined. The capacity of the slab is limited by the maximum strain of the reinforcement bars, dictated by the ductility limits of the Eurocodes, table 6.1. The limiting deflection, w_t, in a 1-way spanning

Class	Diameter	ϵ_{uk}
N(ormal)	$\leq 16mm$	2.5%
H(igh)	$> 16mm$	5%

Table 6.1: ductility limits for reinforcing bars according to EC2

slab can be calculated by considering the maximum deflection as a result of the maximum allowable mechanical strain, ϵ_{uk}, and the thermal strain:

$$w_t = \frac{L}{\pi}\sqrt{4(\epsilon_{uk} + \alpha T_s)} \tag{6.12}$$

For reinforcing steel in a 2-way spanning concrete slab compatibility dictates that the largest strains will occur across the shorter of the two spans, i.e. $\epsilon_{yy} > \epsilon_{xx}$. Therefore the limiting deflection of a 2-way spanning slab is given by:

$$w_t = \frac{B}{\pi}\sqrt{4(\epsilon_{uk} + \alpha T_s)} \tag{6.13}$$

Having determined the limiting strain of the reinforcement in the floor slab and the limiting deflection, the internal and external work required to move the floor slab from the thermal deflection to the limiting deflection can be determined by increasing the displacement incrementally. Where the concrete is in tension, the poisons ratio is 0, and thus equations 6.10 and 6.10 have to be modified to be:

$$\sigma_{xx}(y) = \frac{w_n^2\pi^2 E_s}{8L^2}\left(1 - cos\frac{2\pi y}{B}\right) - E_s\alpha T_s \tag{6.14}$$

$$\sigma_{yy}(x) = \frac{w_n^2\pi^2 E_s}{8B^2}\left(1 - cos\frac{2\pi x}{B}\right) - E_s\alpha T_s \tag{6.15}$$

Where w_n is the slab deflection at the n'th increment. The increment in the internal work for each rebar between deflections w_T and w_n is obtained by integrating the stress with respect to the strain over the volume of the bar. To obtain the total internal work for the current increment, this has to be done for every rebar:

$$\Pi_{int} = \sum_{n=1}^{no.ofrebar}\left[V_n \int_{\epsilon_{w_T}}^{\epsilon_{w_n}} \sigma(\epsilon)d\epsilon\right] \tag{6.16}$$

And the external work increment for a 1-way spanning slab by:

$$\Pi_{ext} = \int_{0}^{L} \left(q_{n-1} + \frac{\Delta q_n}{2} \right) \Delta w \frac{4L}{\pi^2} \tag{6.17}$$

Or for a 2-way spanning slab by:

$$\Pi_{ext} = \int_{0}^{L} \int_{0}^{B} \left(q_{n-1} + \frac{\Delta q_n}{2} \right) \Delta w \frac{4LB}{\pi^2} \tag{6.18}$$

Where q_n is the total load at the n'th increment, and Δq_n is the load at the current increment. The internal and external work must equal each other, and therefore these equations can be re-arranged and solved for Δq_n and the ultimate capacity can be determined from:

$$q_{ult} = \sum_{\forall n} \Delta q_n \tag{6.19}$$

6.6 Catenary and Membrane Mechanisms

Because a 1-way spanning slab will not develop a membrane action supported on all sides by horizontal members, a distinction is made here between a simple catenary mechanism and a tensile membrane mechanism. In the catenary mechanism of a 1-way spanning slab, the capacity is enhanced via thermal strains induced in the available steel, whereas in a 2-way spanning slab this is enhanced further by compatibility of the mechanical strains in the embedded reinforcement.

Since the slab is adopting a catenary mechanism, the resistance to load is based upon the steel spanning between the supports, i.e. the steel spanning in the shorter span. For slabs with small aspect ratios, i.e. where $B/L < 2/3$, the slab can be assumed to be 1-way spanning since the deflected shape will be governed by the behaviour of the system in the short span.

6.7 Thermally Pre-stressed Yield Line

As demonstrated in preceding parts of this chapter, increasing rigidity of the floor slab actually leads to a decrease in the thermal deflections and the final available tensile membrane capacity of the floor system. The numerical modelling above suggests that at low deflections a large amount of compressive stress is present to a varying degree through the depth of the slab. It follows that at low deflections of floor slab large reserves of flexural resistance may be available for carrying loads, and these reserves may be enhanced by a thermal pre-stressing where the restraint to thermal expansion remains above the plane of the upper surface at the centre of the slab.

6.7.1 Numerical Modelling

The effect of heating on yield line capacity can be illustrated using the previously described finite element model. The slab was subjected to the total thermal loading equivalent to a ΔT of 200^OC and a $T_{,z}$ of -5^OC/mm. Three cases were considered, firstly static loading with no thermal loading to illustrate bending only; secondly thermal loading to illustrate in-plane compressive forces developing as the slab heats up; and thirdly thermal and static loading to illustrate the reduction in compressive forces as the slab moves through the static deflection. Since this model is intended to illustrate only the distribution of thermal strains and stresses through the depth of the section the concrete was again assumed to be perfectly elastic, accounting for a reduction of stiffness with increasing temperature, according to EC2.

Under static loading only, the displacement at the mid-point is approximately equal to the depth of the slab. Since the only significant tensile stresses present are in the reinforcement; compressive stresses alone are considered for the concrete. Compressive stress vectors along the diagonal (yield line) of the slab are shown in figure 6.23. The increase in compressive forces at the perimeter of the slab as the slab is moved through the displacement is clearly visible at the upper surface of the slab; this is similar to an 'arching' effect as the slab boundaries push against the in-plane restraint to adopt the deflected shape shown. Coincident with a reduction of in-plane restraint due to central deflection of the slab, the compressive stresses in the middle of the slab tend towards those required to sustain bending.

Under thermal loading only, the displacement is approximately 1.5 times the depth of the slab. Compressive stress vectors are plotted in figure 6.24. Similar to static loading only, the boundary of the slab is subjected to large compressive forces, creating the well documented 'compressive ring' due to restraint against in-plane expansion and out of plane deflection of the slab at the perimeter. However, the thermal gradient leads to compressive strains in the bottom of the concrete as the thermal expansion of the lower concrete is 'restrained' by the ambient concrete of the upper part of the section which is not in compression. This thermal strain couple is what causes the thermal deflection of the slab under elevated temperatures.

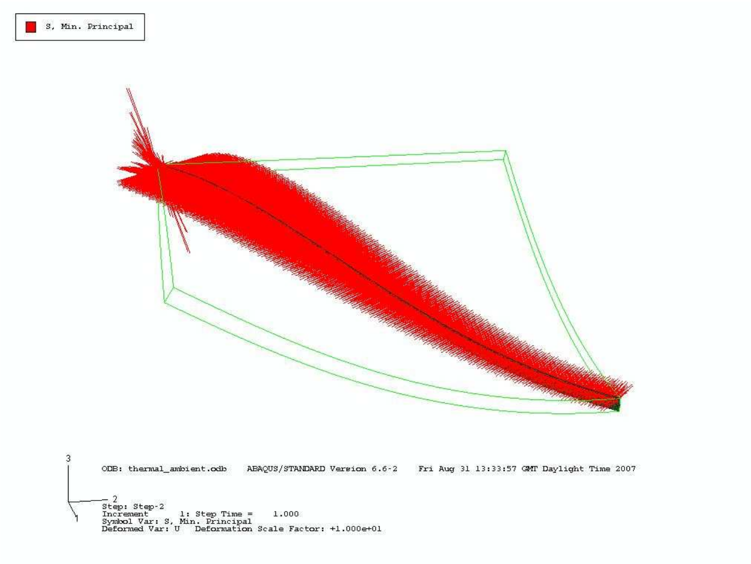

Figure 6.23: compressive stress vectors along the diagonal of a quarter model square floor slab under static loading

When static loading is introduced to the thermally loaded model, the resulting increase in deflection at the midpoint of the slab effectively balances and then overcomes the thermal compression in the middle of the slab, figure 6.25. Although compressive stresses remain in the plane of the yield line, figure 6.26, it is the compressive stresses about the yield line which create the tension-compression couple resisting the applied moment. When these compressive stresses are no longer available and only tensile stresses remain in the steel of the slab then the slab begins to adopt a catenary mechanism and no bending resistance is available in the region. The compressive region of concrete disappears with increasing deflection.

Figure 6.27 shows the compressive stress along the top of the plane of the yield line. At the corner the uplift to restraint causes a relief in the com-

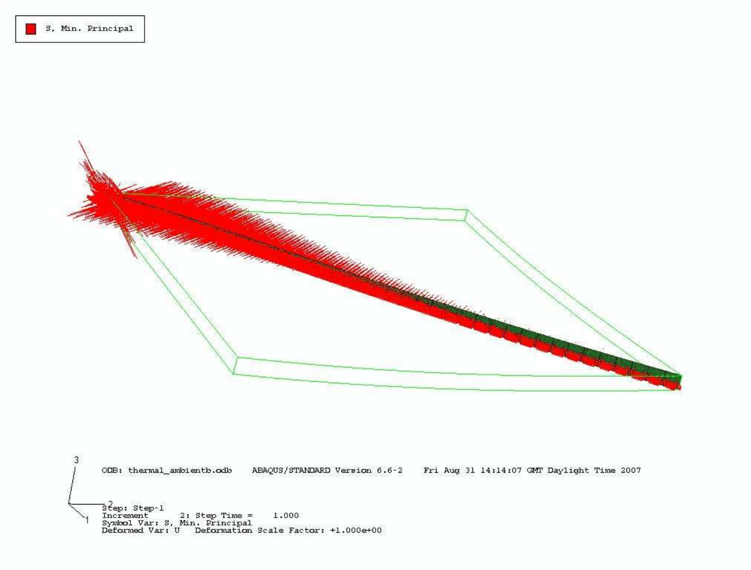

Figure 6.24: compressive stress vectors along the diagonal of a quarter model square slab under thermal loading only

pressive stress. 2.5 metres along the yield line, the compressive stress is zero. Figure 6.28 shows the deflection along the yield line for comparison. It can be seen that the point where compressive stress is no longer present coincides with a deflection of 150mm.

In summary, there are two effects caused by geometrical changes induced by thermal expansion on the ultimate moment of a section which have to be considered:

1. Thermal loading induced by temperature increases in the slab; i.e., a thermal force generated by the average temperature increase and a thermal moment induced by the difference in temperatures between the heated and unheated surfaces. This causes an increase in the area of the cross section under mechanical compressive strain (assuming that the fire is below the slab and that there is restraint to lateral translation

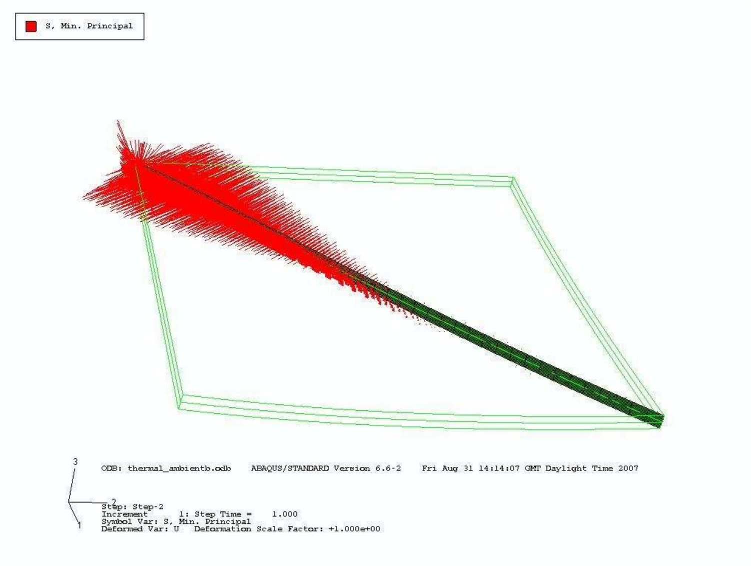

Figure 6.25: compressive stress vectors along the diagonal of a quarter model square slab under thermal and static loading

at the edges).

2. The downward deflection of the section removes the available in-plane restraint to compression in the slab, effectively moving the neutral axis for bending upwards through the depth of the slab.

These two actions are similar to the effect of pre-stressing on the concrete section: the thermal loading (1) is equivalent to the compressive force caused by pre-stressing tendons; the downward deflection (2) controls the eccentricity of the pre-stressing, this has a negative effect when the eccentricity becomes large enough that it is above the upper surface of the slab.

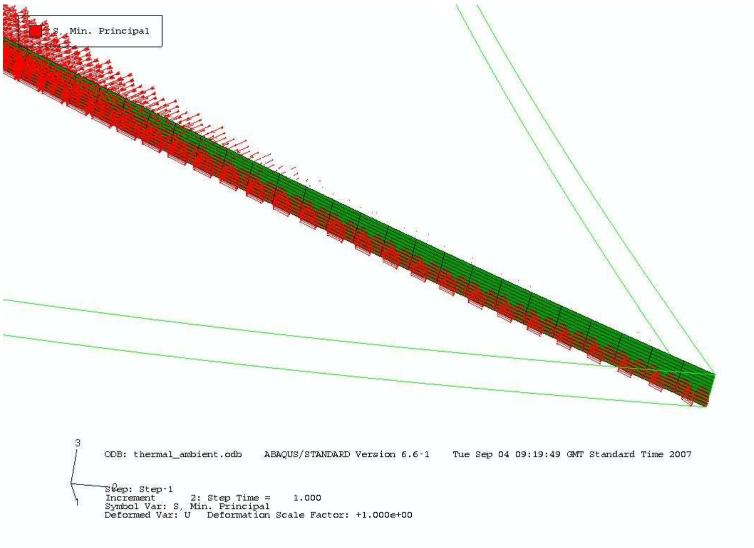

Figure 6.26: compressive stresses remain in the plane of the yield line but are not available in the tension-compression couple about the yield line

6.7.2 Ultimate Moment of a Heated Section

The strains in a fully restrained section as a result of thermal loading are shown in figure 6.29. Assuming that no deflection is allowed in the section, the result of the thermal strain is an effective non-linear pre-strain, $\Delta T(z)$, applied to the section. The total strain in the steel before failure is increased by an amount equivalent to the thermal strain in the reinforcing bar, ΔT_s.

From compatibility, the depth to the neutral axis can be calculated by considering the strains in the concrete and the steel at the ultimate state, i.e. where concrete has reached its ultimate compressive strain. For a pre-stressed section assuming full bond between the concrete and the steel, this is [66]:

$$\frac{h_{na}}{h_e} = \frac{\epsilon_{cu}}{\epsilon_{cu} + \epsilon_{pb} - \epsilon_{pe} - \epsilon_e} \tag{6.20}$$

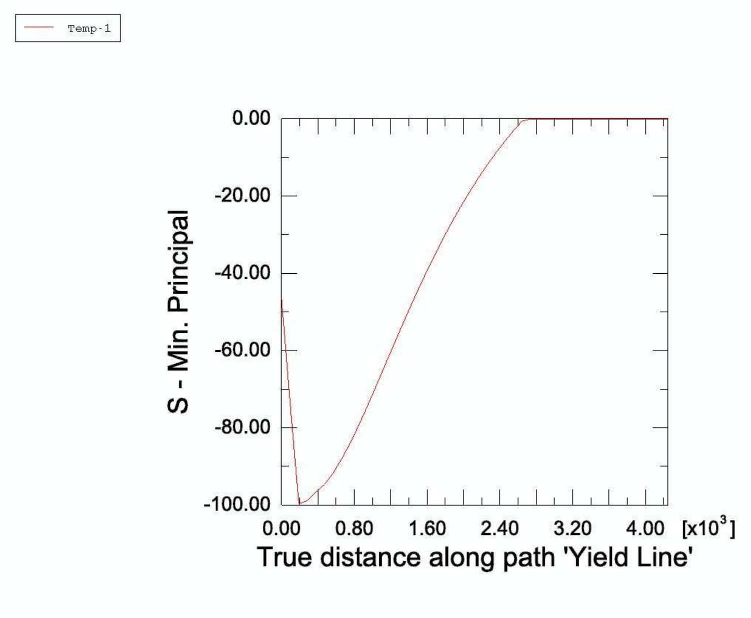

Figure 6.27: compressive stress along the top of the yield line

Where h_{na} is the depth to the neutral axis, h_e is the effective depth of the section. ϵ_{cu} is the ultimate compressive strain of the concrete, ϵ_{pb} the strain in the steel at the ultimate state, ϵ_{pe} the strain due to the effective pre-stress, and ϵ_e is the concrete pre-stress at the depth of the steel.

For the thermal pre-stressing proposed, equation 6.20 becomes:

$$\frac{h_{na}}{h_e} = \frac{\epsilon_{cu}}{\epsilon_{cu} + \epsilon_{pb} + \epsilon_{Ts} - \epsilon_{Tc}(d)} \tag{6.21}$$

Where ΔT_s is the thermal strain in the steel and $\Delta T_c(d)$ is the thermal strain in the concrete at the effective depth.

From horizontal equilibrium of the section:

$$\sigma_s(T)A_s = \sigma_{cu} b h_{na} \tag{6.22}$$

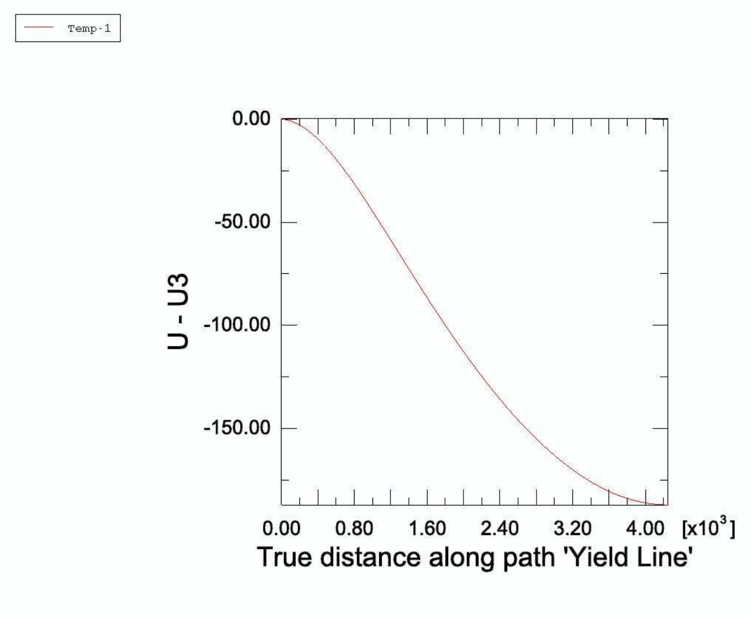

Figure 6.28: deflection along the top of the yield line

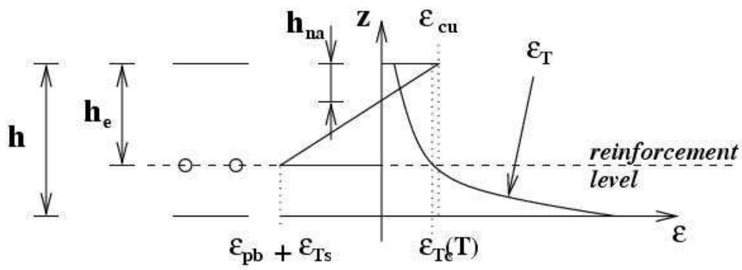

Figure 6.29: strains in the floor section as a result of thermal and static load

Where $\sigma_s(T)$ is the temperature dependant stress in the steel at the limit state of the section, $\epsilon_c u$ is the stress in the concrete at the limit state, b is the breadth of the section and A_s is the area of steel in the section.

The stress and strain in the steel at the ultimate state of the section can be found by substituting 6.22 into 6.21 and rearranging for σs:

$$\sigma_s(T) = \frac{\sigma_{cu} b h_e}{A_s} \frac{\epsilon_{cu}}{\epsilon_{cu} + \epsilon_{pb} + \epsilon_{Ts} - \epsilon_{Tc}(d)} \tag{6.23}$$

This gives the relationship between the stress and the strain in the reinforcement at the ultimate state. These can then be determined from the stress-strain curve.

Having determined the stress and strain in the rebar at the ultimate limit state, the value of ϵ_{pb} can then be inserted into equation 6.21 and the neutral axis location calculated. This can be used to calculate the residual moment in the section from, assuming that the concrete stress block is rectangular:

$$M_R = \sigma_s(T) A_s \left(h_e - \frac{h_{na}}{2} \right) \tag{6.24}$$

Where M_R is the residual moment of the section given the current thermal loading.

6.7.3 Thermally Prestressed 1-way Spanning Slab

The membrane force in a 1-way spanning slab is given by [27]:

$$F_x = EA \frac{\pi^2 w_T^2}{4L^2} - N_T \tag{6.25}$$

Where w_T is as given by equation 6.1.

Considering the slabs thermal deflection, the horizontal restraining force at the supports will have some eccentricity to the section. For a one way spanning slab this eccentricity will vary with the distance from the supports, and is denoted $e(x)$. For a neutral axis coinciding with the plane of restraint, the eccentricity is equal to the deflection of the slab; $w_T(x)$, figure 6.30. Whereas if the neutral axis does not coincide with the depth to the plane of restraint at the boundaries, the restraining force, F_x, will have an additional eccentricity equal to the distance from the plane of support to the neutral axis:

$$e(x) = w(x) - \left(\frac{h_e}{2} - h_{na}\right) \tag{6.26}$$

The residual moment of resistance of the section about the y-axis at a

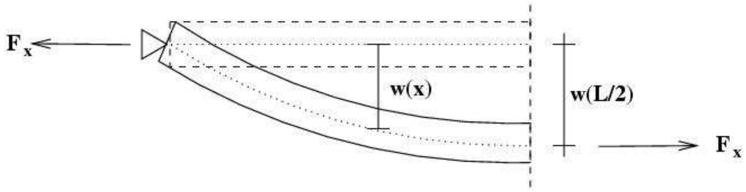

Figure 6.30: the eccentricity of the restraining force varies with the deflection of the slab.

thermal deflection, w_T, is the moment of resistance of an un-deflected section minus the moment induced by the restraining force and its eccentricity:

$$M_{Ry} = \sigma_s(T)A_s\left(h_e - \frac{h_n a}{2}\right) - F(x)e(x) \tag{6.27}$$

The yield line method is based upon the principal of virtual work. Yield lines in a 1-way spanning simply supported slab will tend to run along the middle of the slab where the larger applied moment is. The capacity of the 1-way spanning slab can be calculated by comparing the internal and the external work of the system at failure. These should be equal, i.e. [67]:

$$\text{work done in yield lines rotating} = \text{work done in loads moving}$$

The internal work per unit breadth is the integral of the ultimate moment of the section at $x = L/2$ multiplied by the rotation of the section; for all sections:

$$\Pi_{int} = 2M_R\Theta \tag{6.28}$$

Where Θ is the rotation of the yield line at failure for a unit displacement; i.e.:

$$\Theta = \frac{1}{L/2} \tag{6.29}$$

The external work per unit breadth is the load per unit breadth multiplied by the displacement it goes through for a unit displacement at the centre of the slab:

$$\Pi_{ext} = 2q\frac{L}{4} \tag{6.30}$$

6.7.4 Thermally Pre-stressed 2-way Spanning Slab

For a two way spanning slab the eccentricity will vary with the position of the section in the slab from both of the boundaries and is denoted $e(x, y)$.

$$e(x, y) = w(x, y) - \left(\frac{h_e}{2} - h_{na}\right) \tag{6.31}$$

The membrane force at the perimeter of the slab varies along the perimeter, figure 6 25, and can be calculated per unit length by integrating equations 6.10 and 6.11 with respect to the relevant axes.

The residual moments of resistance of the section at position x, y can be calculated, as before, by taking moments about the section.

$$M_{Rx}(x, y) = \sigma_s(T)A_s\left(h_e - \frac{h_n a}{2}\right) - F_y e(x, y) \tag{6.32}$$

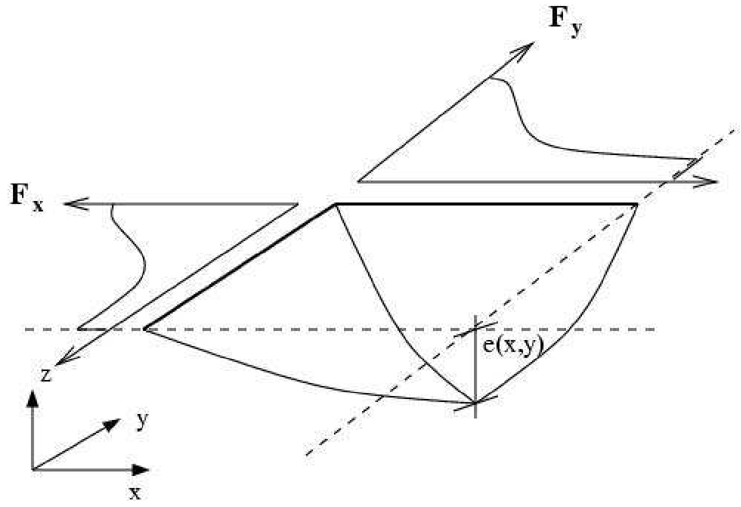

Figure 6.31: membrane force variation along the perimeter of a slab

$$M_{Ry}(x,y) = \sigma_s(T)A_s\left(h_e - \frac{h_n a}{2}\right) - F_x e(x,y) \tag{6.33}$$

The internal work done is the integral of the moment of resistance of the section along the yield line multiplied by the angle of rotation of the section through a unit displacement. For yield lines which do not run parallel with the boundaries, the yield lines are integrated along their lengths projected parallel with the boundaries. Thus the internal work is given by:

$$\Pi_{int} = \sum_{\forall yieldlines}\left(\int_0^{L_x} M_{Ry}(x,y)\Theta dl + \int_0^{L_y} M_{Rx}(x,y)\Theta dl\right) \tag{6.34}$$

The external work is then given by, as for a 1-way spanning slab:

$$\Pi_{ext} = \sum Q\delta \tag{6.35}$$

Where Q is the resultant of the distributed load, q, on the section, and δ is the vertical displacement of Q with unit displacement of the centre of the slab.

6.8 Ultimate Capacity Assessment

To illustrate the transition from one mechanism to another, a 6m 1-way spanning floor slab was analysed. The slab had an assumed depth of 150mm, and steel reinforcement of 1130mm^2/m placed 50mm from the unheated surface of the floor slab. The slab was exposed to a British standard fire of duration 1 hour.

Figure 6.32 shows the evolution of the ultimate moment at the position of the yield lines of the floor slab. Initial expansion of the floor slab at low deflections increases the ultimate moment of the floor slab, until large deflections allow for a release of the pre-stressing force.

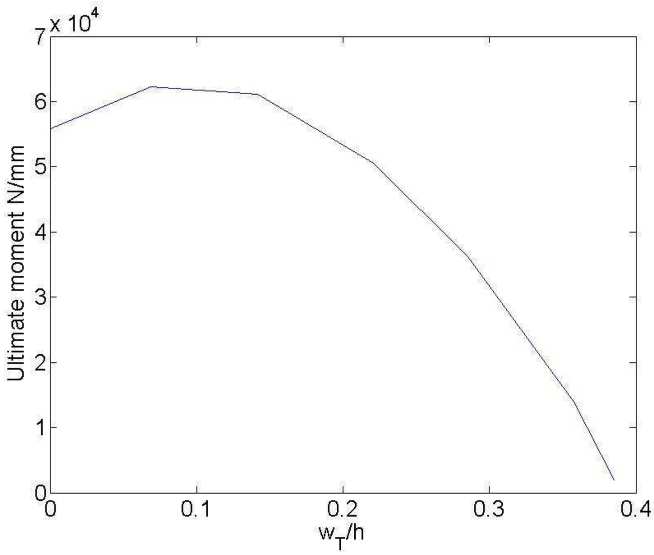

Figure 6.32: evolution of ultimate moment at the yield lines of the slab

Similarly, for a 2-way spanning slab, the ultimate moment varies with the position along the yield line. Since the centre of the slab experiences the largest deflection, the pre-stressing force there is the lowest. At the perimeter of the slab the pre-stressing force is the highest since it experiences the lowest deflections, figure 6.33. For a 2-way spanning slab, flexural capacity resides around the perimeter of the slab for large displacements of the centre of the slab. Although these 'strips' of flexural capacity become increasingly smaller with increasing displacement of the floor slab as the region in tension increases. The complete deflection behaviour of 1- and 2-way spanning floor slabs is illustrated in figure 6.34. If the capacities of the two mechanisms

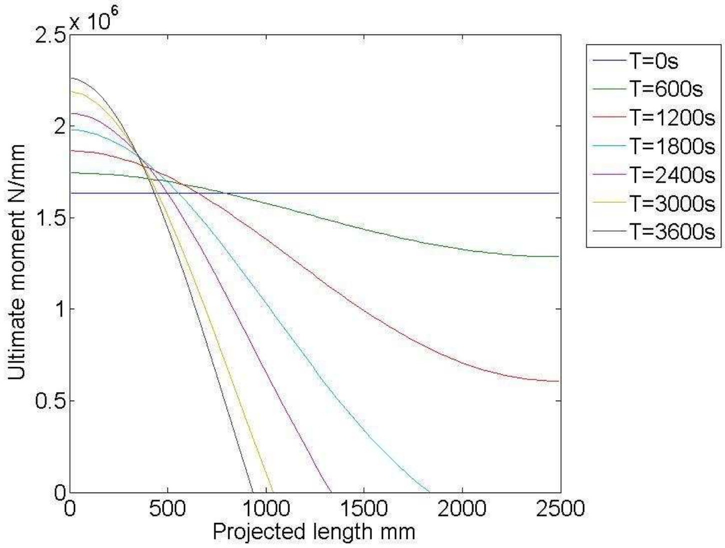

Figure 6.33: evolution of ultimate moment along yield line projected onto slab boundary for a 5 m square slab of 200mm depth, As=1130mm2/m 50mm from the heated surface exposed to a British standard fire

are plotted against the span / depth ratio there are 3 distinct regions in the behaviour of different floor slabs at elevated temperatures and thermal displacements, dependant on their span/depth ratio, figure 6.35. One where

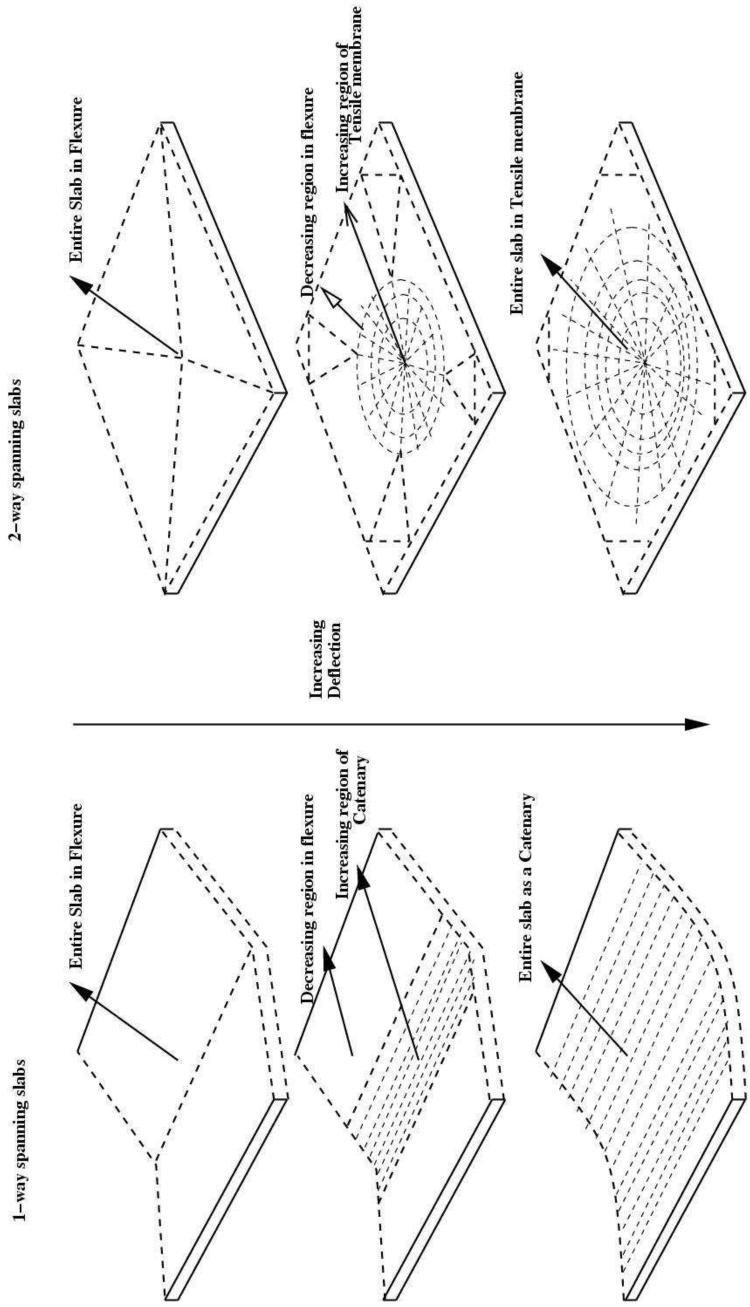

Figure 6.34: transition between flexural and a tensile membrane mechanism with increasing deflection for 1- and 2- way spanning floor slabs

Region	Dominant Mechanism
A	Flexural Only
B	Flexural and Membrane
C	Membrane Only

Table 6.2: summary of capacity dominance in figure 6.35

flexural capacity is dominant, one where membrane capacity is dominant over flexural capacity and one where there is some cross over between the two mechanisms where it can be expected that the mechanisms may work together to provide an enhanced mechanism beyond that which is calculated by one of the theories alone. These are summarised in table 6.2.

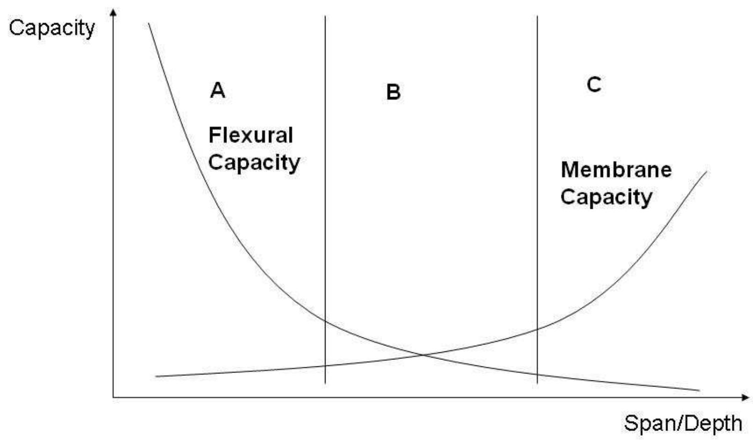

Figure 6.35: schematic capacity variation with span/depth ratio

Comparing the two mechanisms after 20 minutes of a British standard fire over a range of span/depth ratios (depth=200mm, $A_s = 1130mm^2/m$ 50mm from the heated surface), Figure 6 30, the span/depth ratio where transition from one mechanism to another occurs is clear. As shown, the assessment of the capacity of floor slabs must be rationalised by consideration of the cur-

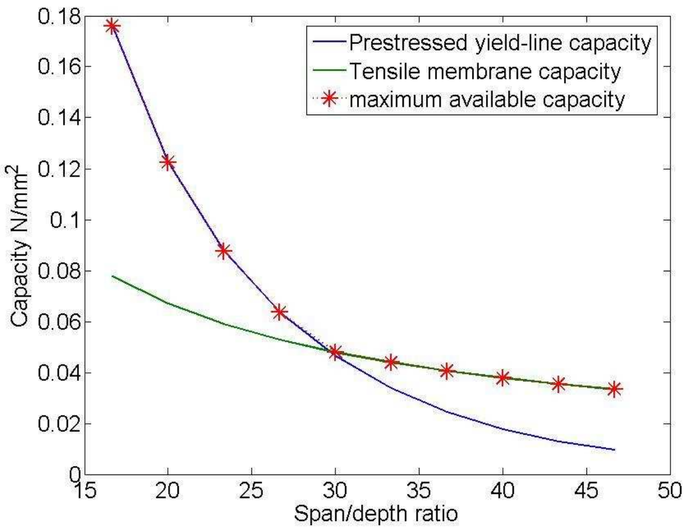

Figure 6.36: after a 20 minutes of a British standard fire, the capacity of the two mechanisms over a range of span/depth ratios

rent mechanism. At low displacements, a yield line mechanism forms over the slab. This can be enhanced by taking account of the thermal 'pre-stressing'. Increasing deflection leads to cracking of the central region of the slab and an onset of tensile membrane action. The tensile membrane hangs at this point from a region of decreasing width around the perimeter. This is the point at which transition to a tensile membrane mechanism described is more likely to occur as the tensile region of the concrete grows and the deflection increases until the load is 'caught' by the steel reinforcement. In the derviation of the thermally prestressed yield line methodology, creep and transient strains are effectively ignored, since the thermal deflection is take directly from the tensile membrane calculations above. These components may have a larger effect on the final capacity of the section, since the ultimate moment is dependant upon the residual concrete strength, more work may therefore be required to fully understand this.

6.9 Conclusions

For the design of floor slabs under thermal loading, research has tended to rely upon a membrane mechanism which requires large deflections to develop in order for the mechanism to mobilise. However, the transition between the ambient flexural, low displacement, design and the tensile membrane mechanism has never been satisfactorily addressed. This omission ignores the positive effect on bending capacity of large compressive forces which occur during a fire.

A new design method was derived here which takes account of the thermal pre-stressing of the concrete floor at developing thermal deflections. By considering the typical yield pattern for a slab, and its evolution as the deflection increases, two distinct cases for the response of slabs under thermal loading have been defined: 1 where the thermal deflection is low enough that a thermally pre-stressed yield line theory still applies and where deflections are not yet large enough for a tensile membrane mechanism to mobilise; and 2, where the deflection is large enough that the pre-stressed yield line theory is no longer applicable due to tensile stresses across the slab but where the deflection is developed enough that a tensile membrane mechanism can develop. The area of region 2 increases with the deflection, decreasing the length of the yield lines and lowering the capacity as calculated by the yield line method, and is associable with the instability which occurs between low and high deflections in concrete floor slabs.

For a tensile membrane mechanism, the ultimate load can be increased by encouraging larger deflections using a thinner slab, or by allowing for a larger thermal strain in the steel of which the membrane is composed by placing it lower in the slab. For the thermal pre-stressing method, the capacity can be enhanced by increasing the lever arm or by increasing the depth of the section. For very high deflections, the membrane capacity is clearly dominant over the flexural capacity, whereas for very low deflections the flexural capacity is dominant.

7

Tall Building Stability

7.1 Introduction

Despite the events of September 11th 2001, there has been very little research carried out into the stability of tall buildings in multiple floor fires. Quiel and Garlock [68, 69], calculate the capacity of beam-columns based upon the axial elongation of the beam, using the column as a spring resisting this elongation; this, however, did not consider the beams acting as a catenary to support the static loading; and it did not consider the potential for failure of the columns given fire on multiple floors. Analysis carried out at the University of Edinburgh on the world trade centre towers focused on identifying and understanding the mechanisms which may have led to their collapse as a result of thermal loading alone. Initial findings and a proposed collapse mechanism were presented in 2003 [70], with additional work presented in 2005 [71]. This collapse mechanism, referred to as a weak-floor collapse mechanism relies is dependant upon the floors adjacent to the fire floors being unable to resist the axial load placed upon them as a result of adjacent floors adopting a catenary mechanism.

Further investigation into the mechanism identified led to the postulation of a further collapse mechanism [72], which can occur when the floors are strong enough axially to resist the forces required to support the fire floors in a catenary mechanism. Although the method of collapse is different, the chain of events leading to the two mechanisms is governed by the same underlying structural mechanics.

7.2 Weak Floor Failure Mechanism

In the weak floor failure mechanism identified, illustrated in figure 7.1 for a 3-floor fire, fire starts simultaneously on multiple floors. Initially, the floors are in a 'push-out' stage, where central deflection of the floor system is relatively low, and a flexural mechanism is still active. Top and bottom fire floors push out against the column; the middle fire floors adopt tensile forces due to compatibility. Floors adjacent to the fire floors, 'pivot floors', which remain cool are also in tension as they restrain the column against lateral displacement. With increasing thermal deflection of the fire floors, resistance to buckling decreases and the top and bottom fire floors are unable to sustain the compressive axial load which is generated by thermal expansion. Top and bottom fire floors lose flexural stiffness and adopt a catenary mechanism first. The middle fire floors and pivot floors adopt compatibility compression as a result of the pull-in forces applied to the column from the catenary of the top and bottom fire floors. All fire floors eventually lose flexural stiffness and adopt a catenary mechanism. This transition is a smooth one which results from a gradual increase in pull-in forces and a decrease in the stiffness of the heated floor systems.

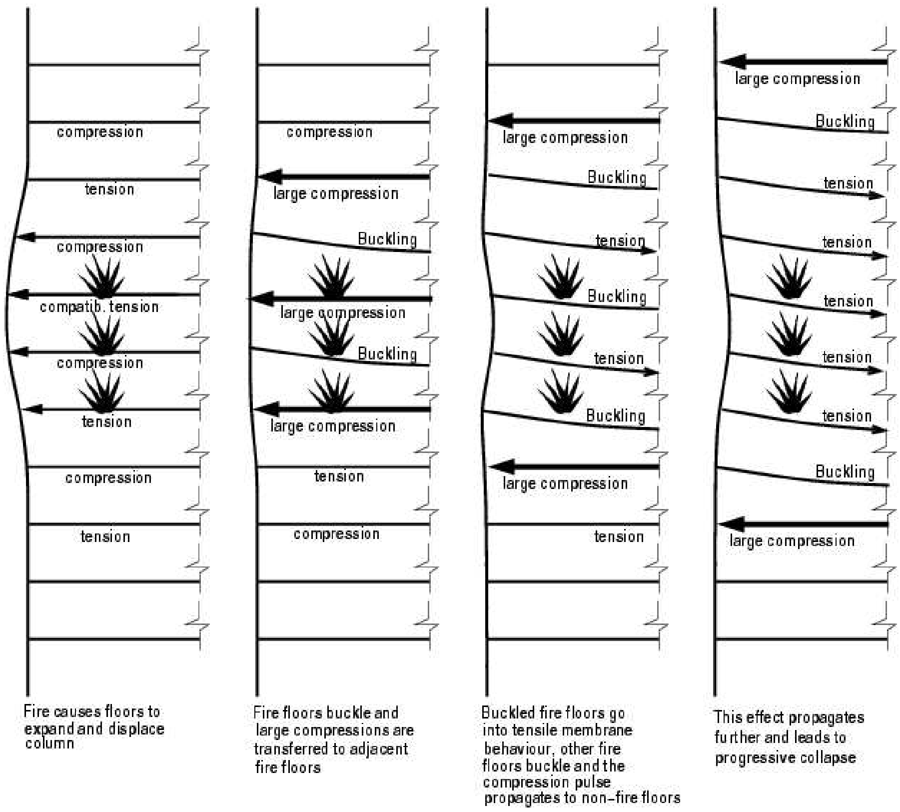

Figure 7.1: weak floor collapse mechanism

Where the pivot floors are unable to sustain the horizontal pull-in forces which result from the catenary of the fire floors, they buckle and the force is transferred to the adjacent floors. Progressive collapse ensues as the buckling 'wave' is propagated along the length of the column.

7.3 Strong Floor Failure Mechanism

In the strong floor failure mechanism, figure 7.2, initial response is similar to that of the weak floor failure mechanism. At the point where all fire floors lose have lost flexural stiffness and adopt a catenary mechanism, the stronger pivot floors are able to resist the induced axial load.

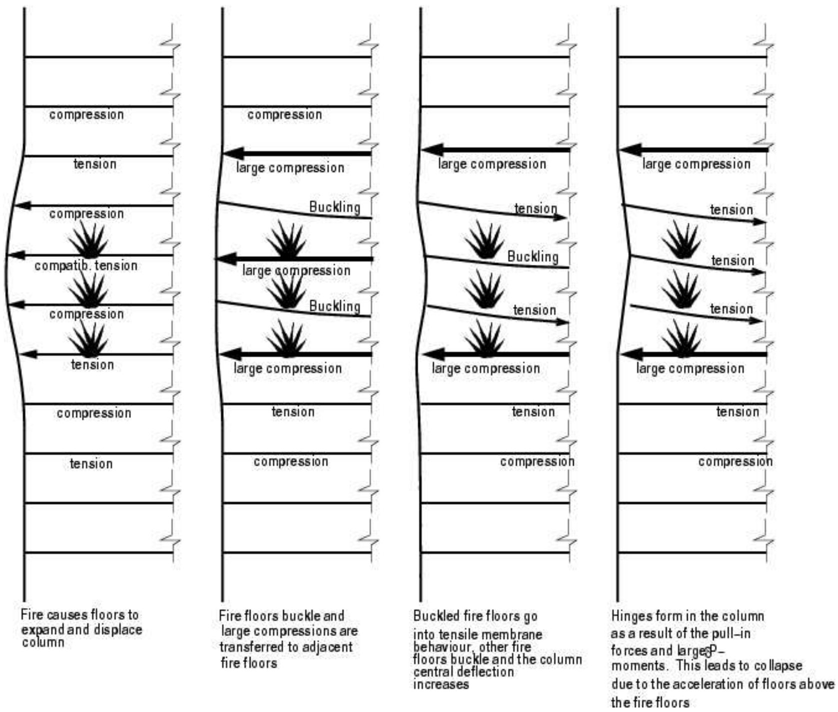

Figure 7.2: strong floor failure mechanism

In this instance, the pull-in forces exerted on the column by the fire floors acting as membranes causes the formation of 3 plastic hinges (column reaches full plastic yield through a combination of axial compression and bending), thus initiating collapse. This collapse is initiated by localised hinge formation, which is not as inherently progressive as the weak floor mechanism, however once the three hinges are formed then the loads from the superstructure will perpetuate the collapse.

7.4 Numerical Modelling

Although the collapse mechanisms described were initially identified for very specific tall buildings in fire, subsequent work has shown them to be relevant for regular multiple storey buildings so long as it can be represented by the frame shown in figure 7.3.

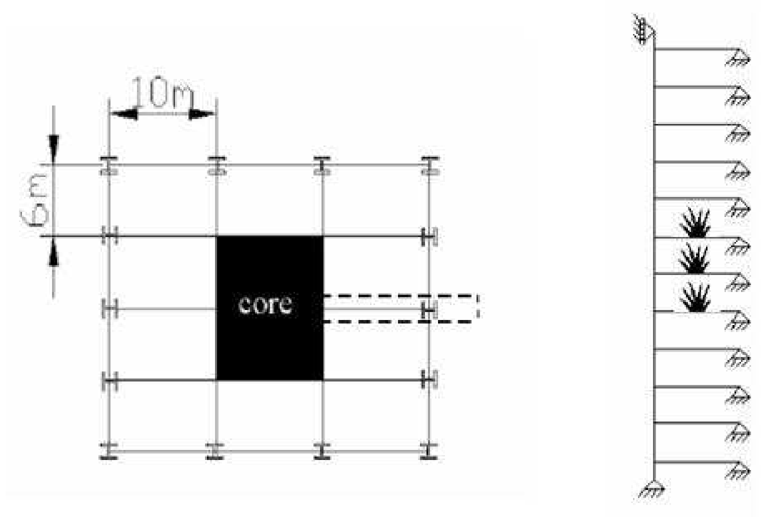

Figure 7.3: typical multi-storey building plan and representative section

The external bays are assumed to be restrained by a stiff internal core [72], i.e. as shown in figure 7.3. This is represented by a 2-dimensional cross section of the column and floor system, as shown, although this representation can be extended to include steel frames without a stiff concrete core so long as sufficient stiffness can be shown to be provided by the bays interior to those on fire.

To illustrate the applicability of the collapse mechanisms to more common structures a conventional composite steel frame was analysed [73]. The beams forming the floor system are laterally restrained by the stiff concrete core but are free to rotate, as shown. They are fully fixed to the exterior column, since much of the floor rotation will be transferred to the column via edge beams under torsion. The column is fixed at the bottom but restrained only in the horizontal direction at the top, allowing vertical displacement. A composite steel/concrete floor system is modelled using beam elements tied together. The structure is subjected to uniform loading on the floor system at each level, as well as a point load on the column representing the load from the structure above the model. The distributed load on the floor systems includes the self weight of the concrete slab as well as the imposed load. To compare the behaviour of the models several parameters were changed to obtain a wide variety of results [10]. This includes changing loads, section sizes and spans. The assumed material properties are in accordance with Euro Code 3-1. In the analysis, the fire was assumed to affect three floors (floors 6, 7 and 8). The steel was assumed to be unprotected and thus experienced a uniform temperature increase equal to that of the fire. This allows for 1-way spanning floor behaviour to develop, where the entire heated floor system adopts a catenary mechanism. The maximum and ambient temperatures were taken as 800^{O}C and 20^{O}C respectively with an exponential increase and the columns are protected and are restricted to a maximum temperature of 400^{O}C.

Two of the resulting models are shown in figure 7.4 which illustrate the two collapse mechanisms. In both models a UC section size 305 x 305 x 198 was used. For the weak floor collapse mechanism a UB section size 305 x 102 x 28 was used and in the strong floor mechanism a UB 533 x 210 x 92 was used. Details of the structures are given in table 7.1.

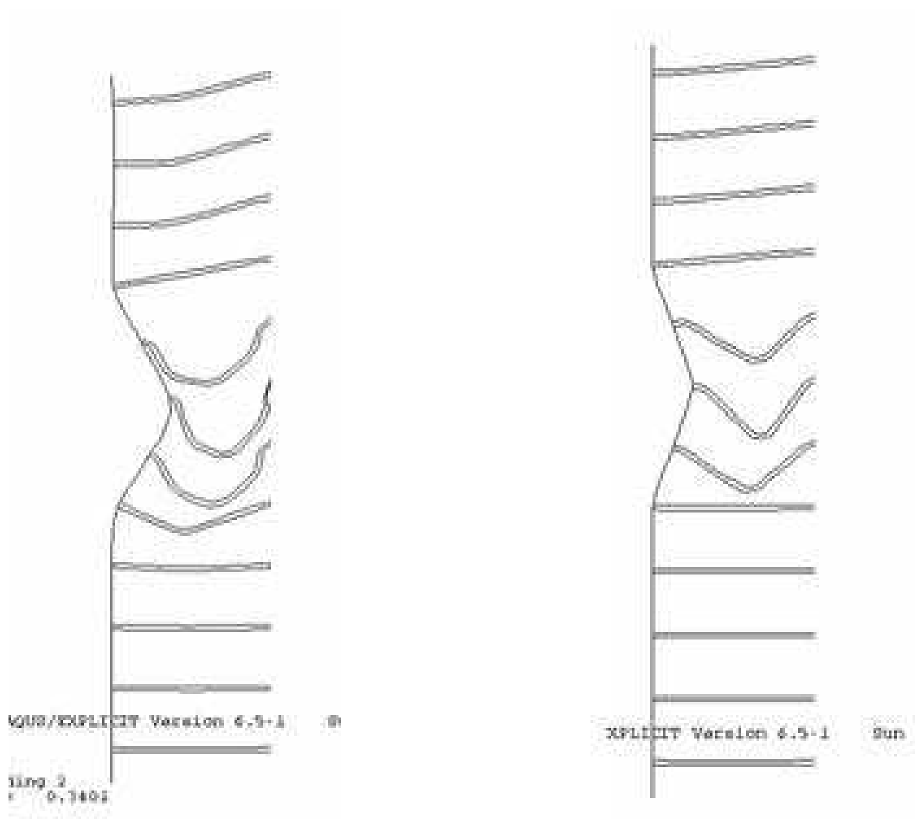

Figure 7.4: weak and strong floor collapse mechanisms: 2D FE Model [10]

	Weak floor system	Strong floor system
Structure		
Column section	305 x 305 x 198	305 x 305 x 198
Beam section	305 x 102 x 28	533 x 210 x 92
Beam depth	309mm	533mm
A_s	$36.3cm^2$	$117cm^2$
I_s	$5420cm^4$	$55230cm^4$
E_s	$200000N/mm^2$	$200000N/mm^2$
Distance between floors	$4000mm$	$4000mm$
Concrete slab:		
Depth	$100mm$	$100mm$
Width	$6000mm$	$6000mm$
Span	$10000mm$	$10000mm$
A_c	$0.6m^2$	$0.6m^2$
E_c	$14000N/mm^2$	$14000N/mm^2$
Loading:		
Distributed load	$45N/mm$	$45N/mm$
Column axial load	$6900kN$	$6900kN$

Table 7.1: details of the numerical models

In the weak floored model, collapse was initiated at approximately 550 seconds. This is almost immediately following the buckling of the upper and lower fire floors and the onset of catenary action of the fire floors. Reaction Forces at the connection of the 4th to the 10th floors and the stiff core of the building are shown in figure 7.5, where the buckling time and the time of onset of collapse are indicated.

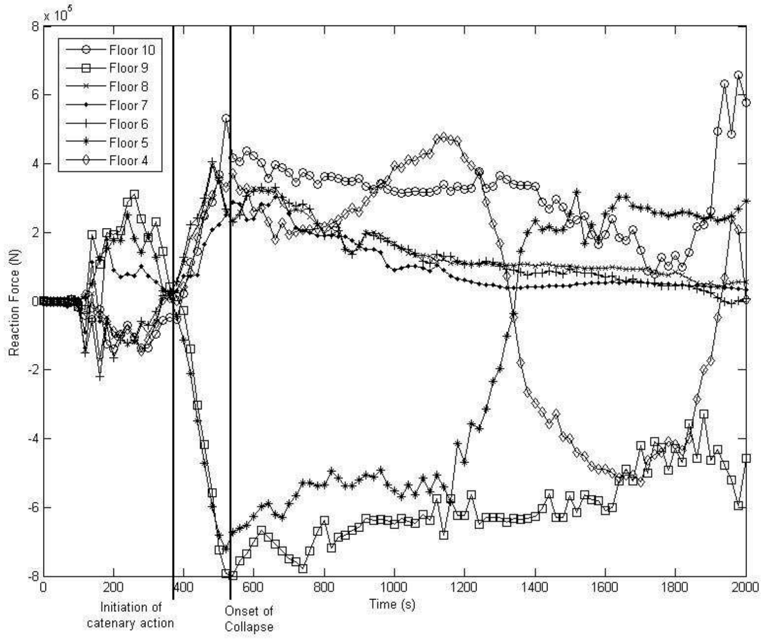

Figure 7.5: weak floor horizontal reaction forces

In the strong floored model, the initiation of the collapse mechanism occurs after approximately 1000 seconds. Again this is immediately following the transfer of the mechanism from a predominantly flexural to a catenary one, figure 7.6. This collapse mechanism takes longer to initiate due to the increased stiffness of the floors and their increased bending stiffness.

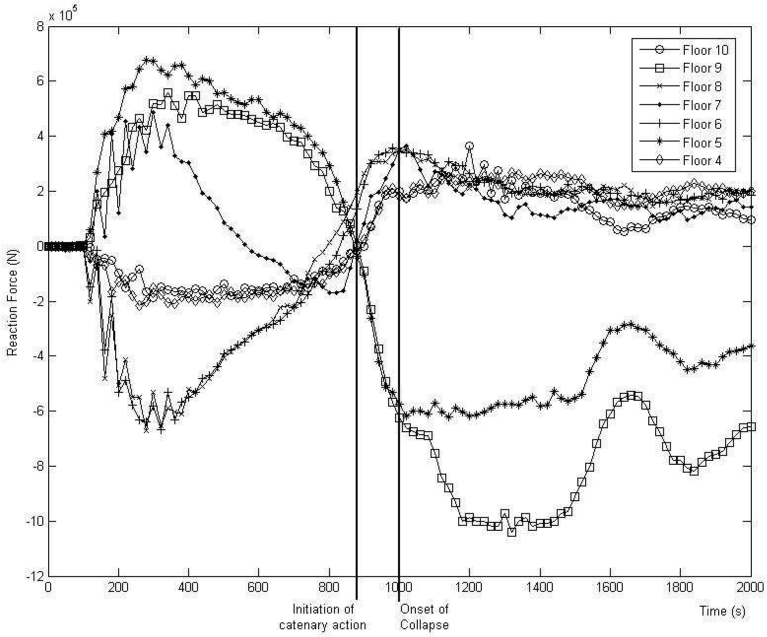

Figure 7.6: strong floor horizontal recation forces

The initiation of both weak and strong floor collapse mechanism for the two generic structural models shown illustrates the validity of these two mechanisms for a range of structures which can be idealised by the 2D representation shown.

7.5 Analytical Modelling

The first stage in the analytical assessment of the two collapse mechanisms identified is to determine the floor response as a result of the thermal loading. Thermal loading can be calculated using a simple one dimensional heat transfer code, or via an appropriate finite difference calculation [74]. Alternatively, BS7974 [75], offers a simplified calculation method for the temperature of concrete slabs in fire.

7.5.1 Thermal Deflection and Thermal Force

Since the mechanisms described rely upon the floor system adopting a catenary mechanism which in turn relies upon the presence of large mid-span deflections, the thermally induced displacements of the floor system must first be calculated.

For a composite steel building, the deflected shape of the floor is calculated based upon the thermal stresses and strains in the concrete deck alone. The application of catenary forces to the column is dependant upon the loss in stiffness of the primary beam supporting the floor system. This is viable for either an exceptionally severe fire in the case of a protected primary beam, or for unprotected steel beams.

In instances where the beam is protected and does not experience a severe temperature increase it is generally assumed that the beam will be able to support the surrounding concrete floor systems as they adopt 1 or 2-way spanning catenary mechanisms as described previously.

However, at the stage where bending is no longer a viable action of any primary steel beams, the material is assumed to be ductile enough that the deflected shape is governed by that of the concrete slab, figure 7.7. In this case the steel of the beam will yield at the connections due to large thermally induced expansion stresses and the steel will effectively hang from the support, adopting the deflected shape of the concrete slab.

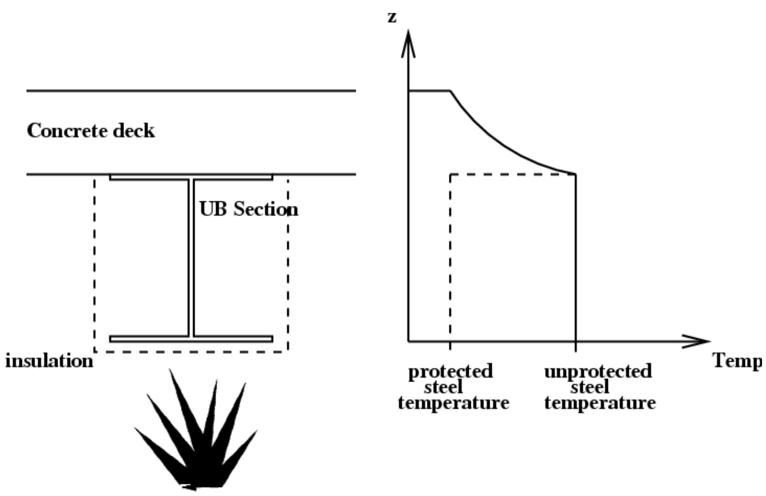

Figure 7.7: exposed and unexposed steel temperatures

7.5.2 Floor Boundary Conditions

During the early stages of fire where the floor system carries the load via a flexural mechanism, the adjacent floors can be assumed to provide lateral support to the column and therefore the stiffness of the column against lateral displacement is high, allowing compressive forces to develop within the floor slab with little or no deflection of the exterior column.

Similarly, where the fire exists on only one floor the translational stiffness of the column is relatively large as a result of the supporting floors. With increasing number of fire floors, this lateral stiffness is reduced, allowing larger horizontal deflections of the exterior column at the fire floors and larger mid-span deflection of the fire floors.

The horizontal stiffness of the column is calculated using the stiffness method, as shown in figure 7.8, assuming an adequate 2-dimensional representation of the structure. Increasing number of floors adopting a catenary mechanism will decrease the stiffness of the column by increasing its effective length. 'Pivot' floors, i.e. floors above and below the fire floors, are represented by a rotational spring.

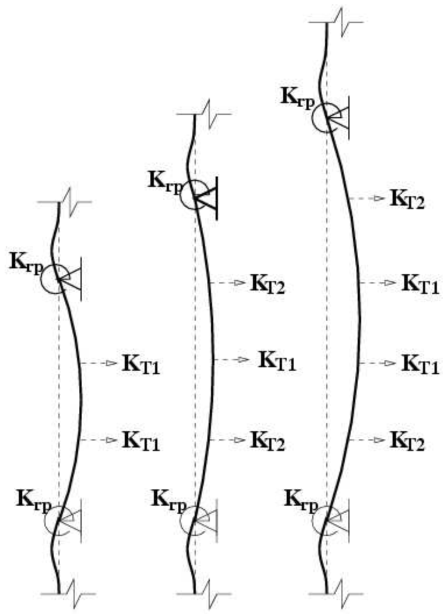

Figure 7.8: lateral stiffness of the exterior column

7.5.3 Horizontal Reaction

Upon initial heating, the floor is in a 'push-out' stage. Forces are compressive and push against the column, figure 7.9. At this stage, the column load is simply the push-out force, N_T, from the thermal loading in both the concrete and the steel. However, for simplicity, it is assumed that $\epsilon_T \approx \epsilon_\Phi$, i.e. no net thermal force is transferred to the column, and little or no initial horizontal displacement is induced at the column. No catenary tension is present while the floor supports load via a bending mechanism.

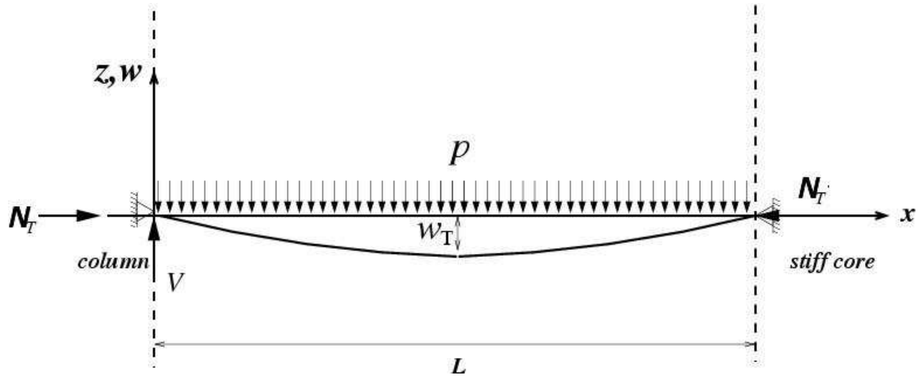

Figure 7.9: displacements and forces as a result of initial heating

Increasing thermal displacements reduce the flexural capacity of the floor, forcing the uniformly distributed mechanical load on the floor to be supported by the system via a catenary, or membrane, action, figure 7.10. This leads to a horizontal pull-in force, N_p, to be exerted on the perimeter framing (column and edge beams). The column resists the pull-in force as a translational spring as discussed, of stiffness K_T, and provides the supporting reaction for the catenary tension in the floor system.

$$N_p = K_T up \tag{7.1}$$

7.5.4 Vector Resolution

Considering the tension in the floor system, at a distance x along the span, it is clear that, dependant upon the deflected shape of the floor system, the horizontal reaction is given by the product of the vertical reaction and the inverse of the gradient at $x = 0$. Assuming that the deflected shape adopted

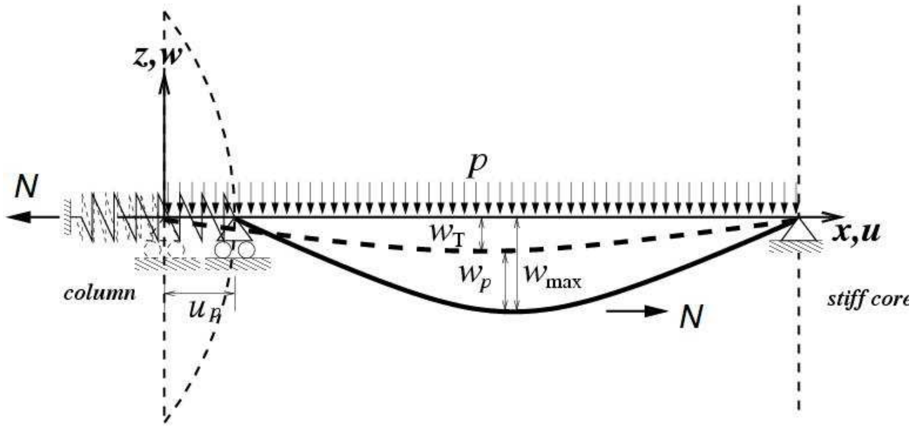

Figure 7.10: total deflections and forces on the floor system under mechanical loading

is that of a sine curve, the reaction is given by:

$$N_p = \frac{pL^2}{2\pi w_{max}} \tag{7.2}$$

7.5.5 Catenary Tension

The components of the tension in the floor system are shown in figure 7.11. The tension in the floor at any point is the resultant of the shear forces at that point and the horizontal force. By resolving the shear force and the pull-in force vector, the tensile force in the floor is given by:

$$F(x) = \sqrt{N_p(x)^2 + V(x)^2} \tag{7.3}$$

The horizontal force is constant across the span, and therefore tension in

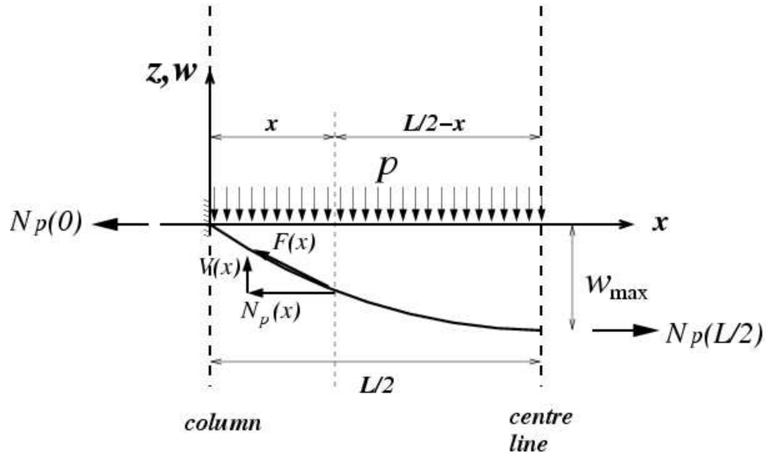

Figure 7.11: components of the tension in the floor system

the floor varies only with the shear force.

$$N_p(0) = N_p(x) = N_p \tag{7.4}$$

$$V(x) = p\left(\frac{l}{2} - x\right) \tag{7.5}$$

7.5.6 Floor Elongation

At large displacements, the contribution from concrete to the floor system is ignored due to widespread tensile cracking of the concrete. The horizontal pull-in force should therefore be calculated based upon the total tensile force in the steel in the floor system, at a vertical deflection where the available steel carries the applied load.

$$F(x) = A_s E_s(T)\epsilon_s(x) \tag{7.6}$$

Substituting equation 7.3 into equation 7.6, the increase in length, ΔL_p, can be calculated by integrating the strain along the length of the floor.

$$\epsilon_s(x) = \frac{\sqrt{{N_p}^2 + p^2 \left(\frac{l}{2} - x\right)^2}}{A_s E_s(T)} \tag{7.7}$$

$$\frac{\Delta L_p}{2} = \int_0^{l/2} \epsilon_s(x)dx = \frac{1}{A_s E_s(T)} \int_0^{l/2} \left({N_p}^2 + p^2 \left(\frac{l}{2} - x\right)^2\right)^{1/2} dx \tag{7.8}$$

$$\begin{aligned} \frac{\Delta L_p}{2} &= \frac{1}{A_s E_s(T)} \left[\frac{2p^2x^2 - p^2 l}{4p^2} \left({N_p}^2 + p^2\left(\frac{l}{2} - x\right)^2\right)^{1/2} \right. \\ &+ 4p^2 \left({N_p}^2 + p^2 \frac{l^2}{4}\right) \\ &\left. - \frac{p^4 l^2}{8p^2} ln \left(2 \left(p^2 \left({N_p}^2 + p^2 \left(\frac{l}{2} - x\right)^2\right)\right)^{1/2} + 2p^2 x - p^2 l \right)_0 \right. \end{aligned} \tag{7.9}$$

7.5.7 Floor Catenary Deflection

w_{max}, and u_p in equations 7.1 and 7.2 are related by the change in length of the floor system under mechanical loading, ΔL_p. Recalling the assumption that the lateral thermal deflection of the floor system is negligible, i.e. $\epsilon_T \approx \epsilon_\phi$, the maximum deflection is given by equation (8.10).

$$w_{max} = \frac{2L}{\pi} \sqrt{\frac{L_T + \Delta L_p}{L} + \frac{\left(\frac{L_T + \Delta L_p}{L}\right)^2}{2}} \tag{7.10}$$

Equations7.1, 7.2, 7.9 and 7.10 can now be solved to obtain the pull-in forces resulting from the mechanical load.

7.5.8 Composite Beam Pull-in Force Example

To illustrate the calculation of pull-in forces resulting from a fire under a floor slab, the system shown in figure 7.12 is analysed. The steel beam is assumed to be unprotected, and the temperature of the beam is assumed to follow the compartment temperature time curve. The pull-in force is calculated for the steel beam alone, in this case ignoring the contribution of the reinforcing steel. Since steel is a thermally thin material, i.e. high conductivity, thermal gradient is very low in the steel beam. Uniform high temperatures will increase ductility of the steel and induce large compressive forces in the section causing it to yield plastically at the connections early on in the fire. Therefore the thermal deflection is calculated based upon the thermal gradient and thermal expansion of the concrete floor slab spanning between primary beams.

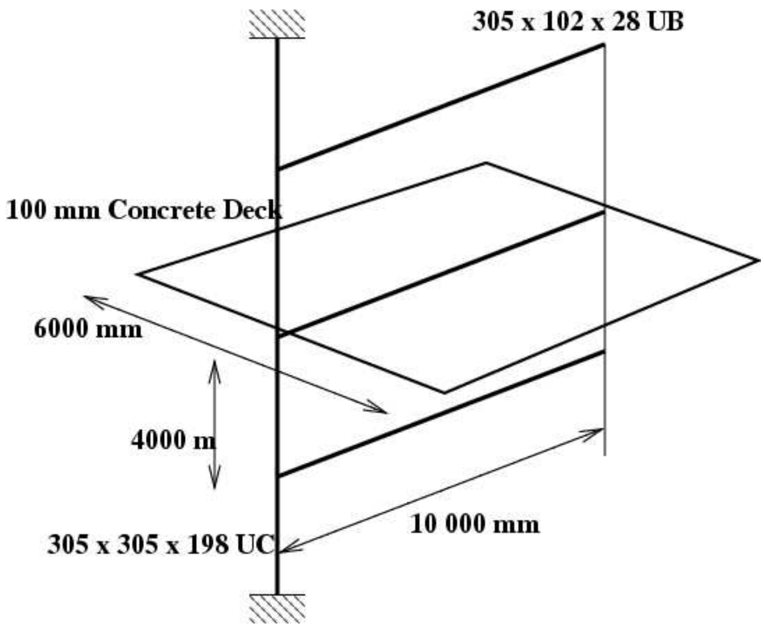

Figure 7.12: pull-in force example structure

A generalised exponential fire is applied to the underside of the floor system, as described by equation 7.11, where α controls the heating rate. Maximum temperature is 800^{O}C, total duration is 3600seconds and α is 0.005. Heat transfer to the slab is calculated using a one dimensional finite element script, resulting in a uniform temperature increase, ΔT; and an equivalent thermal gradient, $T_{,z}$. As already stated, the steel beam is assumed unprotected and therefore its temperature follows the compartment temperature.

$$T(t) = T_0 + (T_{max} - t_0)(1 - e^{-\alpha t}) \tag{7.11}$$

Mechanical loading was applied to the beam via a $45N/mm$ line load, representing the total distributed load on the floor of $7.5 \times 103N/mm^2$. The resulting thermal deflections of the floor system are shown in figure 7.13.

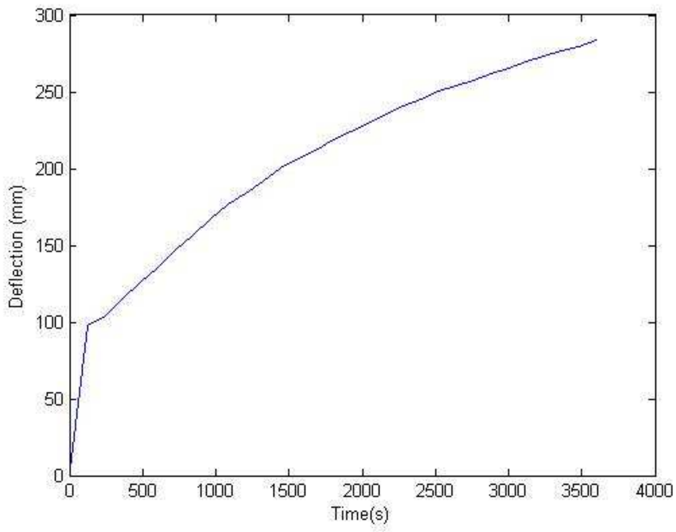

Figure 7.13: thermal deflection of the floor system in figure 7.12

In order to verify the analytical study, a simple numerical analysis was carried out using the finite element software ABAQUS. For the numerical study, the bending resistance of the floor system was kept to a minimum in order to encourage catenary action by using a very thin beam element to represent the floor system. The element had the same area as the analytical model, but a very small moment of inertia. Assuming that the beam is at constant temperature equal to the maximum compartment temperature, the numerical model showed that at a deflection of approximately 910mm, the pull-in force was 6.1×10^5N.

Pull-in forces for the beam obtained from the analytical model are shown in figure 7.14. From the same analysis, the total resulting deflection of teh floor system is shown in figure 7.15. Comparison with the results of the numerical analysis shows that the thermal deflection and the resulting pull-in force of the floor system at 400 seconds is comparable with the numerical analysis.

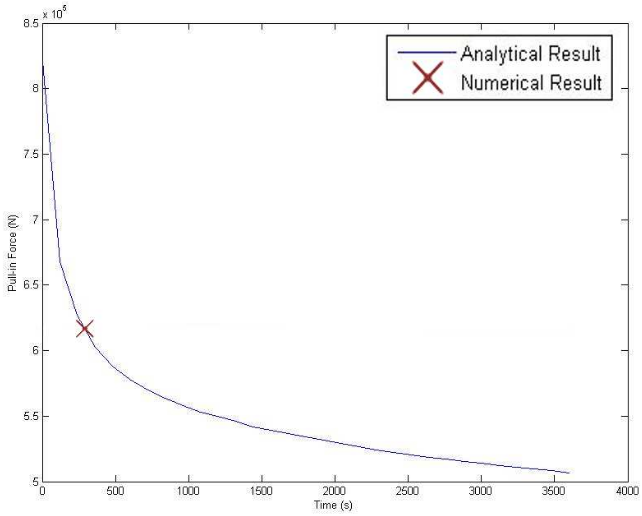

Figure 7.14: pull-in forces based upon the primary beam only

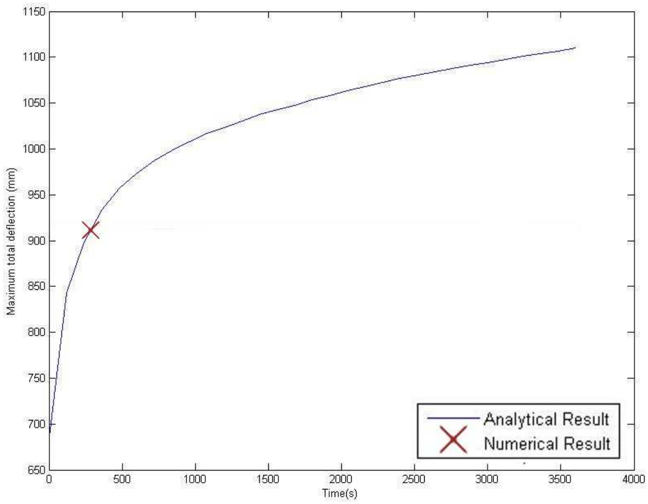

Figure 7.15: total vertical deflection of the floor system

The analytical deflection shown in figure 7.15 increases over the numerical result shown after approximately 240 seconds have elapsed. In the analytical model, the primary beam is forced to follow the deflected shape of the floor slab, and so additional tension is created in the beam as a result of the concrete deflection. This increased deflection reduces the horizontal component of the tension in the beam, and therefore the horizontal pull-in forces decrease past this point, the corresponding decrease is seen in figure 7.14.

7.5.9 Reinforcement Mesh Pull-in Force example

In reality, membrane resistance will come from the reinforcement in the floor slab, embedded within the entire span of concrete deck. Therefore the steel used in calculating the pull-in forces should be that of the anti-cracking mash spanning parallel to the beam as well as any additional reinforcement in the slab. This steel will be much cooler than that of the primary beam.

The beam in figure 7.12 is replaced by an A142 anti-cracking mesh, typical of steel reinforcement supplied in composite concrete panels. The mechanical loading remains unchanged; however, the reinforcement is assumed to lie at mid-depth in the concrete slab and therefore is at a much lower temperature. The resulting pull-in forces from this steel arrangement are shown in figure 7.16. This is the total pull-in force applied across the entire span of the floor system. The pull-in forces in this case are substantially larger due to the lower ductility of the steel at the current temperature, and the corresponding deflections are therefore lower, as shown in figure 7.17. Numerical results from the same analysis as before are also shown in figures 7.16 and 7.17 for comparison with the analytical results. In this case, however, the steel representing the reinforcing mesh in the numerical model is subject to an increase in temperature over the course of the analysis representative of the actual temperature of the reinforcing steel in the floor system. Overall good correlation is shown to occur between the two methods, with peak forces being very similar.

Where additional structural steel in the form of primary beams is available, equation 7.6 should include an additional term representing this. Unless the steel is at a low temperature, i.e. in the case of unprotected steel, the resulting material degradation will be such that the steel will have very low strength and stiffness. Assuming that this additional steel has yielded due to the applied thermal force, the tensile force becomes:

$$F(x) = A_s E_s(T)\epsilon_s(x) + A_b\sigma_{yb}(T) \tag{7.12}$$

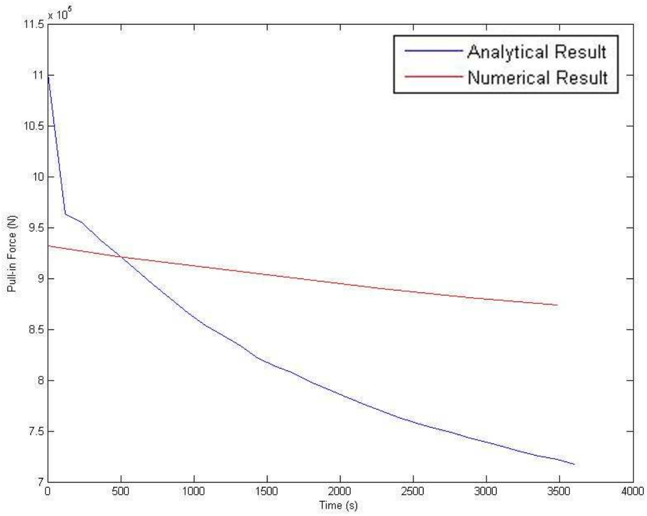

Figure 7.16: pull-in forces on the structure from an A142 steel anti-cracking mesh

The highest pull-in forces occur after transition of the mechanism from a flexural one to a catenary because of the high horizontal component of the resulting axial load in the floor system at low deflections. Therefore the surrounding structure should be designed to withstand these peak forces.

7.6 Column Loading

The result of the floor system adopting a catenary mechanism will be that the tensile force of the reinforcement is transferred to perimeter beams via shear studs and bent over reinforcement bars at the floors edge, and this pull-in force is then transferred to the exterior column, figure 7.18. Where the primary beam spanning between the exterior column and the stiff internal core of the building adopts a catenary, any additional pull-in force from the beam will also be transferred to the column via the connection.

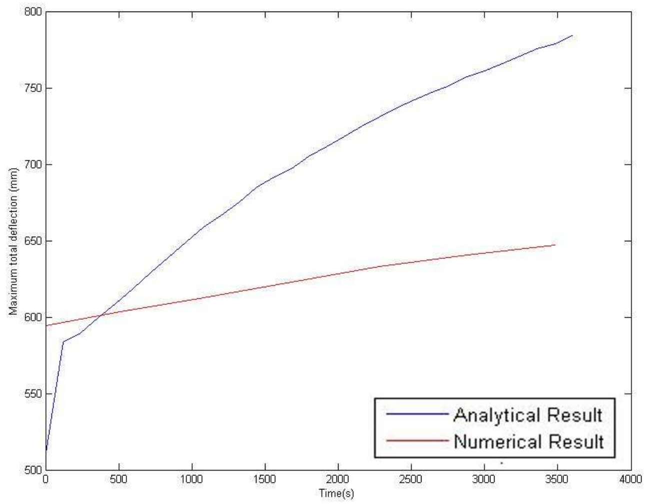

Figure 7.17: vertical deflection from the catenary action of the reinforcement

The resulting horizontal forces, in conjunction with the removal of lateral restraint as a catenary mechanism is adopted by adjacent fire floors, will cause large displacements in the column. The total moment on the column is the sum of the P-δ moment from the axial load on the column and the moment induced by the pull-in forces.

7.7 Minimum Deflection Required

For the one-dimensional model considered, the floor needs to adopt a catenary response to the loading before any tensile forces can be applied to the column. No provision is made for the floors ability to carry the load via a flexural mechanism in the calculation method presented. The earliest time at which the analysis can reasonably be applied to the columns corresponds

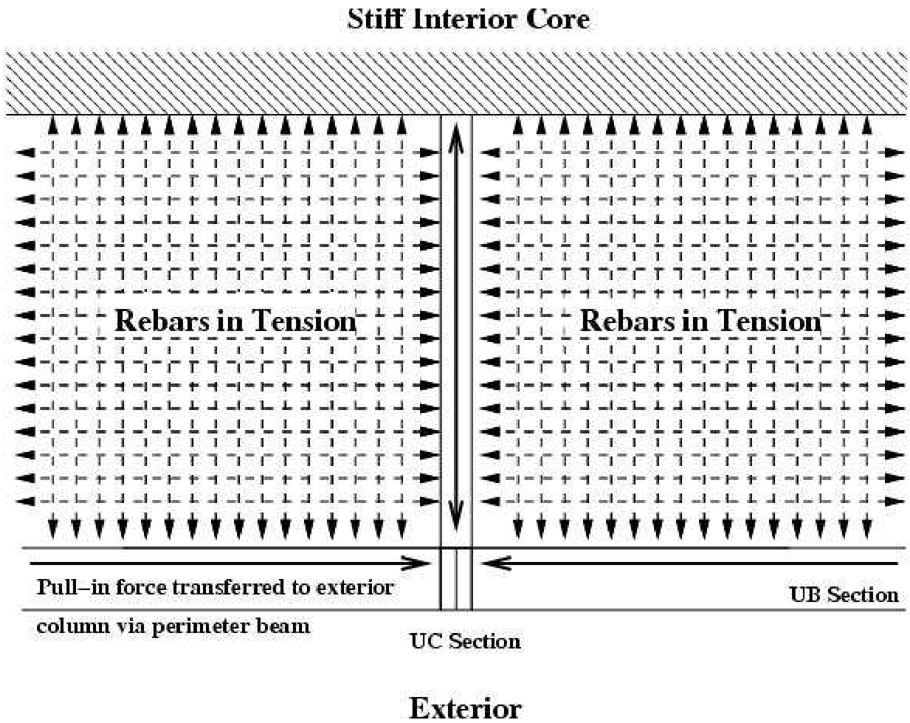

Figure 7.18: transfer of the pull-in forces from the steel reinforcement in the floor to the column

to the time at which the floor system stops carrying the applied loading via a flexural mechanism and starts to carry the load via a catenary or membrane mechanism.

This can be estimated from the slab models described in the previous chapter. However, since full axial restraint is assumed in both axes when determining the resistance of the floor slab the evolution of the membrane force at the floors boundary is larger than would be present given the translational spring provided by the column.

Alternatively, Usmani suggests that the minimum deflection required for the adoption of a catenary mechanism is approximated by the following inequality, based on empirical observations made during the analysis of the Cardington tests:

$$w_T > \frac{L}{10} \tag{7.13}$$

7.8 Failure Mechanism Assessment

Having calculated the mechanical response of the floor, i.e. the horizontal pull-in force, the increase in length, and the horizontal deflection of the sprung support, there are three checks which need to be made to assess the stability of the structure.

Firstly, the ability of the floor to sustain the required tensile load as a catenary has to be determined; this should also include some consideration of the transmission of the pull-in forces to the perimeter beam.

Secondly, the ability of the pivot floors to sustain axially the reaction required preventing lateral displacement of the column at levels above and below the fire floors should be determined.

Thirdly, the moment resulting from the pull-in forces as well as the P-δ moment resulting from the axial load on the column and the lateral displacement should be determined.

7.8.1 Floor Failure

The floor system applies a very large horizontal pull-in force to the column. It should be checked that the floor is able to sustain the load which it is applying. The largest mechanical strains occur in the steel at the supported edges of the floor system. From equation7.7:

$$\epsilon_{max} = \frac{\sqrt{{N_p}^2 + p^2 \left(\frac{l}{2} - x\right)^2}}{A_s E_s(T)} \tag{7.14}$$

In addition to this, the shear connectors around the edge of the floor system which transfer the pull-in force to the perimeter beam should be able to resist the pull-in force applied to the column, distributed along the entire length of the perimeter beam. The force on the connectors, N_s distributed at pitch ϕ, for a floor of width L applying a pull-in force N_p to the column is:

$$N_s = N_p \frac{L}{\phi} \tag{7.15}$$

7.8.2 Weak Floor Collapse Mechanism

The pivot floors, the floors above and below the fire floors, must be able to resist axially the reaction required to resist horizontal translation of the column. The axial resistance of the floor system should include a contribution from both the steel and the concrete decking. According to Eurocode 4 [76], the effective width of a concrete deck acting compositely with a steel beam is equivalent to one quarter of the composite length:

$$B_{eff} = \frac{L_{comp}}{4} \tag{7.16}$$

This effective width should be used to calculate the axial resistance of the floor system as well as a bending stiffness using the reduced modular ratio to determine the buckling resistance of the section.

It should be noted at this stage that equation 7.16 is intended for use in calculating the effective width of the composite deck for bending. It is suggested here for lack of a better value for the effective width and further research may yield a more suitable value.

7.8.3 Strong Floor Collapse Mechanism

In the strong floor failure mechanism identified the pivot floors above and below the fire floors are strong enough axially to resist the total horizontal pull-in force. They are also strong enough to resist any P-δ moments associated with the cool floor deflection and the pull in force caused by the fire floors. If the floors are strong enough and are shown not to buckle, the column should be checked for the 3-hinge mechanism shown in figure 7.2.

The three hinge mechanism is caused by a combination of the moments induced in the column by the horizontal pull-in force and the large P-δ moment resulting from the horizontal displacement of the column under loading and the vertical load above the pivot floor from the superstructure above the fire floors.

For the column to withstand the pull-in forces, the following inequality should be satisfied (where n=2 for a rectangular section; n≈1.3 for an I-section bending about it's major axis or a box section; and n≈2 for an I-section bending about its weak axis):

$$\frac{M}{M_p(T)} + \left(\frac{P}{P_p(T)}\right)^n < 1 \qquad (7.17)$$

7.9 Proposed Tall Buildings in Fire Stability Assessment Methodology

By carrying out the above checks logically and following the analytical method described, a simple assessment methodology for tall building collapse mechanisms in fire can be derived. Figure 7.19 illustrates such a design methodology.

The steps in the proposed methodology are as follows:

1. Structure and Thermal Loading Based on appropriate risk based criteria, establish the following:
    - An adequate two-dimensional representation of the structural frame, including the exterior columns and the adjacent structural framing, which is assumed to be restrained in the interior by a stiff core;
    - The time dependent magnitude of fire in the compartments adjacent to the exterior columns of the structure (using one of BS476,

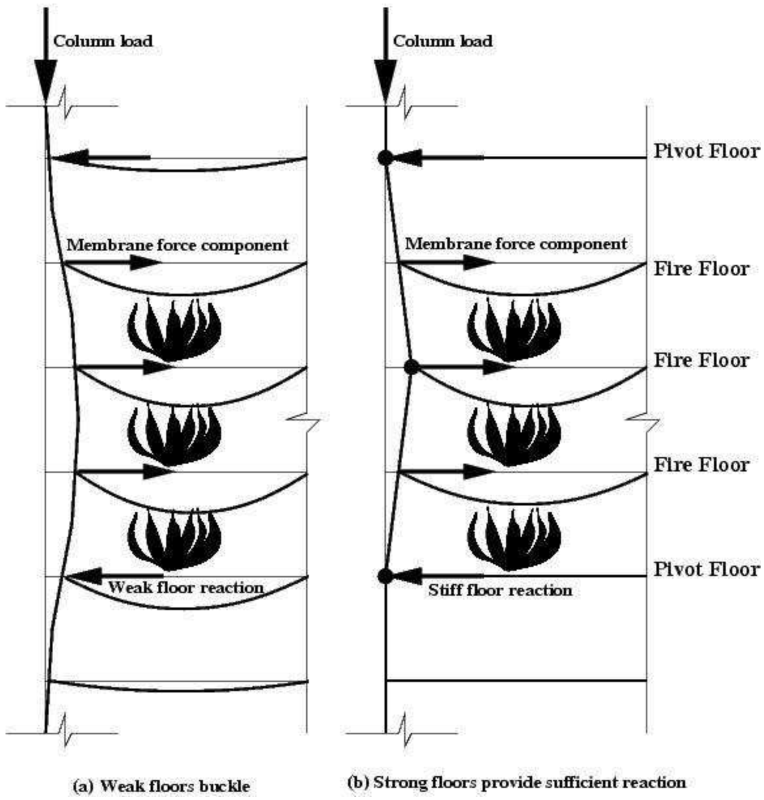

Figure 7.19: simple assessment methodology

ISO834, ASTME119 or Eurocode 1 based curves or other more advanced fire models);

- The number of floors involved in the fire;
- The temperature distribution in the structural members of the frame (columns and floor systems) at the end of the heating curve using appropriate code formulas or tables or heat transfer calculations;
- Convert the temperature distribution at the end of the heating phase to an equivalent uniform temperature and through depth thermal gradient.

2. Floor Mechanical Loading Determine the mechanical state of the floor system after application of the design thermal input (i.e the reduction in strength and stiffness of the component materials and the change in geometry) ignoring the mechanical loading, and follow these steps:

    - Check if the applied uniformly distributed load (using appropriate reduction factors allowed by code) on the floor can be resisted through residual flexural capacity - if this is the case, stop the analysis as the structure can not fail in either of the two collapse mechanisms shown in figure 7.19;
    - If the design udl is greater than the flexural resistance of the floor, check to see if the udl can be resisted by the floor system through catenary action, here the concrete tensile resistance is ignored and only the reinforcement and any composite structural steel are assumed to provide catenary resistance. If the floor system is unable to provide the tensile resistance (limited by rupture of reinforcement and fracture of structural steel connection) than the floor system fails, leading potentially to progressive collapse. The floor system should be redesigned until it is able to resist the udl through flexure or catenary action.
    - Determine the "pull-in" forces applied on the column by the fire floors sagging in catenary action.
    - At this stage determine the ability of the floor system and the shear studs to support the pull-in force

3. Column Mechanical Loading Using the catenary 'pull-in' forces applied by the floors, obtain the moments induced in the columns at the 'pivot' floors (adjacent to the fire floors) and in the centre of the height

between the pivot floors. Use an approximation of the column internal displacement to calculate the additional P-δ moments experienced by the columns.

4. Check for Weak Floor Collapse Mechanism Calculate the reaction of the pivot floors as shown in figure 7.19 counteracting the membrane 'pull-in' forces. If the floor membrane is unable to provide the reaction calculated, a weak floor failure becomes possible. This failure is relatively less likely to occur as it requires the pull in forces from many floors on fire. However a combination of the membrane compression induced in the floor and the additional moment imposed on the sagging floor by the P-δ effect and by the rotation of the column may also cause a combined bending and compression failure of the floor with only a few floors on fire, also leading to a weak floor failure.

5. Check for Strong Floor Collapse Mechanism Perform an analysis to calculate the column deflection under the 'pull-in forces' from the fire floors. Check the temperature dependent moment-force interaction diagram for the column to ensure that the column has not reached yield surface (and thus formed a plastic hinge). If this is the case at all three locations (pivot floors and middle fire floor) then the strong floor failure mechanism identified can occur as the three hinges form a mechanism.

7.9.1 Example

To illustrate the methodology in use, the following structure is checked for either of the two collapse mechanisms presented:

- a 12 storey frame, consisting of a 305 x 305 x 137 UC section, braced to a stiff internal core by a series of composite concrete floors at spacing of 4m;
- floor systems span 8m, have a width of 6m, and concrete depth 100mm with an As of 142mm^2/m positioned mid way through the slabs depth, σ_y of the steel reinforcement is 600MPa;
- Total uniform distributed loading on the floor system is 7.5kN/m^2.

The steel providing the catenary is the steel reinforcement of the floor system. No structural steel is used in calculating the resistance. The rotational stiffness at the pivot floor is provided by the entire composite floor system, including the concrete slab across the full width. A 2 dimensional representation of the structure is shown in figure 7.20. The stiffness matrix required for the calculation of the horizontal stiffness coefficients is as follows:

$$K = \begin{pmatrix} \frac{6EI}{L_1} + \frac{4EI}{L_2} + \frac{3E_F I_F}{L_F} & \frac{6EI}{L_2^2} & \frac{2EI}{L_2} & 0 \\ \frac{6EI}{L_2^2} & \frac{12EI}{L_2^3} + \frac{12EI}{L_3^3} & \frac{6EI}{L_3^2} - \frac{6EI}{L_2^2} & \frac{6EI}{L_3^2} \\ \frac{2EI}{L_2} & \frac{6EI}{L_2^2} - \frac{6EI}{L_3^3} & \frac{4EI}{L_2} + \frac{4EI}{L_3} & \frac{2EI}{L_3} \\ 0 & \frac{6EI}{L_3^2} & \frac{2EI}{L_3} & \frac{4EI}{L_3} + \frac{4EI}{L_4} + \frac{3E_F I_F}{L_F} \end{pmatrix}$$

Using an appropriate modular ratio for the concrete decking, and calculating the rotational stiffness of the column at the height of the pivot floor, the stiffnesses at the fire floors are given in table 7.2.

1. Structure and thermal loading Line loading on the floor representing

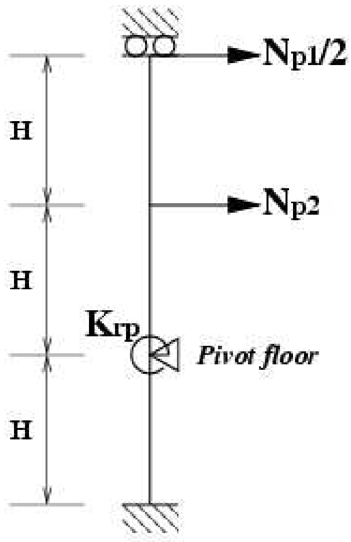

Figure 7.20: 2 dimensional representation of the structure

	Weak floor system	Strong floor system
$K_1, (N/mm)$	4177	4386
$K_2, (N/mm)$	24689	26381

Table 7.2: lateral column stiffness at fire floors

the entire UDL is 45kN/m length of floor. Thermal loading is approximated by an average temperature increase of 150^OC and an equivalent thermal gradient of 5^OC/mm.

Lateral stiffness to translation at the floor levels is calculated taking into account the contribution to the stiffness of the floors immediately above and below the pivot floors.

2. Floor mechanical loading The severe thermal gradient which is imposed

Pull-in force (N)	Vertical Deflection (mm)	Lateral Deflection (mm)	$\Delta L(mm)$
4.6×10^5	785	36.0	98.9

Table 7.3: pull-in forces

on the floor slab will cause large thermal displacements, and therefore it can be assumed that flexural capacity is not available as a viable load carrying mechanism under the prescribed conditions.

Following the method presented, the pull-in force, the vertical deflection, the lateral deflection and the increase in the length from the floor acting on the column are as summarised in table 7.3, for one mid-height floor on fire.

The increase in length of the floor system is 98.8mm, equating to an average strain in the reinforcement of 1.2%, which is less than the rupture strain for standard ductility reinforcement steel as described in EC2 [38]. The pull-in force equates to an average stress of 540MPa on the steel reinforcement, which is less than the yield stress stated.

3. Column mechanical loading Assuming that there are 3 fire floors, above which are 6 non-fire floors the axial load on the column at the level of the top pivot-floor is 2160N. Performing a 2nd order elastic analysis on the structure using the program Mastan 2 [77], the maximum moment on the column as a result of the combined P-δ moment and the pull-in

forces is 1.6×10^6Nm. The horizontal reaction forces at the pivot floors is 1.4×10^6N.

4. Check for Weak Floor Collapse Mechanism The steel beam acting in composite with the floor system should be able to withstand an axial load of 1.4×10^6N without buckling. The capacity of the floor system to withstand the axial load can be enhanced by considering the combined buckling capacity of the steel beam and concrete decking acting in composite, using an appropriate modular ratio.

5. Check for Strong Floor Collapse Mechanism The column section obviously has some effect on the stiffness to lateral translation, and therefore will have a small effect on the pull-in forces calculated in the analysis. However, the column design should be iterated to withstand the maximum moment as calculated.

7.10 Conclusions

Two possible collapse mechanisms for tall buildings in fire have been postulated. Although the analyses carried out have generally been for 2-dimensional structures, most structures are of regular plan and therefore the results can be taken to be representative of the response of a regular multi-storey building subject to fire attack on multiple floors.

Pull-in forces and deflections of floor systems as a result of fire can be simply and effectively calculated using the analytical techniques developed in this chapter, and the resulting forces and deflections compare well with those from finite element analyses. These pull-in forces are transferred via edge beams and primary beams to perimeter columns of buildings, inducing large displacements and moments in the columns leading to one of the two collapse mechanisms described.

The results from the pull-in force calculation can be used in the presented design methodology to provide a quick and simple assessment of tall building stability given fire on multiple floors - something which current codes and design guides omit. Where uncertainty or potential failure of the building is apparent using the method a more complex numerical study can be carried out to provide an additional check, or the structure can be strengthened and rechecked using the method presented. The results can also be used to determine the validity of finite element analyses, providing an initial estimate of the magnitude of pull-in forces in complex structural models.

8

Case Studies

8.1 Introduction

In 1992 the steel construction institute published a document comparing the costs of various construction options in generic commercial buildings. The study was updated in 2003, funded by Corus group plc. in order to compare new technologies being taken advantage of by the construction industry [78]. The results of the project are summarised in a document published by Corus

C&I titled 'Supporting the commercial decision' [79].

Two buildings were considered for the study, a small building of 2600m2 floor area, four storeys high; and a larger commercial building with an atrium of 18000m2 floor area 8 storeys high. For the purposes of the study, the smaller of the two buildings was assumed to be in Manchester, and the larger of the two buildings was assumed to be in London.

In this chapter, the performance in fire of the two buildings is determined for two of the structural schemes considered in the original study, following the proposed assessment methodology and recommendations are made to overcome any deficiencies encountered.

8.2 Building A

The Manchester office building is a four storey office building, the plan and architectural features of which are shown in figure 8.1 and figure 8.2.

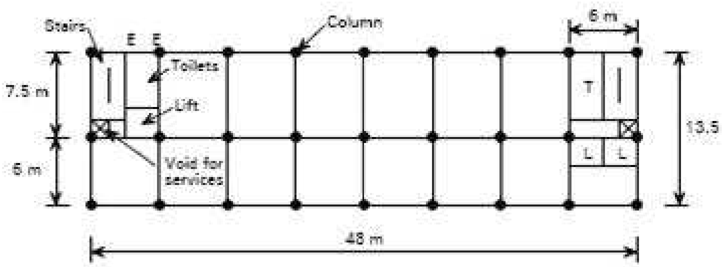

Figure 8.1: building A floor plan layout

Figure 8.2: building A architectural impression

8.2.1 Overview

A number of schemes are presented in the comparative study for the building, 5 short span floor systems, and 8 long span floor systems. The long span floor schemes are designed to allow for the removal of the internal columns except in the cores at either end of the building. The long span floor systems are neglected for this case study, and the performance of the short span systems is determined. The short span systems include:

- Slimflor beams with pre-cast concrete slabs and a 60mm concrete topping;
- Two Slimdek composite floor options, one where the floor spans longitudinally through the building and one where the floor spans transversely;
- Composite concrete beam and slab option, and a;
- Reinforced concrete slab option.

8.2.2 Structural Scheme Studied

The structural scheme studied in this chapter is the composite concrete beam and slab option. The initial design is the design as detailed in the SCI document, and is summarised in figure 8.3. The slabs are modelled with a nominal thickness of 95mm. Strength is based on only the anti cracking mesh in the upper layer of the slab. It is assumed initially that none of the secondary steelwork is protected against thermal effects.

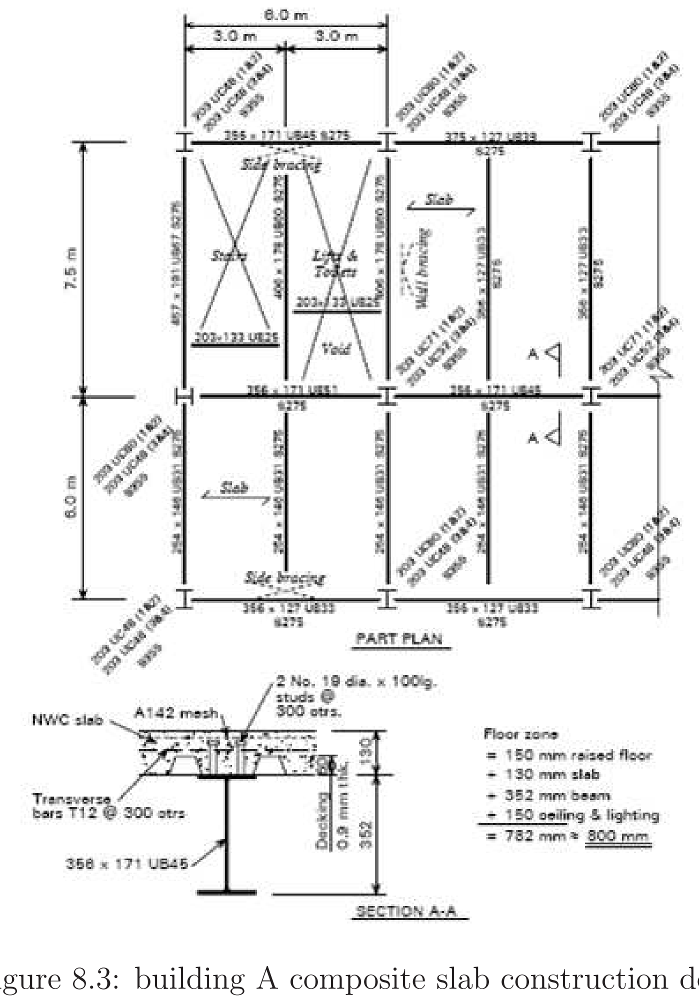

Figure 8.3: building A composite slab construction details

8.2.3 Loading

Design loading and additional information regarding the materials used is presented in table 8.1. All floors, including the roof level are designed to resist the same loading. Although it is not stated, it is assumed that all reinforcing steel has yield strength of 460MPa. The building is divided into two

Design Loading	
Imposed load	$3.5kN/m^2$
Partition loading	$1kN/m^2$
Services, ceiling loading, etc.	$0.7kN/m^2$
Floor	
Concrete	Normal weight concrete
Steel grade	
Columns and primary beams	Grade s355
All other beams	Grade s275

Table 8.1: building A design loading and materials

bays of 6m and 7.5m by the line of columns down the middle of its length. This results in the regular structural grid seen in Figure 9 1. The floors are sited at a vertical spacing of 2.7m.

The total distributed load on the floors of the structure using the composite beams and composite slab construction option consists of the fully factored live load of 5.2kN/m2 plus an additional dead load of 2.4kN/m2 which represents the composite concrete decking.

The original building was designed to have a fire resistance of 60 minutes, using the factors allowed in Eurocode 4 [37], the imposed load on the structure can be reduced by a factor of 0.65 to 2.275kN/m2 from 3.5kN/m2. Fully factored design loading is shown in table 8.2. In the analysis, the un-factored

Live Load	$4.5kN/m^2$
Dead Load	$2.4kN/m^2$
Total Load	$6.9kN/m^2$

Table 8.2: total loading for building A including factored accidental loading

material strengths are used, in accordance with Eurocode 4.

8.2.4 Building Layout

The layout of the building on all four floors is as shown in figure 8.4, figure 8.5, figure 8.6, and figure 8.7. The building runs east to west and the stairwells are located on the north face of the building.

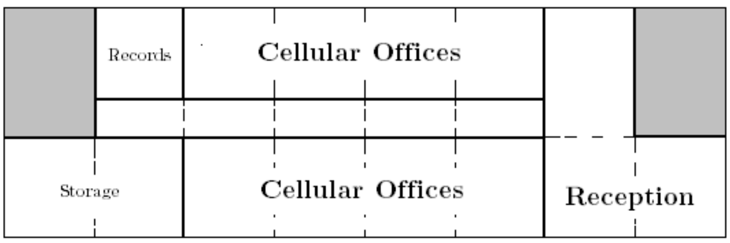

Figure 8.4: building A ground floor plan

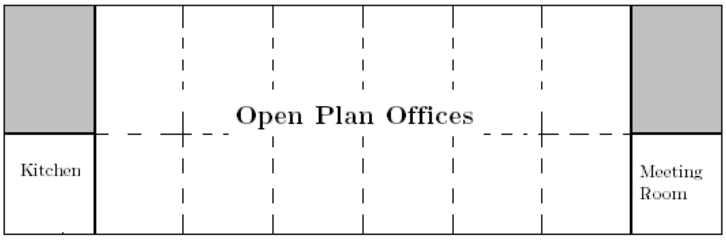

Figure 8.5: building A first floor plan

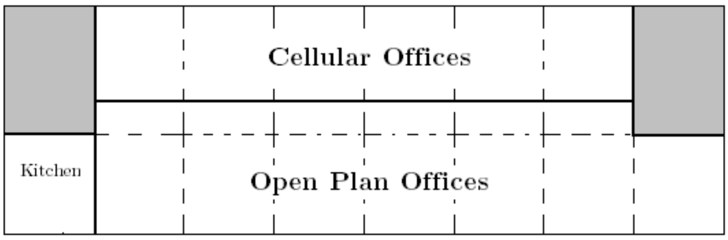

Figure 8.6: building A second floor plan

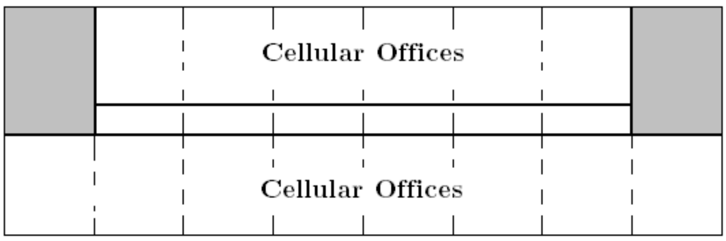

Figure 8.7: building A third floor plan

8.2.5 Building A Risk Assessment

Step 1. Division of the structure or system into suitable compartments and components

Step 1 is the identification of the compartments which will comprise the structural fire risk assessment. These are listed below:

Records (GF)

Kitchen (1F)

Kitchen (2F)

Reception

Cellular Offices (GF)

Cellular Offices (2F)

Cellular Offices (3F)

Open Plan Offices (1F)

Open Plan Offices (2F)

Open Plan Offices (3F)

Storage Room (GF)

Meeting Room (1F)

Step 2. Fuel load ranking

The different compartments are arranged in order of relative potential fuel load. This is the first stage in the development of the relative risk matrix for the project which will lead to the risk ranking. The compartments are arranged against the headings described in Chapter 5 in table 8.3.

Relative potential fuel load	High	Medium	Low	Very Low
Compartments	Records(GF) Storage room (GF)	Cellular Offices(GF) Cellular Offices(2F) Cellular Offices(3F) Open plan offices (1F) Open plan offices (2F)	Kitchen(1F) Kitchen(1F) Reception	

Table 8.3: building A relative fuel load potential

The records room and storage room are expected to have the highest potential fuel load, followed by the offices where there may be some instances of combustibles such as office furniture or reference material. The reception area will have little combustible material present and is expected to be mainly used as a waiting area. Similarly, the kitchen is expected to have little combustible material present although it will have a number of ignition sources present.

Step 3. Ignition source ranking

The potential for ignition in each of the areas identified is summarised in table 8.4.

Relative ignition potential	Very Likely	Likely	Unlikely	Very Unlikely
Compartment		Kitchen (1F) Kitchen (2F)	Cellular Offices (GF) Cellular Offices (2F) Cellular Offices (3F) Open plan Offices (1F) Open plan Offices (2F)	Records (GF) Storage Room (GF) Recpetion

Table 8.4: building A relative ignition potential

Risk Ranking	IV	III	II	I
Compartments	Records (GF) Storage Room (GF) Kitchen (1F) Kitchen (2F)	Reception	Cellular Offices (GF) Cellular Offices (2F) Cellular Offices (3F) Open Plan Offices (1F) Open Plan Offices (2F)	

Table 8.5: building A relative compartment risk ranking

Step 4. Risk Ranking

The relative risk matrix is used in correlation with the tables above to order the compartments into their relative risk from fire and the potential which they may have for a meaningful fire occurring within the building.

The overall relative risk is summarised in table 8.5. This is the list which will be used in determining the order in which the structure should be checked for achieving the reliability required. This list is based on the risk matrix described in the chapter 5 figure 8.8.

		Relative potential ignition likelihood			
		Very Likely	Likely	Unlikely	Very Unlikely
Relative potential fuel load	Very High	IV	III	III	I
	High	IV	III	II	I
	Low	IV	II	I	I
	Very Low	IV	I	I	I

Figure 8.8: Risk matrix

8.2.6 Building A Reliability Assesment

The structural models used in the analysis are those described in previous chapters. For the purposes of tensile membrane action and the pre-stressed yield line method the slab is assumed to by 2-way spanning between the supports.

The slabs are constructed from normal weight concrete 60mm deep ignoring the depth of the ribs, with an A142 anti-cracking mesh positioned 25mm from the heated surface. The steel column section is a UC 203 x 203 x 60. Although in the original study the steel elements were protected with an intumescent coating it is assumed that the steel beam is a 280ASB100 section with an exposed lower flange. All primary steelwork has yield strength of 355MPA. It is assumed that the temperature of the steel beam follows the compartment temperature-time curve.

Step 1. Reliability Goal Definition

From the ASCE 7 standard the building is in performance group 2, i.e. it is a commercial structure where the occupants are unlikely to have reduced mobility. Using the performance matrix of table 4.1, the required frequency of severe structural damage is rare which corresponds to a reliability index of 3.1 according to table 5.2.

Step 2. Fire Scenario Definition

Using the Eurocode parametric fire curve, variation in the fire scenario is defined primarily by the opening factors of the building and the areas of the rooms. For each of the compartments, these are as detailed in table 8.6.

Compartment	Floor area	Windows
Records (GF)	$36m^2$	$1 \times$ (5 x 2 m)
Kitchen (1F)	$36m^2$	$3 \times$ (1.5 x 1.5 m)
Kitchen (2F)	$36m^2$	$1 \times$ (1.5 x 1.5 m)
Reception	$115m^2$	$3 \times$ (5 x 2 m)
Cellular Offices (GF)	$144m^2$	$4 \times$ (5 x 2 m)
Cellular Offices (2F)	$144m^2$	$6 \times$ (1.5 x 1.5 m)
Cellular Offices (3F)	$216m^2$	$14 \times$ (5 x 2m)
Open Plan Offices (1F)	$486m^2$	$36 \times$ (1.5 x 1.5 m)
Open Plan Offices (2F)	$306m^2$	$7 \times$ (1.5 x 1.5 m)
Storage Room (GF)	$72m^2$	$2 \times$ (5 x 2m)
Meeting Room (1F)	$36m^2$	$3 \times$ (1.5 x 1.5 m)

Table 8.6: building A Compartment areas and openings

Variation of the openings is achieved using a normal distribution, truncated at 0 and the maximum opening possible. The mean of all of the openings is taken to be 75% of the opening factor, and the standard deviation is 10% of the opening factor plus 1% per window up to a maximum of 20%.

The limiting time is linearly distributed between 900 and 1500s.

The fuel load is based on the fuel load prescribed by EC 1 [15] for the closest occupancy type. Variation is a normal distribution with mean as described in EC1 and standard deviation of 7.5%.

All other variables required for the analysis are deterministic and are not varied during the analyses. This is chosen arbitrarily, and is intended to represent a range of real fires which may occur within each compartment.

Step 3. Structural component pairing with compartment.

As discussed above, the floor slabs within the building are assumed to be 2-way spanning. They are modelled using the techniques described in Chapter 6.

In this example, it is assumed that fire stopping is adequately installed between the floors and therefore a fire on multiple floors is not considered. However, building stability as a result of a fire on one floor is considered. This is modelled using the techniques described in Chapter 7. It is assumed in this case that the structure outwith the fire compartment provides enough support to adequately restrain the floor system at the interior edge for one of the collapse mechanisms described to occur.

The structural components which correspond to each of the compartments are listed below in table 8.7. Where a compartment boundary lies along a grid line and there are no grid lines within the compartment the floor system is assumed to be supported by the compartment boundary and therefore catenary action is unable to form which means that the column is not exposed to any additional pull-in forces. In these cases, the column in the table which pertains to the floor length is left blank and columns are not analysed in these compartments.

The structural detailing is similar for all components and is detailed in 8.2.2, above. It is therefore not summarised again here.

Step 4. Targeted Reliability Analysis.

The reliability analysis of the components listed in table 8.7 follows the order dictated by the risk ranking in table 8.5. It is based on deterministic structural details and the details provided on the fire loading as detailed in the previous step.

The first targeted analysis is performed on those components which are associated with the highest risk compartments. The results of this reliability analysis are detailed in table 8.8. These results are based upon a study of 100 samples. None of the slabs in the compartments are able to sustain the static loading required under a deterministic analysis using the means of the input variables; using the varied input variables to perform a reliability study of the components highlights the fact that the margin of safety is negative, indicating failure in most cases.

Increasing the diameter of the steel reinforcement used in the calculation

Compartment	Floor slab Quantity	Floor slab Dimensions	Column Floor Length
Records (GF)	1	6×6m	
Kitchen (1F)	1	6×6m	
Kitchen (2F)	1	6×6m	
Reception	2	6×6m	6m
	1	6×7.5m	
Cellular Offices (GF)	4	6×6m	6m
Cellular Offices (2F)	5	6×6m	6m
Cellular Offices (3F)	6	6×6m	6m
	8	6×7.5m	
Open Plan Offices (1F)	6	6×6m	6m
	6	6×7.5m	7.5m
Open Plan Offices (2F)	8	6×6m	6m
Storage Room (GF)	2	6×6m	6m
Meeting Room (1F)	1	6×6m	

Table 8.7: structural details by compartment

from 6mm to 7mm, i.e. changing the mesh from an A142 mesh to an A193 changes the reliabilities of the floor slabs to those shown in table 8.9. Increasing the diameter of the anti-cracking mesh which the membrane capacity is reliant upon dramatically increases the reliability of the floor plates in fire, more than doubling the reliability indices of the floor plates in question.

The risk acceptance criteria proposed in the design framework requires that the reliability analysis should continue through successive risk levels until the

Compartment	Component	Dimensions	μ(M)	σ(M)	β	Pass/Fail
Records (GF)	Slab	6 × 7.5m	1.0 kN/m^2	0.53 kN/m^2	1.89	Fail
Storage room (GF)	Slab	6 × 6m	1.0 kN/m^2	0.56 kN/m^2	1.79	Fail
Kitchen (1F)	Slab	6 × 6m	1.1 kN/m^2	.38 kN/m^2	2.89	Fail
Kitchen (2F)	Slab	6 × 6m	0.96 kN/m^2	0.47 kN/m^2	2.04	Fail

Table 8.8: level IV risk targeted reliability analysis

solution satisfies the requirements 'as is'. The reliability analysis is therefore extended to encompass components which are associated with compartments which have been allocated the next level of risk, table 8.10.
Table 8.10 shows all of the components which are associated with the compartments having the next level of risk to meet the reliability goals. The floor slabs meet them satisfactorily. Since the fire is considered to occur on only one floor and the floor to floor spacing is relatively low the reliability of the columns is very much higher than the reliability goal.

8.3 Building B

The prestige office block in London, figure 8.9, is an 8 storey high quadrangle consisting of 2 structural bays which circle around a closed roof atrium. The reliability of the atrium roof structure is not considered in this study,

Compartment	Component	Dimensions	μ(M)	σ(M)	β	Pass/Fail
Records (GF)	Slab	6 × 7.5m	3.9 kN/m^2	0.65 kN/m^2	6	Pass
Storage room (GF)	Slab	6 × 6m	4.0 kN/m^2	0.55 kN/m^2	7.3	Pass
Kitchen (1F)	Slab	6 × 6m	3.9 kN/m^2	.67 kN/m^2	5.8	Pass
Kitchen (2F)	Slab	6 × 6m	3.9 kN/m^2	0.56 kN/m^2	7.0	Pass

Table 8.9: revised level IV risk targeted reliability analysis

and it is assumed that appropriate ventilation is included in the overall fire strategy for the building to ensure that the gas temperature in the atrium is controlled and maintained below a temperature at which it may become of relevance to the surrounding structure. Therefore the atrium is effectively ignored.

The building is 45m wide by 60m in length and the atrium measures 15m x 30m. The structural bays are arranged on a regular grid of 7.5m squares, figure 8.10.

Compartment	Component	Dimensions	μ(M)	σ(M)	β	Pass/Fail
Reception	Slab	6 × 6m	1.2 kN/m^2	.36 kN/m^2	3.3	Pass
(GF)	Slab	6 × 7.5m	1.2 kN/m^2	0.35 kN/m^2	3.4	Pass
	Column	6m floor length	6.6 kNm	.068 kNm	97	Pass

Table 8.10: level III risk targeted reliability analysis

Figure 8.9: architectural features of building B

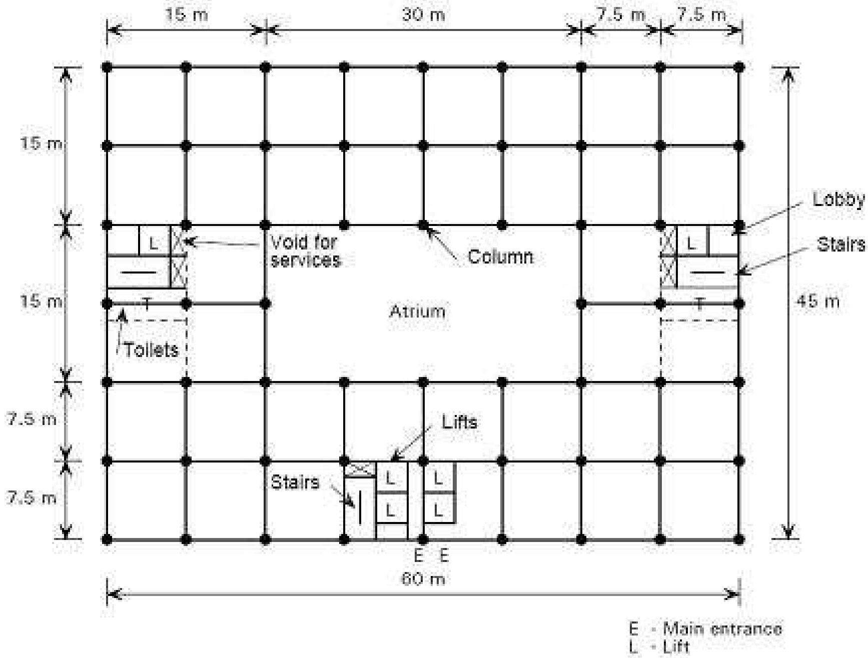

Figure 8.10: structural layout of building B

8.3.1 Structural Scheme Studied

As with building A, a number of structural schemes were considered in the original SCI study. In this study, the scheme comprising a composite beam and slab is chosen. The structural details are summarised in figure 8.11.

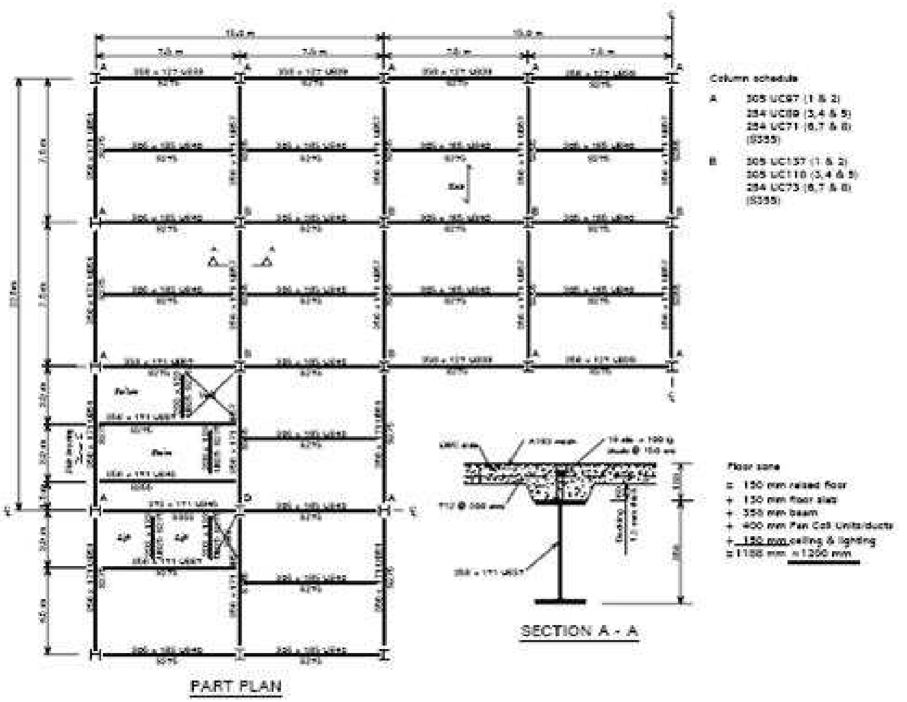

Figure 8.11: building B composite beam/slab detail

8.3.2 Design Loading

Design loading in building B is the same as in building A, table 8.2.

8.3.3 Building Layout

The building layout is as shown in figures 8.12, 8.13, 8.14, 8.15 and 8.16. Floors 2-5 have the same layout and are treated as one floor in the analysis.

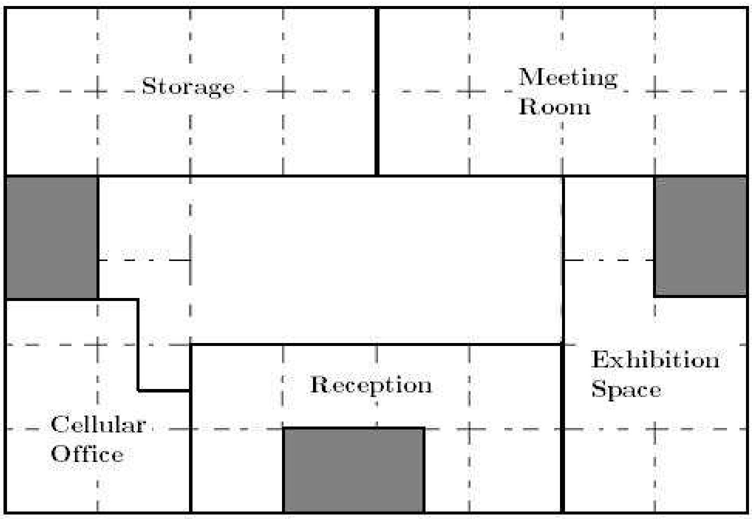

Figure 8.12: building B ground floor layout

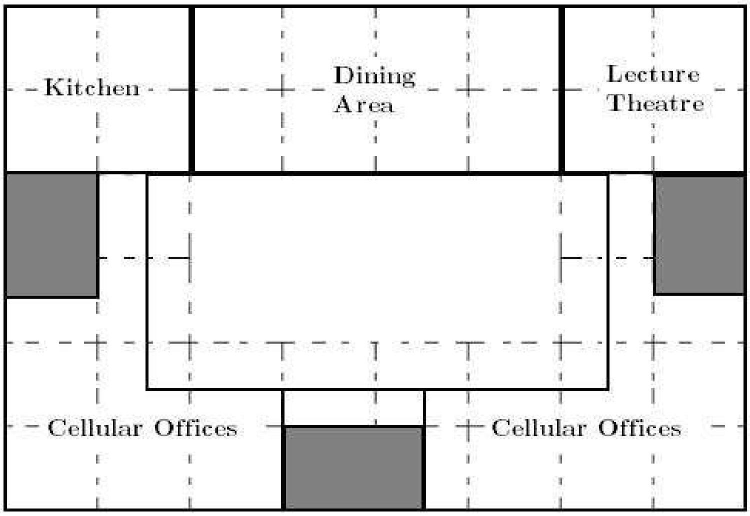

Figure 8.13: building B 1^{st} floor layout

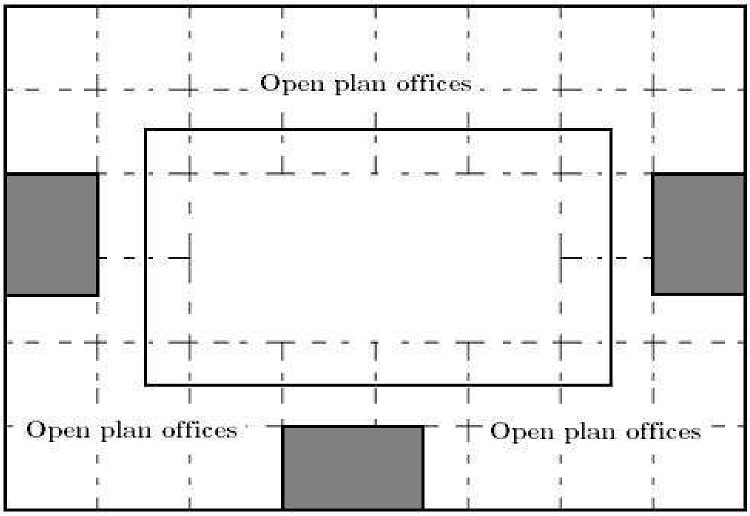

Figure 8.14: building B 2^{nd} floor layout

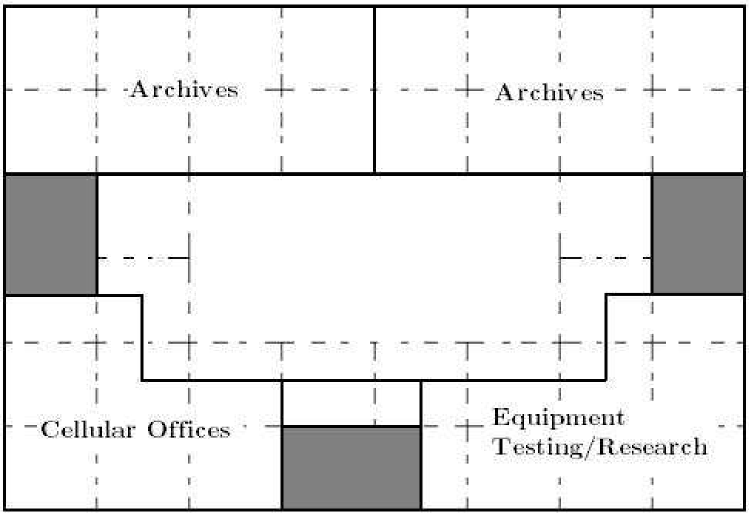

Figure 8.15: building B 6^{th} floor layout

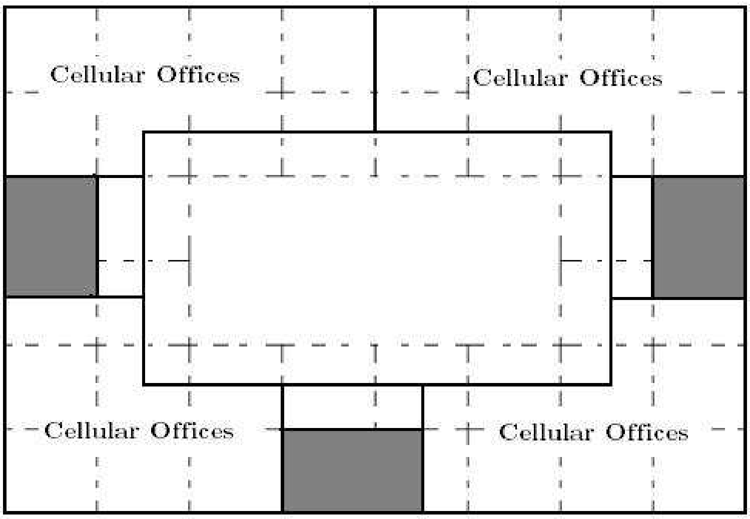

Figure 8.16: building B 7^{th} floor layout

8.3.4 Building B Risk Assessment

Step 1. Division of the structure or system into suitable compartments and components

As before, step 1 is the identification of the compartments which will comprise the structural fire risk assessment.

Storage (GF)

Meeting / Conference room (GF)

Exhibition space (GF)

Reception (GF)

Cellular offices (GF)

Kitchen (1F)

Dining area (1F)

Lecture theatre (1F)

Cellular offices (1F)

Open plan office (2-5)

Archive store (6F)

Cellular offices (6F)

Equipment testing benches (6F)

Cellular offices (7F)

Step 2. Fuel load ranking

The different compartments are arranged in order of relative potential fuel load. This is the first stage in the development of the relative risk matrix for the project which will lead to the risk ranking. The compartments are arranged against the headings described in Chapter 5 in table 8.11.

The records room and storage room are expected to have the highest potential fuel load, followed by the offices where there may be some instances of combustibles such as office furniture or reference material. The reception area will have little combustible material present and is expected to be mainly used as a waiting area. Similarly, the kitchen is expected to have little combustible material present although it will have a number of ignition sources present.

Step 3. Ignition source ranking

The potential for ignition in each of the areas identified is summarised in table 8.12.

Step 4. Risk Ranking

The relative risk matrix is used in correlation with the tables above to order the compartments into their relative risk from fire and the potential which they may have for a meaningful fire occurring within the building.

The overall relative risk is summarised in table 8.13. This is the list which will

Relative potential fuel load	High	Medium	Low	Very Low
Compartments	Storage (GF) Archive store (6F)	Cellular offices (GF) Cellular offices (1F) Open plan offices (2-5) Cellular offices (6F) Equipment testing benches (6F) Cellular offices (7F)	Meeting/Conference room (GF) Exhibition space (GF) Reception (GF) Kitchen (1F) Dining area (1F) Lecture theatre (1F)	

Table 8.11: building B relative fuel load potential

be used in determining the order in which the structure should be checked for achieving the reliability required.

Relative ignition potential	Very Likely	Likely	Unlikely	Very Unlikely
Compartment		Kitchen (1F) Equipment testing benches (6F)	Cellular Offices (GF) Cellular Offices (1F) Open plan offices (2-5) Cellular offices (6F) Cellular offices (7F)	Storage (GF) Archive store (6F) Meeting/conference room (GF) Exhibition space (GF) Reception (GF) Dining Area (1F) Lecture Theatre (1F)

Table 8.12: building B relative ignition potential

8.3.5 Building B Reliability Assessment

The structureal models used in the analysis are those described in previous chapters. For the purposes of tensile membrane action and the pre-stressed yield line method the slab is assumed to be 2-way spanning between the supports.

The slabs are constructed from normal weight concrete 60mm deep ignoring the depth of the ribs, with an A142 anti-cracking mesh positioned 25mm from teh heated surface. The steel column is a UC 204 x 203 x 60. Although in the original study the steel elements were protected with an intumescent

Risk Ranking	IV	III	II	I
Compartments	Storage (GF) Archive store (6F)	Cellular offices (GF) Cellular offices (1F) Open plan offices (2-5) Cellular offices(6F) Cellular offices (7F) Equipment testing benches (6F)	Kitchen (1F)	Meeting/conference room (GF) Exhibition space (GF) Reception (GF) Dining area (1F) Lecture theatre (1F)

Table 8.13: building B relative compartment risk ranking

coating it is assumed that the steel beam is a 280 ASB 100 section with an exposed lower flange. All primary steelwork has yield strength of 355MPa. It is assumed that the temperature of the steel beam followes the compartment temperature-time curve.

Step 1. Reliability goal definition

From the ASCE 7 standard the building is in performance group 2, i.e. it is a commercial structure where the occupants are unlikely to have reduced mobility. Using the performance matrix of table 4.1, the required frequency of severe structural damage is rare which corresponds with a reliability index of 3.1 according to table 5.2.

Step 2. Fire Scenario Definition

Using the Eurocode paramteric fire curve, variation in teh fire scenario is achieved by varying the opening factors of the building, the limiting time and the fuel load per unit area. For each of the compartments, areas and openings are detailed in table 8.14.
The variation of the openings is the same as with the previous example, i.e. it is As with building A, the limiting time is linearly distributed between 900 and 1500s.

The fuel load is based on the fuel load prescribed by EC 1 [15] for the closest occupancy type. Variation is a normal distribution with mean as described in EC1 and standard deviation of 7.5%.

All other variables required for the analysis are deterministic and are not varied during the analyses. This is chosen arbitrarily, and is intended to represent a range of real fires which may occur within each compartment.

Step 3. Structural Component Pairing with Compartment

As discussed above, the floor slabs within the building are assumed to be 2-way spanning. They are mdoelled using the techniques desscribed in Chapter 6.

In this example, it is assumed that fire stopping is adequately installed between the floors and therefore a fire on multiple floors is not considered. However, building stability as a result of a fire on one floor is considered. This is modelled using the techniques described in Chapter 7. It is assuemd that the tructure outwith the fire compartment provides enough support to adequately restrain the floor system at the interior edge for one of the collapse mechanisms described to occur.

The structural components which correspond to each of the compartments are listed below in table 8.15. Where a compartment boundary lies along a grid line and there are no grid lines within the compartmnet the floor system is assumed to be supported by the compartment boundary and therefore catenary action si unable to form which means that the column is not exposed to any additional pull-in forces. In these cases, the column in the table which pertains to the floor length is left blank and columns are not analysed in these compartments.

The structural detailing is similar for all components and is detailed in section 8.3.1, above. It is therefore not summarised again here.

Step 4. Targeted Reliability Analysis.

The first reliability analysis of building B is on those components which ahave been allocated the highest level of risk. These are teh storage and the archive rooms. The results of this reliability analysis are detailed in table 8.16.

All of the components of building B meet the reliability targets as set out in Stage 1 of the reliability assessment without any further revision. Since no revision is required to the components which comprise the compartments with the highest risk no further analysis is necessary for the remaining compartments. As with building A, the reliability of the columns is very much higher than the reliability goal of the project. If a fire on multiple floors was considered or if the floor to floor spacing was lower then the reliability of the columns would be expected to be lower.

Compartment	Floor area	Windows
Storage (GF)	$450m^2$	$6 \times (7 \times 2m)$
Meeting/conference room (GF)	$450m^2$	$6 \times (7 \times 2m)$
Exhibition space (GF)	$366m^2$	$3 \times (7 \times 2m)$
Reception (GF)	$366m^2$	$2 \times (7 \times 2m)$
Cellular offices (GF)	253^2	$3 \times (7 \times 2m)$
Kitchen (1F)	225^2	$4 \times (7 \times 2m)$
Dining area (1F)	450^2	$4 \times (7 \times 2m)$
Lecture theatre (1F)	$225m^2$	$4 \times (7 \times 2m)$
Cellular offices (1F)	$380m^2$	$4 \times (7 \times 2m)$
Open plan offices (2-5)	$1603m^2$	$22 \times (7 \times 2m)$
Archive store (6F)	$450m^2$	$6 \times (7 \times 2m)$
Cellular offices (6F)	$337.5m^2$	$5 \times (7 \times 2m)$
Equipment testing benches (6F)	$337.5m^2$	$5 \times (7 \times 2m)$
Cellular offices (7F)	$380m^2$	$5 \times (7 \times 2m)$

Table 8.14: building B Compartment areas and openings

	Floor slab		Column
Compartment	Quantity	Dimensions	Floor Length
Storage (GF)	8	$7.5 \times 7.5m$	$7.5m$
Meeting / conference room (GF)	8	$7.5 \times 7.5m$	$7.5m$
Exhibition space (GF)	7	$7.5 \times 7.5m$	$7.5m$
Reception (GF)	7	$7.5 \times 7.5m$	$7.5m$
Cellular offices (GF)	5	$7.5 \times 7.5m$	$7.5m$
Kitchen (1F)	4	$7.5 \times 7.5m$	$7.5m$
Dining area (1F)	8	$7.5 \times 7.5m$	$7.5m$
Lecture theatre (1F)	4	$7.5 \times 7.5m$	$7.5m$
Cellular offices (1F)	8	$7.5 \times 7.5m$	$7.5m$
Open plan offices (2-5)	30	$7.5 \times 7.5m$	$7.5m$
Archive store (6F)	8	$7.5 \times 7.5m$	$7.5m$
Cellular offices (6F)	10	$7.5 \times 7.5m$	$7.5m$
Equipment testing benches (6F)	10	$7.5 \times 7.5m$	$7.5m$
Cellular offices (7F)	8	$7.5 \times 7.5m$	$7.5m$

Table 8.15: building B structural details by compartment

Compartment	Component	Dimensions	μ(M)	σ(M)	β	Pass/Fail
Storage (GF)	Slab	7.5 × 7.5m	1.8 kN/m^2	0.46 kN/m^2	3.88	Pass
	Column	7.5m floor × 7.5m length	3.6 kN/m^2	.096 kN/m^2	37.8	Pass
Archive store (6F)	Slab	7.5 × 7.5m	1.8 kN/m^2	0.46 kN/m^2	3.88	Pass
	Column	7.5m floor × 7.5m length	5.3 kN/m^2	.096 kN/m^2	55.2	Pass

Table 8.16: level IV risk targeted reliability analysis (building B)

8.4 Summary

In the original study by the SCI, buidling A was designed to have a 60 minute fire resistance and building B was designed to have a 90 minute fire resistance. This was provided via a combinationof board encasement, spray on intumescent coating applied both ons and offsite as well as a cementitious spray protection.

The approach suggested here will hopefully reduce the cost of the fire protection required. Especially for building A where, although a number of the floor plates require additional reinforcement to be applied, it is expected that some saving can be achieved by omitting fire protection from all secondary beams using the design principles given here. The motivation for employing the techniques described here is further enhanced by the added security and safety that the more scientific approach taken here to the assessment of the structure for high temperatures will provide.

There were very few changes required to building A, these comprise an increase in the anti-cracking mesh size for only a few hazard rooms. If the use and / or occupancy of building A is expected to change over its life time then additional measures may be requried to mitigate against any additional risks introduced as a result of this.

Building B meets the performance goals as it is currently designed, however as with building A if any changes are expected to occur during the buildings life time then additional work may be required to identify and to mitigate against any additional risks.

The amount of work introduced to a project by this methodology is limited, especially where the structure is designed around a simple grid system as the buildings described in this chapter. The work required does not require any specialist tools or software and as such the cost introduced to a project in order to carry out these analyses will be very low.

9

Conclusions

9.1 Summary

The aim of this thesis has been to develop a performance based design methodology for structures in fire, addressing the concepts of risk and reliability. This goal was complemented by the need to develop further suitable analytical techniques for the assessment of a structures response in fire.

A methodology for the performance based design of structures in fire has been proposed, based on the concepts of risk and reliability and drawing on the common aspects of a performance based design framework. The framework is not dependant upon statistical means to define fire scenarios for a building to resist and takes a more holistic approach which allows the design fires to be based upon the likely distribution of fuel, ignition sources and ventilation within a building.

The framework is demonstrated in use by assessing the performance of two 'standard' buildings in fire. The buildings are assessed using a complete model describing floor plate behaviour at increasing deflection and a simple assessment methodology for stability of tall buildings in fire. These two techniques are developed and described in earlier chapters and are analytical methods which are based on the fundamental principles of structural behaviour in fire.

The floor plate methodology is a continuation and modification of a theory for describing tensile membrane capacity of heated floor plates. The membrane forces are used to derive a thermally pre-stressed yield line theory for floor plates which are sufficiently rigid that they do not experience large thermal deflections at their mid-span and therefore do not lend themselves well to tensile membrane action.

The tall building assessment methodology is based on the results of exhaustive numerical studies carried out to identify potential collapse mechanisms of tall buildings in fire. Analytical techniques are derived which describe the contributing forces for these mechanisms.

Following assessment of the risk and reliability of the two structures in fire, improvements are made based upon the results of the analysis to increase the reliability of the structures such that they meet simple reliability targets.

9.2 Discussion and Possible Further Work

The structural work and assessment of capacities in this thesis has been primarily concerned with the growth and burning phase of a compartment fire. It is becoming increasingly clear to researchers, however, that the large strains which develop in a structure or frame during the cooling phase of a fire can and do have a significant effect on the resulting stability of the structure after fire. Despite this, the design methodology presented and the method for the assessment of the performance of the building during fire is applicable to all design situations. Since performance based design methodologies are inherently modular, cooling, and any additional design situations for which a performance goal can be defined can be addressed in the methodology in one of three ways:

1. The modules which comprise the assessment procedure can be changed to take account of the cooling effects of fire on the structure;
2. Additional modules can be introduced to describe and assess the structures response to other design scenarios; or,
3. Entirely new modules can be developed as required or as new knowledge and understanding becomes available to the designer.

The risk assessment methodology proposed draws together a lot of the concepts which are currently in use for structural fire safety design for exceptional structures, such as identification of locations of high fuel loads and compartments where a fire is likely to be of greater magnitude than in another compartment. The methodology proposed draws these concepts together into a coherent methodical framework which has been shown to be suitable for the assessment of more regular structures. However, the framework at present does not incorporate the structural detailing and the vulnerability of some, e.g. long span, systems to fire. This vulnerability can have a serious impact on the risk from fire. It may be possible to incorporate this aspect into future iterations of the framework by including a subsequent ranking of the components analysed in each compartment by their own relative hazard.

The arrangement and grouping of the compartments by relative fuel load (hazard) and ignition likelihood is potentially very subjective. Guidelines for consistent selection of the groupings could be based upon the occupancy - in the examples, office areas are considered to be of medium or low combustible loading, and to have an unlikely ignition potential driven by a failure in a standard piece of electrical equipment. Other areas, such as public areas may have a higher ignition potential as would kitchens and work benches, etc. Storage areas will have a higher fuel load, and large open spaces will have lower fuel loads.

The reliability goals which are used in the case studies are based on the Eurocode reliability goals, and selected from a performance matrix and the ASCE 7 standard. This draws on a number of standards and proposed standards which may have different foundations and goals. As such the reliability goals may seem high for such a low probability event. However, their use is justified by the fact that no alternative reliability goals exist at present for fire. These are an initial suggestion for the reliability goals, and lower less onerous reliability goals may be equally suited to the purpose.

The selection of fire scenarios in the analyses is based upon an arbitrary selection of random distributions for the non-deterministic variables. The examples are chosen such that the fire scenarios will represent the range of possible fires which may occur within the compartment; however this selection will vary from user to user and will be dependant upon the modelling approach taken.

There is at present no scientific method for determining the probability of an event within a compartment. However, the field of fire engineering is constantly evolving and structural design for fire safety on a performance basis is in its infancy. It is highly likely that new developments and methods will become available for the estimation of these probabilities and the techniques described here will need to be adapted to reflect these.

For ambient design, loads and material strengths are multiplied by some factor which is intended to ensure that the final design meets the reliability goal of the system. These safety factors are derived from the reliability methodologies described in this thesis; however no such factors, aside from the reduced live design load, exist for elevated temperatures. It would be possible to develop a range of partial factors for the material strengths to be used in the design methodologies described in this thesis, based on the results of repeated, physical or analytical, reliability testing to prevent the necessity for such a subjective arbitrary variation in the thermal loading suggested here. These factors would be easier to use than the proposed methodology and would facilitate a more widespread growth in the use of performance based structural design for fire safety.

The methodologies described for the determination of floor slab capacity in fire assume a low deflection and a large deflection respectively. The pre-stressed yield line methodology when it yields will allow the slab to adopt a large deflection, increasing towards that of a tensile membrane capacity. Through this increase in the deflection, a large amount of external work is released without a correspondingly large increase in the internal work as the concrete cracks across the slabs surface. Where the thermal effects on the slab are high enough, this transition will be arrested by the reinforcement mesh as it adopts a tensile mechanism. However, where the capacity of a tensile membrane mechanism is not high enough to arrest the load on the slab the slab will fail.

It is likely that regions of concrete at low deflection will continue to provide a laterally compressed support through this transition, with the level of support decreasing correspondingly with an increasing area having adopted a tensile membrane mechanism. Further study into this is possible, and may yield a further enhancement to the capacity calculated via tensile membrane mechanisms and provide greater confidence in the ability of a floor slab to sustain static loading despite large central deflections.

References

[1] S. Lamont. Behaviour of steel framed structures in fire. *The University of Edinburgh*, 1997.

[2] Pd 7974-3: 2003 application of fire safety engineering principles to the design of buildings - part 3: Structural response and fire spread beyond the enclosure of origin (sub-system 3).

[3] B. Tubbs. Icc performance codes for buildings and facilities structural fire protection provisions. 2001.

[4] S.R. Hamilton, C.A. Menun, and G.G. Deierlein. Probabilistic aspects of performance-based engineering methodologies for fires and earthquakes. 2002.

[5] T.F. Barry. Risk informed - performance based industrial fire protection. first edition. *Tennessee Valley Publishing*, 2002.

[6] F.W. Mowrer. A performance framework for structural fire safety.

[7] J.L. Torero, J.G. Qunitiere, and T. Steinhaus. Fire safety in high-rise buildings, lessons learned from the wtc. *Vereinigung zur Forderung des Deutschen Brandschutzes e.V*, 2002.

[8] Nfpa 551 guide for the evaluation of fire risk assessments 2007 edition.

[9] J.M.J. Watts. Fire risk ranking. *The SFPE Handbook of Fire Protection Engineering, 2nd Edition, 1995.*

[10] C. Roben. Fire induced instability in multi-storey frames. *The University of Edinburgh*, 2006.

[11] En 1990:2002 eurocode - basis of structural design.

[12] J. Twilt, J. Van Oerle, and U. Kirchner. Fire characteristics for use in a natural fire design of building structures, in competitive steel buildings through the natural fire safety concept. *Profil Arbed*, 1999.

[13] Bs iso/tr 13387-2:1999 fire safety engineering - part 2: Design fire scenarios and design fires.

[14] A.H. Buchanan. Structural design for fire safety. 2001.

[15] En 1991-1-2:2002 eurocode 1: Actions on structures - part 1-2: General actions - actions on structures exposed to fire.

[16] J. Zehfuss and D. Hosser. A parametric natural fire model for the structural fire design of multi-storey buildings. *Fire Safety Journal*, 42:115–126, 2007.

[17] J.M. Franssen and J.-F. Cadorin. Natural fire models in competitive steel buildings through the natural fire safety concept.

[18] Nist, fire dynamics simulator (fds).

[19] Ansys, ansys cfx.

[20] Bre, jasmine.

[21] G.T. Rein, W. Jahn, J. Stern-Gottfried, N.L. Ryder, S. Desanghere, M. Lazaro, F. Mowrer, A. Coles, D. Joyeux, D. Alvear, J.A. Capote, A. Jowsey, and P. Reszka. A priori modelling of fire test one, in the dalmarnock fire tests: Experiments and modelling. 2007.

[22] W. Jahn, G. Rein, and J. Torero. A posteriori modelling of fire test one, in the dalmarnock fire tests: experiments and modelling. 2007.

[23] A.M. Sanad, S. Lamont, A.S. Usmani, and J.M. Rotter. Structural behaviour in fire compartment under different heating regimes - part 1 (slab thermal gradients). *Fire Safety Journal*, 35:99–116, 2000.

[24] A.M. Sanad, S. Lamont, A.S. Usmani, and J.M. Rotter. Structural behaviour in fire compartment under different heating regimes - part 2 (slab mean temperatures). *Fire Safety Journal*, 35:117–130, 2000.

[25] Behaviour of steel framed structures under fire conditions. *Main report, DETR PiT project*, 2000.

[26] M. Gillie. The behaviour of steel-framed composite structures in fire conditions. *The University of Edinburgh*.

[27] N. Cameron. The behaviour and design of composite floor systems in fire. *The University of Edinburgh*, 2003.

[28] British Steel plc. The behaviour of multi-storey steel framed buildings in fire. *Swinden Technology Centre*, 1999.

[29] Y.C. Wang, T. Lennon, and D.B. Moore. The behaviour of steel frames subject to fire attack. *Journal of Constructional Steel Research*, 35:291–322, 1995.

[30] M. Gillie, A. Usmani, and M. Rotter. A structural analysis of the first cardington test. *Journal of Constructional Steel Research*, 57:581–601, 2001.

[31] M. Gillie, A. Usmani, and M. Rotter. A structural analysis of the cardington british steel corner test. *Journal of Constructional Steel Research*, 58:427–442, 2002.

[32] M. Gillie, A. Usmani, M. Rotter, and M. O'Connor. Modelling of heated composite floor slabs with reference to the cardington experiments.

[33] S. Lamont, A.S. Usmani, and M. Gillie. Behaviour of a small composite steel frame structure in a "long-cool" and a "short-hot" fire. *Fire Safety Journal*, 39:327–357, 2004.

[34] J.M. Rotter and A.S. Usmani. Thermal effects. *Proceedings of the 1st International workshop, Structures in Fire*, 2000.

[35] A.S. Usmani, J.M. Rotter, S. Lamont, A.M. Sanad, and M. Gillie.

[36] A.S. Usmani and N.J.K Cameron. Limit capacity of laterally restrained reinforced concrete floor slabs in fire. *Cement and Concrete Composites*, 26:127–140, 2004.

[37] En 1994-1-2:2003 design of composite steel and concrete structures - part 1-2: General rules - structural fire design.

[38] En 1992-1-2:2002 eurocode 2: Design of concrete structures - part 1-2: Structural fire design.

[39] G.V. Hadjisophocleus, N. Benichou, and A.S. Tamim. Literature review of performanced based fire codes and design environment. *Journal of Fire Protection Engineering*, 9:12, 1998.

[40] Performance based design of steel structures in fire, work in progress 1st draft. *Structural Engineering for Fire Resistance, Short course at Tianjin University of Technology*, 2002.

[41] A. Irfanoglu. Structural design under seismic risk using multiple performance objectives. *PhD thesis, CalTEC: California*, 2000.

[42] D. Beller, G. Foliente, and B. Meacham. Qualitative versus quantitative aspects of performance based design regulations. *4th International conference on performance based codes and fire severity design methods*, 2002.

[43] M.H. Faber, O. Kubler, M. Fontana, and M. Knobloch. Failure consequences and reliability acceptance criteria for exceptional building structures - a study taking basis in the failure of the world trade centre twin towers. *Institute of Structural Engineering, Swiss Federal institute of Technology.*

[44] En 1993-1-2:2005 eurocode 3: Design of steel structures - part 1-2: General rules - structural fire design.

[45] Y.-S. Lin. Estimations of the probability of fire occurrences in buildings. *Fire Safety Journal*, 40:728–735, 2005.

[46] G. Ramachandran. The economics of fire protection. 1998, london: E and fn spon.

[47] P.G. Holborn, P.F. Nolana, and J. Golt. An analysis of fire sizes, fire growth rates and times between events using data from fire investigations. *Fire Safety Journal*, 39:481–524, 2004.

[48] K. Helm. Statistical information, twelve month analysis of 250 000 - plus fires. *Fire prevention and Fire Engineers Journal*, April 2005.

[49] S. Hostikka and O. Keski-Rahkonen. Probabilistic simulation of fire scenarios. *Nuclear Engineering and Design*, 224:301–311, 2003.

[50] D.J. Rasbash, G. Ramachandran, B. Kandola, J.M. Watts, and M. Law. Evaluation of fire safety. *Chichester: John Wiley and Sons, Ltd*, 2004.

[51] M.E. Harr. Reliability-based design in civil engineering. *McGraw Hill, Inc*, 1987.

[52] G.N. Berlin. Probability models in fire protection engineering. *The SF-PE Handbook of Fire Protection Engineering*, pages 4–43 – 4–52, 1988.

[53] J. Van Bowen Jr. Reliability. *The SFPE Handbook fo Fire Protection Engineering*, pages 4–34 – 4–42, 1988.

[54] T. Cheung. A note on knights concepts of "risk" and "uncertainty".

[55] B. M. Ayyub. Uncertainty modelling and analysis in civil engineering. *CRC Press LLC.*, 1998.

[56] D. Diamantidis. Risk acceptance criteria: A review. note prepared for the joint committee on structural safety. 2004.

[57] C.G. Bailey and D.B. Moore. The structural behaviour of steel frames with composite floor slabs sunject to fire: Part 1: Theory. *The Structural Engineer*, 78/11:19–27, 2000.

[58] C.G. Bailey and D.B. Moore. The structural behaviour of steel frames with composite slabs subject to fire: Part 2: Design. *The Structural Engineer*, 78/11:28–33, 2000.

[59] N.J.K. Cameron and A.S. Usmani. A new design method to determine the membrane capacity of laterally restrained composite floor slabs in fire part 1: Theory and method. *The Structural Engineer*, 83/19:28–33, 2005.

[60] N.J.K. Cameron and A.S. Usmani. A new design method to determine the membrane capacity of laterally restrained composite floor slabs in fire part 2: Validation. *The Structural Engineer*, 83/19:34–39, 2005.

[61] M. S. Black. Ultimate strength study of two-way concrete slabs. *Journal of the Structural Division of the ASCE*, page 13, jan 1975.

[62] A.T. Salami. Equation for predicting the strength of fully-clamped two-way reinforced concrete slabs. *Procedures of the Institution of Civil Engineers Structures and Buildings*, 104:101–107, 1994.

[63] M. Gillie, A. Usmani, and M. Rotter. Bending and membrane action in concrete slabs. *Fire and Materials*, 28:139–157, 2004.

[64] G.M. Newman, J.T. Robinson, and C.G. Bailey. Fire safe design: A new approach to multi-storey steel-framed buildings. *Fire and Steel Construction*, 2000.

[65] S. Foster, M. Chladna, C. Hsieh, I. Burgess, and R. Plank. Thermal and structural behaviour of a full-scale composite building subject to a severe compartment fire. *Fire Safety Journal*, pages 183–199, 2007.

[66] F.K. Kong and R.H. Evans. Reinforced and pre-stressed concrete 3rd edition. *Van Nostrand Reinhold (UK) Co. Ltd.*, 1987.

[67] G. Kennedy and C. Goodchild. Practical yield line design. *Reinforced concrete council*, 2003.

[68] S.E. Quiel and M.E.M. Garlock. A performance-based design approach for steel perimeter columns subject to fire. *Fourth International Workshop Structures in Fire*, 2006.

[69] M.E.M. Garlock and S.E. Quiel. Combined axial load and moment capacity of fire-exposed beam-columns with thermal gradients. *Fourth International Workshop Structures in Fire*, 2006.

[70] Chung Y.C. and Torero J.L. Usmani, A.S. How did the wtc towers collapse? a new theory. *Fire Safety journal*, 38:501–533, 2003.

[71] A.S. Usmani. Stability of the world trade center twin towers structural frame in multiple floor fires. *Journal of Engineering Mechanics*, pages 654–657, 2005.

[72] G.R. Flint. Fire induced collapse of tall buildings. *The University of Edinburgh*, 2005.

[73] A.S. Usmani, C. Roben, L. Johnston, G. Flint, and A. Jowsey. Tall building collpase mechanisms initiated by fire. *Fourth International Workshop Structures in Fire*, 2006.

[74] D.D. Drysdale. *An Introduction to Fire Dynamics, Second Edition*. John Wiley and Sons, Ltd., 1998.

[75] Pd 7974-1: 2003 application of fire safety engineering principles to the design of buildings - part 1: Initiation and development of fire within the enclosure of origin.

[76] En 1994-1-1:1994 eurocode 4: Design of composite steel and concrete structures - part 1-1: General rules and rules for buildings.

[77] R.D. Ziemian and W. McGuire. Mastan 2. 2000.

[78] S.J. Hicks, R.M. Lawson, J.W. Rackham, and P. Fordham. Comparative structure cost of modern commercial buildings (second edition). *The Steel Construction Institute*, 2004.

[79] Supporting the commercial decision. *Corus Construction and Industrial*.